

9. SITE 711¹

Shipboard Scientific Party²

HOLE 711A

Date occupied: 0945 L, 11 June 1987
Date departed: 1430 L, 12 June 1987
Time on hole: 28 hr, 15 min
Position: 02°44.56'S, 61°09.78'E
Water depth (sea level; corrected m, echo-sounding): 4429.8
Water depth (rig floor; corrected m, echo-sounding): 4440.3
Bottom felt (m, drill pipe): 4438.7
Penetration (m): 249.6
Number of cores: 26
Total length of cored section (m): 249.6
Total core recovered (m): 203.9
Core recovery (%): 81.7
Oldest sediment cored:
Depth (mbsf): 249.6
Nature: nannofossil chalk
Age: middle Eocene
Measured velocity (km/s): 4.207

HOLE 711B

Date occupied: 1635 L, 12 June 1987
Date departed: 0300 L, 13 June 1987
Time on hole: 10 hr, 25 min
Position: 02°44.56'S, 61°09.78'E
Water depth (sea level; corrected m, echo-sounding): 4429.8
Water depth (rig floor; corrected m, echo-sounding): 4440.3
Bottom felt (m, drill pipe): 4440.2
Penetration (m): 98.3
Number of cores: 11
Total length of cored section (m): 98.3
Total core recovered (m): 89.25
Core recovery (%): 90.8
Oldest sediment cored:
Depth (mbsf): 98.3
Nature: nannofossil ooze
Age: late Oligocene
Measured velocity (km/s): 1.494

Principal results: Site 711 is located in the western equatorial Indian Ocean at 2°44.56'S and 61°09.78'E at a water depth of 4428.2 m (Fig. 1). The site lies on the northern edge of the Madingley Rise,

just a few hundred meters above the abyssal plain which separates the Madingley Rise from the Carlsberg Ridge. An irregular relief characterizes the local topography, although the site was placed in a sheltered basin surrounded by two basement highs. This small basin holds some 350 m of sediments, showing moderately strong and internally coherent reflective layers (see "Seismic Stratigraphy" section, this chapter). Site 711 forms the deep end-member of the bathymetric transect drilled for the purpose of studying the Miocene through Pleistocene flux of biogenic calcium carbonate and its dissolution at depth.

We continuously cored two holes at Site 711. Hole 711A penetrated to 249.7 mbsf, yielding a total of 26 cores. The upper 11 of these were cored with the advanced hydraulic piston corer (APC), and the remaining 15 with the extended core barrel (XCB) system. The total recovery was 81.7% (81.1% with the XCB). Hole 711B was cored from the mud line to 98.6 mbsf. The 11 APC cores had a recovery rate of 90.8%.

Based on differences in biogenic components and carbonate contents, four lithologic units were described from Site 711 (see "Lithostratigraphy" section, this chapter):

Unit I (0.0–17.7 mbsf) consists of alternating light yellowish, clayey nannofossil ooze and dark greyish brown, radiolarian-bearing nannofossil clay and nannofossil-bearing clay. Carbonate content varies between 40% and 60%. This unit comprises the Pleistocene through upper Pliocene interval.

Unit II (17.7–68.0 mbsf) consists of low carbonate (0%–10%) clays, although a few short intermittent intervals show slightly higher carbonate contents. About 25 turbidites (<30 cm thick) occur in this unit, which represents the time interval from the upper/lower Pliocene boundary to the lowermost Miocene.

Unit III (68.0–173.0 mbsf) consists of 105 m of carbonate-rich sediments (about 75%–90%) which are virtually devoid of foraminifers. The sediments thus are characterized as nannofossil oozes or clay-bearing nannofossil oozes which become more lithified toward the bottom of Unit III and turn into clay-bearing nannofossil chalks. Two distinct ash layers, 15 and 5 cm thick, respectively, occur in the upper Oligocene. The entire unit represents the time interval from the earliest Miocene, through the Oligocene, and ending close to the middle/late Eocene boundary (22–41 Ma).

Unit IV (173.0–249.6 mbsf) is distinguished from Unit III by the consistent occurrence of radiolarians. This noncarbonate dilution decreases the carbonate values to about 70%–80%. A few shorter intervals contain an almost pure radiolarian ooze. Unit IV spans the major part of the middle Eocene (41–50 Ma). The cored stratigraphic sequence is summarized in Figure 2.

The time control in the upper 104.5 m (all APC cores) is based on combined biostratigraphy and magnetostratigraphy, and below that level on biostratigraphy alone (see "Biostratigraphy" and "Paleomagnetism" sections, this chapter). Not surprisingly, this deep site is characterized by distinctly low sedimentation rates. Despite the fact that the middle and lower Miocene are strongly condensed, with an average sedimentation rate of about 1–3 m/m.y., the sequence appears to represent continuous deposition when viewed in light of the present stratigraphic resolution. Oligocene and upper Eocene sedimentation rates are on the order of 6–8 m/m.y. A few distinct dissolution events occur across the middle/upper Eocene boundary.

Our preliminary attempt to calculate bulk and carbonate mass accumulation rates clearly illustrates the substantial dissolution which has affected the sediments at Site 711 (Fig. 3). The noncarbonate fraction dominates the bulk accumulation throughout most of the Neogene. It is subdued, however, with respect to the carbonate accumulation during Oligocene and Eocene times except for two short intervals around the middle/upper Eocene boundary. The bulk accu-

¹ Backman, J., Duncan, R. A., et al., 1988. *Proc. ODP, Init. Repts.*, 115: College Station, TX (Ocean Drilling Program).

² Shipboard Scientific Party is as given in the list of Participants preceding the contents, with the addition of Isabella Premoli Silva and Silvia Spezzaferria, Dipartimento di Scienze della Terra, Università di Milano, Via Mangiagalli 34, I-20129 Milano, Italy.

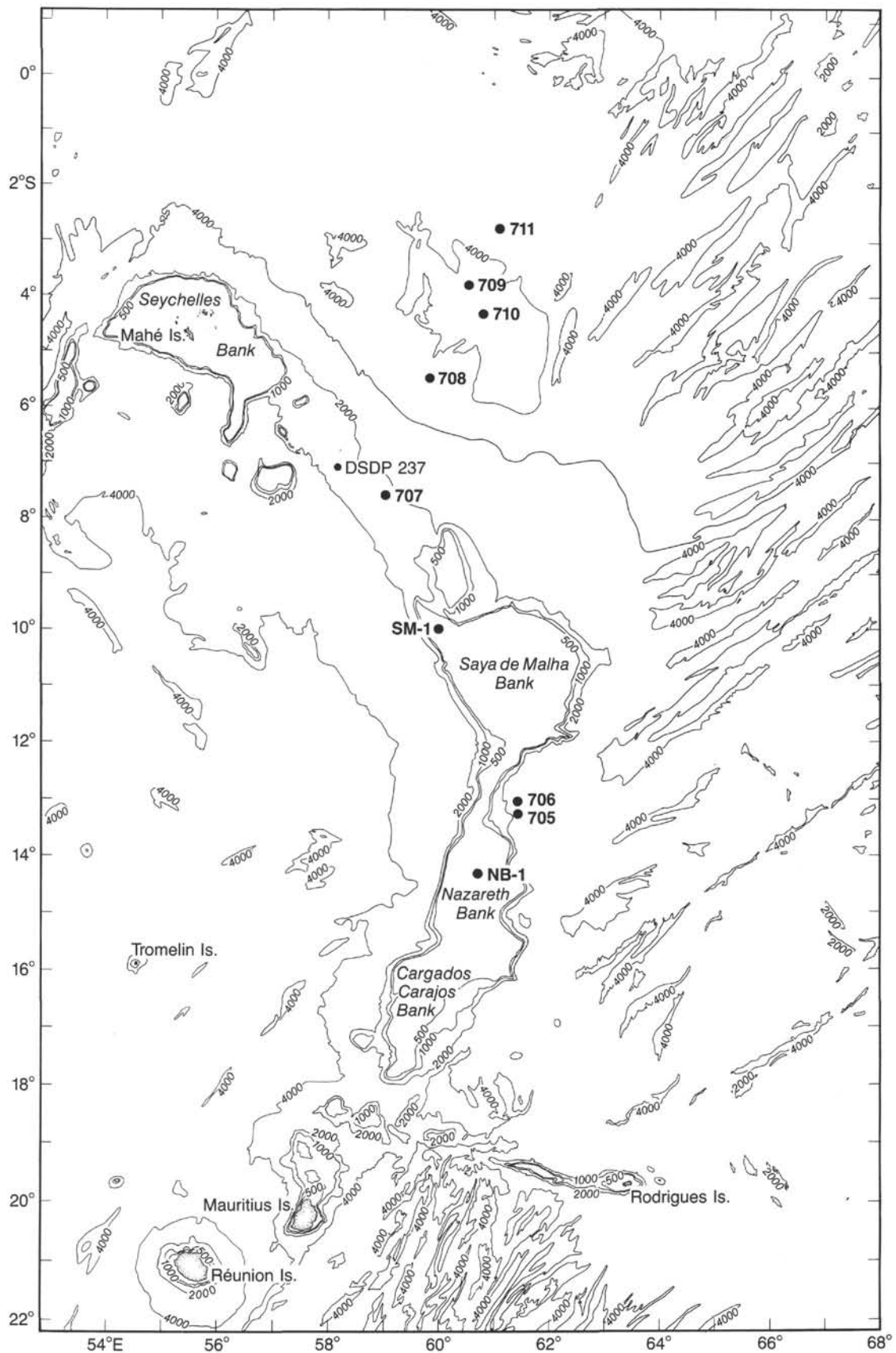


Figure 1. Bathymetric features around the Mascarene Plateau and the location of Site 711 (after Fisher et al., 1971). Depth in meters.

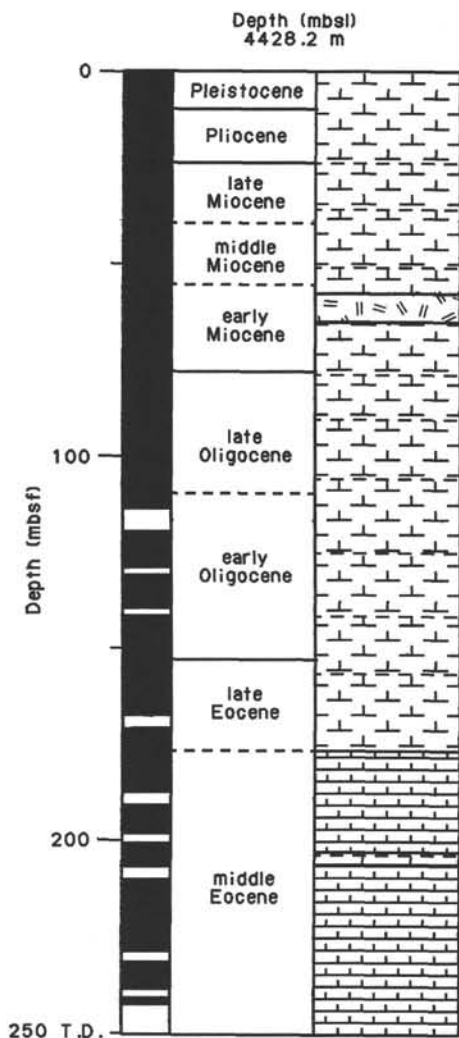


Figure 2. Stratigraphic summary of Site 711. Black column represents recovered section.

mulation rates vary between 0.1 and 0.4 $\text{g/cm}^2/1000 \text{ yr}$ during the Neogene, increase to about 0.6 $\text{g/cm}^2/1000 \text{ yr}$ during the Oligocene and latest Eocene, decrease to an average of 0.3 $\text{g/cm}^2/1000 \text{ yr}$ during the early late and late middle Eocene, and finally increase to about 1.2 $\text{g/cm}^2/1000 \text{ yr}$ during the early half of the middle Eocene. By assuming that the input of the noncarbonate component was similar over the Madingley Rise (Sites 709, 710, and 711) at any given time interval, the general increase in the mass accumulation rate of this component with increasing water depth suggests the influence of downslope transport processes. The only exception to this pattern is in the upper Miocene through Pleistocene intervals at Sites 710 and 711, which show a virtually identical accumulation of the noncarbonate fraction.

Site 711 was near or below the carbonate-compensation depth (CCD) through most of the Neogene. The more carbonate-rich Paleogene sediments are virtually devoid of foraminifers, indicating that the site has been well below the depth of the foraminifer lysocline since 50 Ma and that nannofossils are generally less susceptible to dissolution than foraminifers.

BACKGROUND AND OBJECTIVES

Site 711 is one of five sites in a transect drilled at different water depths from the Mascarene Plateau (Site 707), the Madingley Rise (Sites 709, 710, and 711), and surrounding abyssal plains (Site 708) (Fig. 4). The broader strategy for drilling this bathymetric transect is presented in the Site 707 chapter (see

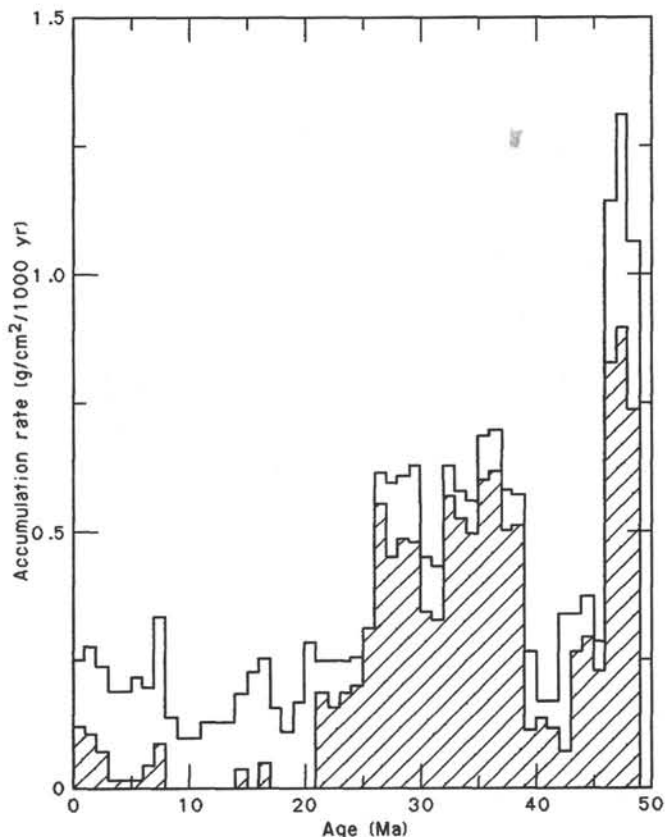


Figure 3. Mass accumulation rates of bulk sediment (unfilled area) and biogenic calcium carbonate (diagonal lines) plotted vs. age at Hole 711A. The data represent mean values within 1-m.y. time increments, based on preliminary shipboard biostratigraphy.

“Background and Objectives” section, “Site 707” chapter, this volume). Located at a water depth of 4428.2 m, Site 711 fulfills the requirement for a deep end-member in the bathymetric transect. The major goal was to retrieve a complete Neogene sediment sequence from the sublysocline transition zone. By definition, the upper boundary of this zone represents the depth horizon where calcite dissolution is drastically increased (the hydrographic lysocline; Peterson, 1966), or where foraminiferal or nannofossil assemblages begin to show marked signs of dissolution (the foraminiferal and nannofossil lysocline, respectively; Berger, 1975). Carbonate dissolution increases progressively throughout the sublysocline transition zone, with its base defined as the depth horizon where the rate of pelagic carbonate “rain” equals the rate of dissolution.

We expect the sediments at Site 711 not only to reveal time-dependent vertical changes in the position of the CCD but also to monitor less dramatic changes such as the time-dependent variability of carbonate preservation within the sublysocline transition zone. The degree of calcite saturation in the oceans varies in order to balance the total carbonate budget (Broecker and Peng, 1982). This transect in the tropical Indian Ocean, therefore, adds a critical piece to the global network of depth transects which are needed in order to produce realistic models of the earth’s carbonate budget, and in order to determine the causes for its variability through time. On geological time scales, such sediment budget models can only be formulated on the basis of a highly resolved chronology. Another major goal at Site 711 was the establishment of an accurate time control based on a combination of biostratigraphy and magnetostratigraphy.

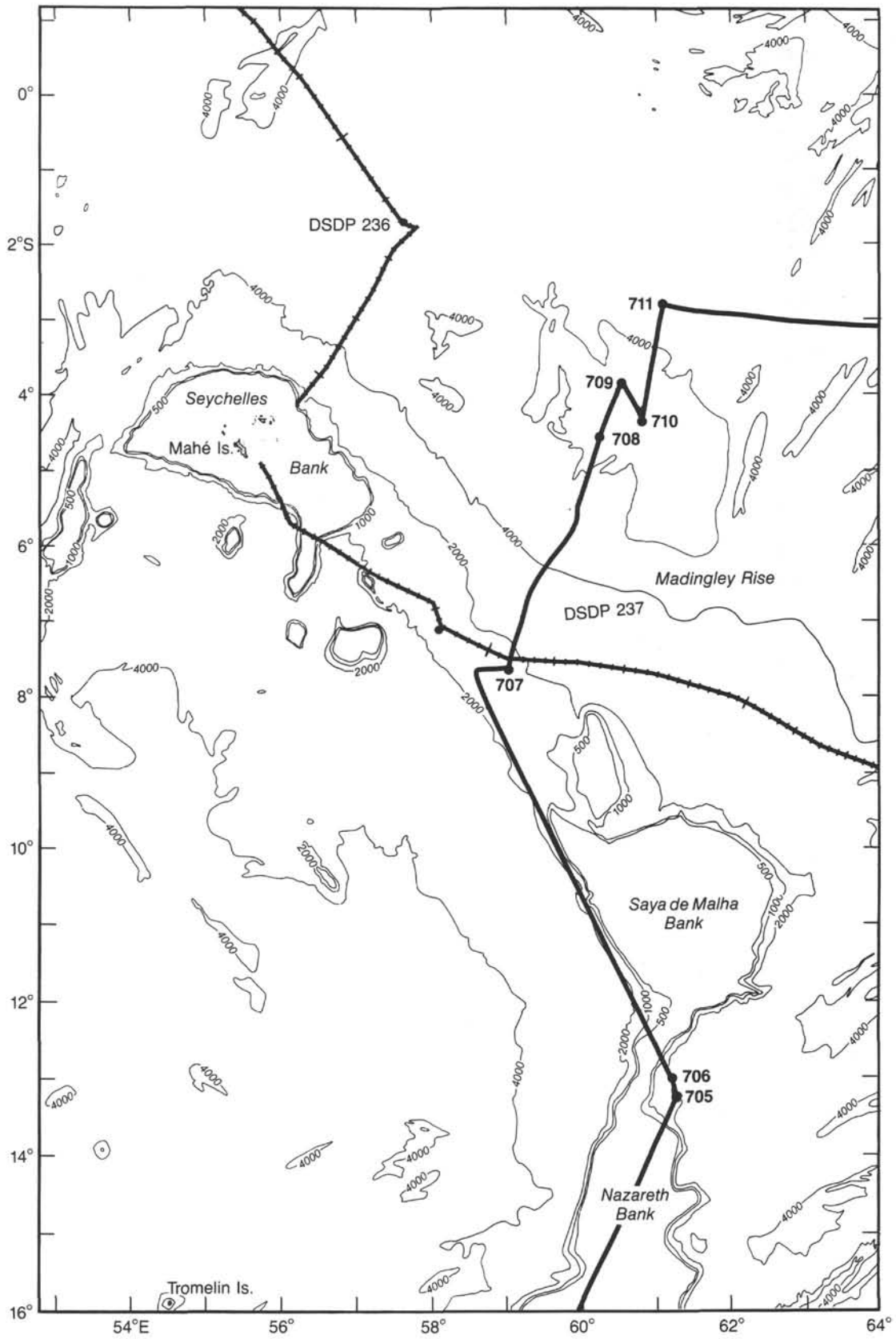


Figure 4. Expanded view of bathymetric features around the northern Mascarene Plateau and the location of Site 711 (after Fisher, Bunce, et al., 1974). Depth in meters. The Leg 115 track line of the *JOIDES Resolution* and the earlier track of the *Glomar Challenger* on Leg 24 are shown for reference.

OPERATIONS

Hole 711A

The recallable beacon was dropped at 0030 hr, 11 June 1987, to establish Site 711. The ship was in dynamic positioning (DP) mode at 0130, and the drill string was tripped in. The same APC/XCB bottom-hole assembly (BHA) used on earlier carbonate-depth transect sites was lowered to the seafloor, and the mud line established at 4428.2 m. The hole was advanced to 4532.7 m (104.5 mbsf) using the APC system, which recovered 95.1 m of core for a recovery rate of 91%. We deployed orientation instrumentation beginning with Cores 115-711A-4H through -11H. When the pull-out force reached 30,000 lb, we changed to the XCB system.

The hole was advanced to 4677.8 m (249.6 mbsf) using the XCB system, recovering 108.7 m of core for an XCB recovery rate of 80%. With our objectives met, the drill string was pulled clear of the mud line and the ship offset 10 m south to initiate Hole 711B. Total penetration was 249.7 mbsf to 4677.8 m with 203.9 m of core recovered for a total recovery rate of 81.7% (Table 1).

Hole 711B

The BHA was lowered to the seafloor, and the mud line established at 4429.7 m. The hole was cored with the APC 11 times to 4528 m (98.3 mbsf). Our objective for this hole was to core the top 100 m of sediments with the APC. When we met this objective, the drill string was tripped out and the transit to Site CB-1 (Chagos Bank) begun. Total penetration was 98.6 mbsf to 4528 m, with 89.25 m of core recovered for a total recovery rate of 90.8% (Table 1).

Site 711 to Site 712 (CB-1)

We made several attempts to recall the beacon, but the beacon would not respond. The same recallable beacon had been used since Site 706. With the drill string on board and everything secured, the 445-nmi transit to Site CB-1 (Chagos Bank) was begun at 1200 hr, 13 June 1987.

LITHOSTRATIGRAPHY

Introduction

Site 711, drilled in 4428.2 m of water, is the deepest site of the carbonate transect on the Madingley Rise. We drilled two holes at Site 711. In Hole 711A, we drilled a 250-m-thick sedimentary sequence. Hole 711B was then offset, and the upper 98.3 m of the sediment column was cored again in order to provide a complete Neogene sequence.

The sedimentary sequence at Site 711 is divided into four major lithologic units based on the composition of the sediment, mainly the different biogenic components and the carbonate content.

Unit I consists of an alternating sequence of clayey nannofossil ooze, radiolarian-bearing nannofossil clay, and nannofossil-bearing clay. It is characterized by alternating light and dark colors, and the carbonate content varies between 20% and 60%.

Unit II consists of three intervals with extremely low carbonate values, usually less than 10%, and is composed of clay and volcanic-glass-bearing clay. The three low carbonate levels are separated by two intervals with higher carbonate content, ranging between 10% and 40%, composed of nannofossil-bearing clay and nannofossil clay.

Unit III consists of a thick, carbonate-rich sedimentary sequence in which carbonate contents, with a few exceptions, range between 75% and 93%. The sediments are either clay-bearing nannofossil oozes and chalks or nannofossil oozes and chalks.

Table 1. Coring summary, Site 711.

Core no.	Date (June 1987)	Time	Depth (mbsf)	Cored (m)	Recovered (m)	Recovery (%)
115-711A-						
1H	11	1000	0-8.1	8.1	8.13	100.0
2H	11	1045	8.1-17.7	9.6	5.03	52.4
3H	11	1130	17.7-27.3	9.6	9.75	101.0
4H	11	1230	27.3-36.9	9.6	9.86	103.0
5H	11	1330	36.9-46.6	9.7	9.78	101.0
6H	11	1430	46.6-56.3	9.7	9.76	100.0
7H	11	1515	56.3-66.0	9.7	9.76	100.0
8H	11	1600	66.0-75.6	9.6	3.86	40.2
9H	11	1700	75.6-85.2	9.6	9.59	99.9
10H	11	1800	85.2-94.8	9.6	9.86	103.0
11H	11	1900	94.8-104.5	9.7	9.81	101.0
12X	11	2000	104.5-114.2	9.7	4.68	48.2
13X	11	2100	114.2-123.9	9.7	8.96	92.4
14X	11	2200	123.9-133.6	9.7	8.48	87.4
15X	11	2300	133.6-143.2	9.6	9.15	95.3
16X	12	0000	143.3-153.0	9.7	9.35	96.4
17X	12	0045	153.0-162.7	9.7	9.47	97.6
18X	12	0130	162.7-172.4	9.7	6.02	62.0
19X	12	0215	172.4-182.1	9.7	9.22	95.0
20X	12	0345	182.1-191.7	9.6	6.65	69.3
21X	12	0445	191.7-201.4	9.7	7.48	77.1
22X	12	0600	201.4-211.1	9.7	5.67	58.4
23X	12	0845	211.1-220.7	9.6	9.17	95.5
24X	12	0945	220.7-230.3	9.6	7.08	73.8
25X	12	1100	230.3-240.0	9.7	6.96	71.7
26X	12	1400	240.0-249.7	9.7	0.33	3.4
115-711B-						
1H	12	1700	0-2.1	2.1	2.28	108.0
2H	12	1800	2.1-11.7	9.6	9.59	99.9
3H	12	1845	11.7-21.4	9.7	9.77	101.0
4H	12	1945	21.4-31.0	9.6	9.48	98.8
5H	12	2030	31.0-40.7	9.7	9.91	102.0
6H	12	2115	40.7-50.3	9.6	9.16	95.4
7H	12	2215	50.3-60.0	9.7	5.21	53.7
8H	12	2300	60.0-69.6	9.6	9.59	99.9
9H	13	0000	69.6-79.3	9.4	8.40	89.3
10H	13	0045	79.3-88.9	9.6	6.32	65.8
11H	13	0300	88.9-98.6	9.7	9.54	98.3

Unit IV is characterized by the ubiquitous occurrence of radiolarians, comprising between 15% and 85% of the bulk sediment. The presence of clay, in addition to radiolarian-produced silica, increases the variability of the carbonate content (0%-85%). The sediments consist of clay- and radiolarian-bearing nannofossil chalk, sponge-spicule- and clay-bearing radiolarian ooze, clay-bearing radiolarian ooze, and some occasional chert.

The occurrence of pelagic turbidite layers is restricted, with some rare exceptions, to the top 100 m of Site 711. The turbidite layers, ranging in thickness from a few to a few tens of centimeters, are usually distinguishable by their white or light color and, in most cases, by the sharp color boundaries and coarser particle size of the bases compared with the underlying pelagic sediments. The upper boundaries are more gradational and are often difficult to locate precisely.

The transition from nannofossil ooze to nannofossil chalk occurs gradationally in Hole 711A over an interval of approximately 30 m. We observed the level where the sediments consist only of chalk 9 m above the Unit III/IV boundary; hence, it does not coincide precisely with our selected lithologic subdivision. The Unit III/IV boundary was based upon the disappearance (less than 10%) of radiolarians in Unit III.

Unit I: Cores 115-711A-1H and -2H (0-17.7 mbsf) and Cores 115-711B-1H and -2H (0-11.7 mbsf); Age: Pleistocene to late Pliocene.

Unit I consists of alternating very pale to pale brown (10YR 7/3, 8/3, and 6/3), light yellowish brown (10YR 6/4) clayey

nannofossil ooze, with yellowish brown, brown, grayish brown, and dark grayish brown (10YR 5/4, 5/3, 5/2, and 4/2) radiolarian-bearing nannofossil clay and nannofossil-bearing clay in both Holes 711A and 711B. All color contacts are gradational, and the extensive bioturbation creates color mottling. Carbonate contents in the clayey nannofossil oozes range between 40% and 60%, whereas the carbonate contents of the radiolarian- and nannofossil-bearing clays vary between 20% and 30%.

We counted several pelagic turbidite layers, ranging in thickness from 1 to 17 cm, in Unit I: four in Hole 711A and five in Hole 711B (Fig. 5). They consist of white (10YR 8/2), very pale brown (10YR 8/3, 7/3), to light brownish gray (10YR 6/2) foraminifer nannofossil ooze or nannofossil foraminifer ooze. Their light colors contrast with the darker intervening pelagic sediments. In addition, they usually display sharp basal contacts with faint graded bedding and gradational upper boundaries where bioturbation features are well developed. Carbonate contents in these turbidites are consistently higher than in the pelagic sediments. Sources of the turbidite material were probably located along the western slopes and crests of the Madingley Rise, reaching water depths as shallow as 3000 m, well above the current foraminifer lysocline.

Unit II: Core 115-711A-3H to Section 115-711A-8H-2, 50 cm (17.7–68.0 mbsf) and Core 115-711B-3H to Section 115-711B-8H-4, 20 cm (11.7–64.7 mbsf); Age: late Pliocene to early Miocene.

Unit II consists of three successive intervals of clay with low carbonate contents (0%–10%), separated by two intervals of higher carbonate contents (between 20% and 40%) in both Holes 711A and 711B. The upper low-carbonate interval consists of clay characterized by colors alternating between light yellowish brown, yellowish brown, and brown (10YR 6/4, 5/4, 5/3), and grayish brown, gray, and dark gray (10YR 5/2, 5/1, 4/1). The clay is moderately bioturbated throughout. The middle and lower low-carbonate intervals consist of dark brown, dark grayish brown, and grayish brown (10YR 3/2, 4/2, and 5/2) volcanic-glass-bearing clay. These core intervals are fairly homogeneous in appearance, with little evidence of bioturbation except for a few light yellowish brown (10YR 6/4) color patches, several centimeters in diameter. These patches have a similar sediment composition as the surrounding sediments (determined by smear slide observations) and are randomly scattered among the dark volcanic-glass-bearing clays. The origin of these lighter color patches is unknown; they could well be infilling of large burrows or they may be due to diagenetic reaction (see below). The two intervals of relatively higher carbonate content consist of very pale brown (10YR 7/3) and light yellowish to yellowish brown (10YR 6/4, 5/4), moderately bioturbated, nannofossil-bearing clay and nannofossil clay.

The stratigraphic distribution of the three low-carbonate intervals is shown in Figure 5. The lower interval occurs during the late early to early middle Miocene, the intermediate one during the late middle to early late Miocene, and the upper one during the late Miocene and early Pliocene.

Turbidite layers are scattered throughout Unit II. We counted 24 turbidite layers (13 clearly discernible turbidites and 11 possible turbidites) in Unit II of Hole 711A and 23 turbidite layers (15 clearly discernible turbidites and 8 possible turbidites) in Unit II of Hole 711B. Because of the light colors of the turbidite layers, white (N9, 10YR, 8/2), very pale brown (10YR 8/3, 7/3), and pale brown (10YR 6/3), which contrast with the dark to very dark colors of the intervening clays, turbidite layers can be separated easily from the pelagic sediments. Clearly discernible turbidites are those with a sharp base and slight graded bedding; possible turbidites are defined only by their contrasting colors and also by reference to the closest true turbidite layers.

Turbidite layers in Unit II of Holes 711A and 711B consist of clay-bearing nannofossil ooze, clay- and foraminifer-bearing nannofossil ooze, and in a few instances clay-bearing foraminifer nannofossil ooze. We analyzed carbonate content (70%) in only one case. There is little doubt, however, that the carbonate content of the turbidite layers is always much higher than the intervening pelagic sediment of Unit II. Particularly within the low-carbonate intervals, the few centimeters of pelagic clays just below the sharp base of the turbidite, as well as in some instances the few centimeters of pelagic clays just overlying the turbidites, are usually lighter in color than the intervening pelagic clays (Fig. 6). This color change may represent a diagenetic chemical front due to the steep carbonate gradient between the carbonate-rich turbidite sediment and the intervening low-carbonate pelagic clays. Finally, though the turbidite layers occur throughout Unit II, their frequency seems to be higher during the two higher carbonate intervals than during the three clayey intervals (Fig. 5).

Unit III: Sections 115-711A-8H-2, 50 cm, to 115-711A-19X-1, 125 cm (68.0–173.0 mbsf) and Sections 115-711B-8H-4, 20 cm, to 115-711A-11H, CC (64.7–98.3 mbsf); Age: early Miocene to late Eocene.

Unit III is fully represented in Hole 711A, whereas only the upper third of Unit III occurs in Hole 711B. Unit III consists of 105 m of carbonate-rich sediments, with carbonate contents between 75% and 93%. Planktonic and benthic foraminifers are totally absent or appear only in trace amounts. The carbonate consists almost entirely of nannofossils. Depending on the carbonate content, the sediments in Unit III can be either nannofossil oozes, clay-bearing nannofossil oozes, or clayey nannofossil oozes. The predominant lithology is clay-bearing nannofossil ooze, with carbonate contents between 80% and 90%. Unit III consists of light-colored sediments, including white (10YR 8/2, 2.5Y 8/2), very pale brown (10YR 8/3, 7/3, 7/2), pale yellow (2.5Y 7/4), and light gray (2.5Y 7/2) to light yellowish brown (2.5Y 6/4). The cores usually appear to be homogeneous and do not display clear evidence of bioturbation.

Toward the lower half of Unit III, the clay-bearing nannofossil ooze grades into a clay-bearing nannofossil chalk. The ooze-to-chalk transition occurs between Sections 115-711A-14X-5 and 115-711A-17X, CC (133.6–162.7 mbsf), a 30-m-long transition. Core 115-711A-18X and underlying cores in Hole 711A display clay-bearing nannofossil chalk only, with the exception of the radiolarian ooze in Cores 115-711A-19X and -20X.

Turbidite layers are seldom observed in Unit III and occur only within the top 30 m of the unit. They are much less frequent than in Units I and II and are quite difficult to distinguish from the light-colored intervening pelagic sediments. The monotony of Unit III is broken by two distinct levels of volcanic-ash particles disseminated within the surrounding pelagic sediments in Samples 115-711A-13X-4, 15–35 cm, and 115-711A-13X-5, 15–20 cm. They give a darker color to the sediments, mottled between a grayish brown (10YR 5/2) and a very pale brown (2.5Y 3/2). The sediments become a clay-bearing ash with up to 80% fresh, unaltered, sand-sized grains.

Unit IV: Sections 115-711A-19X-1, 125 cm, to 115-711A-26X, CC (173.0–249.6 mbsf); Age: late Eocene to middle Eocene.

The 76.6 m of Unit IV are characterized by the ubiquitous occurrence of radiolarians, which can make up to 85% of the bulk sediment, based on smear slide estimates. In a few instances, the presence of clays in addition to the radiolarians pushes the values of carbonate content to zero. The entire spectrum of the different lithologies in Unit IV ranges from (1) a very pale brown (10YR 8/3), clay-bearing nannofossil chalk (in this

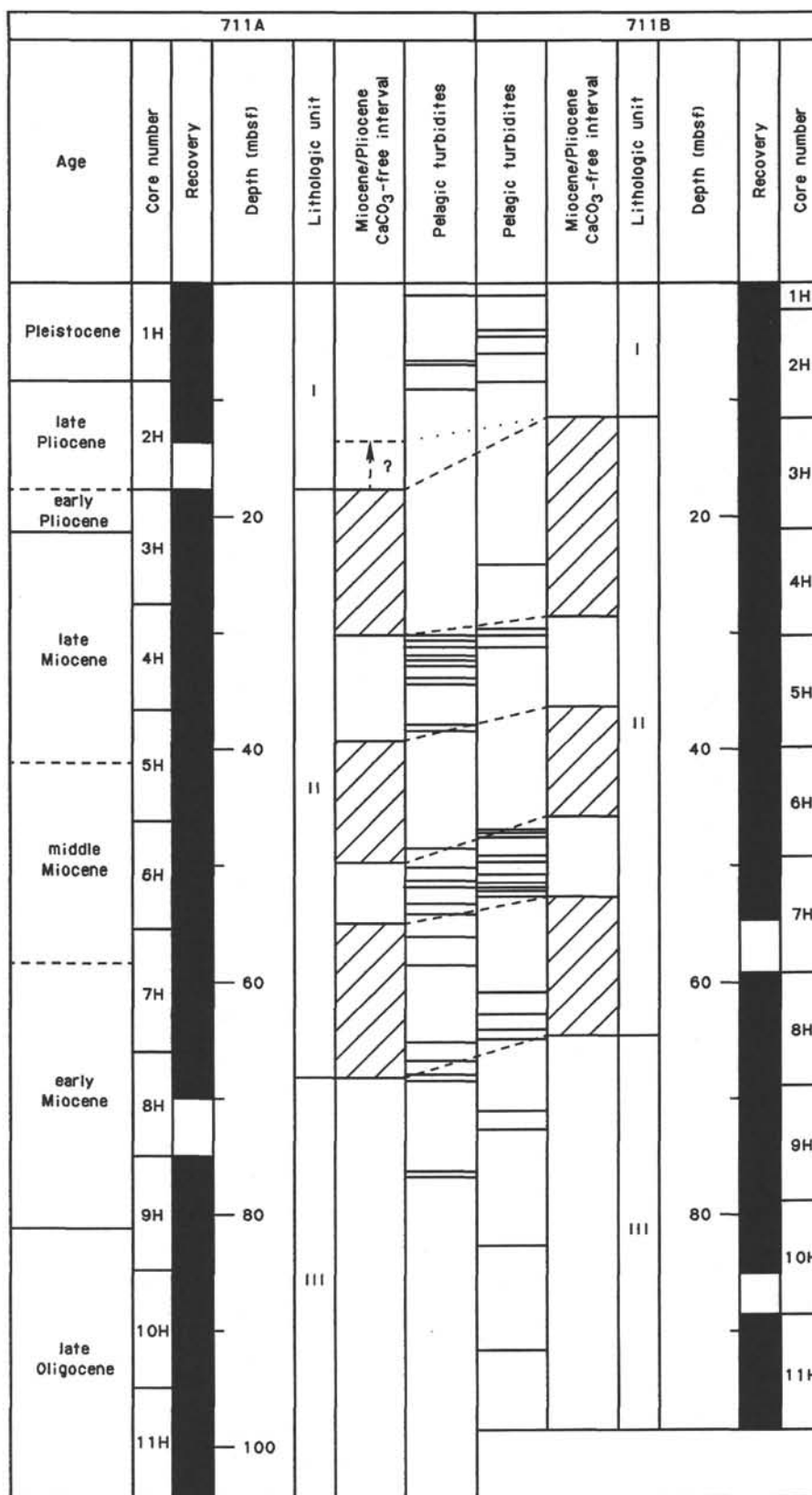


Figure 5. Correlation between the upper 100 m of Hole 711A (left) and the entire 98 m of Hole 711B (right). Stratigraphy is based on paleomagnetism, calcareous nannofossils, planktonic foraminifers, radiolarians, and diatoms (see "Biostratigraphy" and "Paleomagnetism" sections, this chapter). Interhole correlation of boundaries between lithologic units and Miocene/lower Pliocene low-carbonate intervals (diagonal lines) are shown. There is a more or less constant shift of several meters between Holes 711A and 711B. Two to three meters of Pleistocene seem to be missing in Hole 711B, although the mud line was recovered in Core 115-711B-1H. Note the high frequency of pelagic-turbidite occurrence in Unit II (shown as horizontal lines), especially concentrated within the two intervals of nannofossil-bearing clay and nannofossil clay separating the three low-carbonate intervals of Unit II.

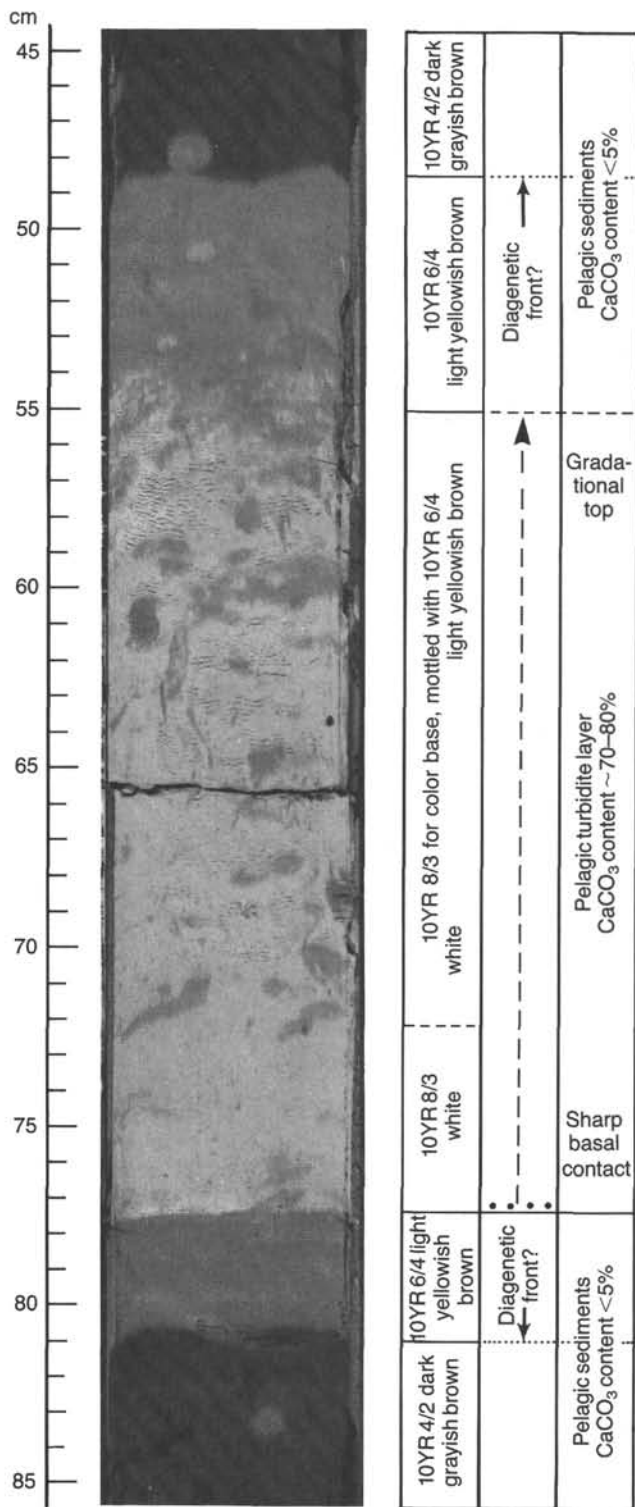


Figure 6. A pelagic-turbidite layer in the lower low-carbonate interval of Unit II (Miocene/lower Pliocene), with the sharp base of the turbidite layer at 77.5 cm and its gradational top around 55 cm (115-711B-8H-3, 45-85 cm). Note the possible diagenetic chemical front 3 cm below the sharp base of the turbidite layer, and 6 cm above its gradational top due to the steep carbonate gradient between the carbonate-rich (70%-80%) turbidite sediment and the intervening low-carbonate (less than 5%) pelagic clay.

particular case, radiolarians comprise less than 10% of the bulk sediment); (2) a pale brown to light yellowish brown (10YR 8/3, 6/3, 6/4) clay- and radiolarian-bearing nannofossil chalk; (3) a darker grayish brown (10YR 5/2), clay-bearing radiolarian nannofossil chalk; (4) a brownish yellow, yellow-orange (10YR 6/6, 7/6), to very dark gray (10YR 3/1) clay-bearing radiolarian ooze; and, finally, (5) a dark yellowish brown to yellowish brown (10YR 4/6, 4/4, 5/4) chert (radiolarite). The lower half of Unit IV (Cores 115-711A-22X through -25X) consists mainly of clay- and radiolarian-bearing nannofossil chalk and clay-bearing radiolarian-nannofossil chalk. Core 115-711A-26X recovered only pebble-sized pale brown and yellowish brown (10YR 8/4, 5/4) chert pieces in the core catcher.

The upper half of Unit IV is richer in radiolarians than its lower part. Two intervals, 100-150 cm thick, of almost pure, brownish yellow-orange (10YR 6/6) radiolarian ooze, characterized by its sugary texture, occur in Cores 115-711A-19X and -20X. At these levels, carbonate contents reach zero. These levels are surrounded by very dark grayish brown (10YR 3/2), manganese-oxide(?) stained, clay-bearing radiolarian ooze, possibly related to alteration of volcanic ashes. Within the pure clay-bearing radiolarian ooze levels in Core 115-711A-20X, we observed two 5-cm-thick chert (radiolarite) layers (Samples 115-711A-20X-3, 0-5 cm, and 115-711A-20X-5, 30-35 cm). Bioturbation occurs throughout Unit IV. When Unit IV is considered as a whole, the proportion of radiolarians increases toward the upper half of Unit IV, to reach two maxima in its upper part. Radiolarian proportions decrease drastically at the Unit III/IV boundary. Radiolarians comprise less than 10% of the sediment in Unit III.

Summary

Site 711 displays a major difference between the Paleogene (Units III and IV) carbonate-rich sediments (averaging 75%-80%) and the Neogene carbonate-poor sediments (averaging 30%). In spite of the high carbonate values in Units III and IV, planktonic and benthic foraminifers are usually absent or comprise only a minor percentage of the bulk sediment. This observation might indicate either a low production of foraminifers or a drastic dissolution of their tests at the seafloor. Either as a major or minor constituent, radiolarians (always in proportions larger than 10%) occur throughout the middle Eocene. The Miocene/lower Pliocene interval, Unit II, is characterized by the lowest carbonate content values of the past 50 m.y. During the three Miocene/early Pliocene low-carbonate intervals, Site 711 was apparently located near or well below the CCD. High carbonate content values during that period of time are observed only within a few pelagic turbidite layers due to the importation of carbonate by gravity flows from surrounding elevated areas.

BIOSTRATIGRAPHY

Introduction

The two holes drilled at Site 711 penetrated a 250-m-thick sedimentary sequence that is characterized by strong carbonate dissolution throughout the entire Neogene and upper Paleogene.

The sequence, apparently continuous from the Pleistocene through the uppermost lower Eocene, consists from top to bottom of (1) 17.7 m (0-17.7 mbsf) of alternating clayey nannofossil ooze and radiolarian-bearing nannofossil clay of Pleistocene-Pliocene age; (2) 50.3 m (17.7-68.0 mbsf) of low-carbonate clays of late Pliocene to early Miocene age; and (3) 181.6 m (68.0-249.6 mbsf) of carbonate-rich sediments of earliest Miocene to latest early Eocene age.

Calcareous nannofossils have undergone strong dissolution in the Neogene section, and certain Miocene intervals are en-

tirely barren of calcareous nannofossils. The fossils are generally abundant and well preserved in the Paleogene.

Planktonic foraminifers are almost entirely absent in the highly dissolved Neogene, Oligocene, and upper Eocene sediments, whereas lower and middle Eocene assemblages are moderately well preserved.

Benthic foraminifers are present as dissolution residues in the Neogene section and were rarely found in the Paleogene.

Radiolarians are present and moderately well to well preserved in the Quaternary and in the lower Oligocene through middle Eocene sequence. Elsewhere in the section, radiolarians are absent or are too poorly preserved to be identified.

Diatoms are rare and poorly preserved in the Pleistocene. A few specimens of early Oligocene and late Eocene ages occur in the Paleogene section.

A biostratigraphic summary for Site 711 is presented in Figure 7.

Calcareous Nannofossils

Middle Eocene to Pleistocene calcareous nannofossils were recovered at Hole 711A. Nannofossils are generally abundant and well preserved in the Paleogene, whereas they are impoverished and strongly dissolved in the Neogene sequence. Many of the analyzed Miocene and lower Pliocene samples are barren of calcareous nannofossils, especially in the later early and late middle Miocene and in the Pliocene. These barren intervals correlate with the time intervals of maximum dissolution or hiatuses in Site 709 and Site 710.

Pleistocene

Pleistocene nannofossils underwent strong to moderate dissolution, although we detected no effects of overgrowth. Because of the poor state of preservation, some evolutionary events were difficult to identify.

Abundant *Emiliania huxleyi* occur above Sample 115-711A-1H-1, 100 cm, and we placed the base of Zone CN15 between this sample and Sample 115-711A-1H-2, 40 cm. Because of the severe dissolution, the presence or absence of *Pseudoemiliania lacunosa* could not be confirmed in Sample 115-711A-1H-3, 40 cm, and the last occurrence of *P. lacunosa* (base of Subzone CN14b) was tentatively placed between Samples 115-711A-1H-2, 110 cm, and 115-711A-1H-3, 110 cm.

We did not identify the top of the small *Gephyrocapsa* Zone in Core 115-711A-1H. Sample 115-711A-2H-1, 40–41 cm, though heavily contaminated with reworked forms, yielded an assemblage referable to the lower part of Subzone CN14a. The Pliocene/Pleistocene boundary can be placed between this sample and the underlying Sample 115-711A-2H-1, 138 cm.

Pliocene

The Miocene/Pliocene boundary is difficult to locate due to extensive dissolution, but it probably occurs within Core 115-711A-3H. In Sample 115-711A-3H-2, 60 cm, *Ceratolithus acutus* and *Discoaster quinqueramus* co-occur. The ranges of these two species are not known to overlap, and their respective first (FO) and last (LO) occurrence are used to locate an approximate Miocene/Pliocene boundary (Berggren et al., 1985). Thus, the observed specimens of *D. quinqueramus* are probably reworked. Since the FO of *C. acutus* is close to the Miocene/Pliocene boundary, this stage boundary was tentatively located at about 21.3 mbsf in the sample mentioned above. The Pliocene Epoch is therefore represented by only about 12 m of sediments.

Core 115-711A-2H yielded upper Pliocene assemblages. The upper part of Core 115-711A-3H (above the FO of *C. acutus*) is barren of nannofossils, and the lower Pliocene Zones CN10c and CN11 were not recognized.

Miocene

We placed the Oligocene/Miocene boundary at approximately 78–79 mbsf on the basis of the LOs of *Sphenolithus ciproensis* and *Dictyococcites bisectus*. The Miocene Epoch is thus represented by approximately 55 m of sediments. *Discoaster quinqueramus*, the marker for the base of the upper Miocene Zone CN9, was recorded at the top of Core 115-711A-5H (37.5 mbsf). Calcareous nannofossils are strongly dissolved in the upper Miocene (Zone CN9), with many samples barren. Within the fossiliferous samples, only the most solution-resistant forms, such as *Discoaster*, *Amaurolithus*, and *Triquetrorhabdulus* were found. These groups are easily identified due to the lack of overgrowth, which usually hampers the species identification of these genera.

In Sample 115-711A-4H-3, 130 cm, the first *Amaurolithus primus* was identified, thus allowing the placement of the boundary between Subzones CN9a and CN9b at this level.

All samples examined from Section 115-711A-5H-2 to the top part of Core 115-711A-6H are barren; thus, no zonal assignment is possible for this interval. The next fossiliferous sample is Sample 115-711A-6H-2, 80 cm, which contains *Sphenolithus heteromorphus*, indicative of Zones CN3–CN4. Therefore, the late Miocene Zones CN6–CN7 were not recognized.

We observed the FO of *S. heteromorphus* (base of Zone CN3) in Sample 115-711A-7H-1, 113 cm. Between the latter sample and Sample 115-711A-7H-5, 125 cm, sediments are barren of nannofossils. Section 115-711A-7H-6 and Core 115-711A-8H, in which *Triquetrorhabdulus carinatus* occurs together with *Discoaster druggii*, belong to Zone NN2 (CN1c).

The preservation varies in the basal Miocene Zone CN1 between good and poor, with evidence of dissolution.

Oligocene

Well- to moderately well-preserved Oligocene nannofossils were found in Cores 115-711A-9H through -17X. Heavy reworking is evident in many samples throughout the sequence, but some samples are relatively free of reworked specimens. Sections 115-711A-9H-2 and 115-711A-9H-3 are contaminated by reworked Oligocene forms, but underlying Sections 115-711A-9H-4 and 115-711A-9H-5 yielded no Oligocene sphenoliths. The top of the Oligocene sequence, therefore, was placed between Samples 115-711A-9H-5, 40–41 cm, and 115-711A-9H-6, 40–41 cm.

We assigned the interval between Sections 115-711A-9H-6, 40–41 cm, and 115-711A-10H-7, 40–41 cm, to the uppermost Oligocene Subzone CP19b. Sections 115-711A-10H, CC, and 115-711A-11H-1 contain many reworked fossils, and the LO of *Sphenolithus distentus* (base of Subzone CP19b) was tentatively placed between Samples 115-711A-10H-7, 40–41 cm, and 115-711A-11H-2, 40–41 cm. The FO of *Sphenolithus ciproensis* (base of Subzone CP19a) was recognized between Samples 115-711A-12X-1, 40–41 cm, and 115-711A-12X-2, 40–41 cm.

As we observed in previous sites of Leg 115, *S. distentus* occurs in two separate intervals. It is generally common in Cores 115-711A-11H through -13X, is absent in Core 115-711A-14X and in the upper section of Core 115-711A-15X, and is present again in the interval between Sections 115-711A-15X-6 and 115-711A-16X-6.

Many samples taken from Cores 115-711A-12X through -17X are heavily contaminated by reworked Eocene and lower Oligocene forms, making difficult the determination of the lower Oligocene zones, which are based upon LOs of key species. We tentatively assigned the interval between Sections 115-711A-12X-2 through 115-711A-16X-4 to lower Oligocene Zone CP18 to Subzone CP16b.

Sample 115-711A-17X-2, 40–41 cm, contains no Eocene discoasters. The underlying Sample 115-711A-17X-3, 40–41 cm, is

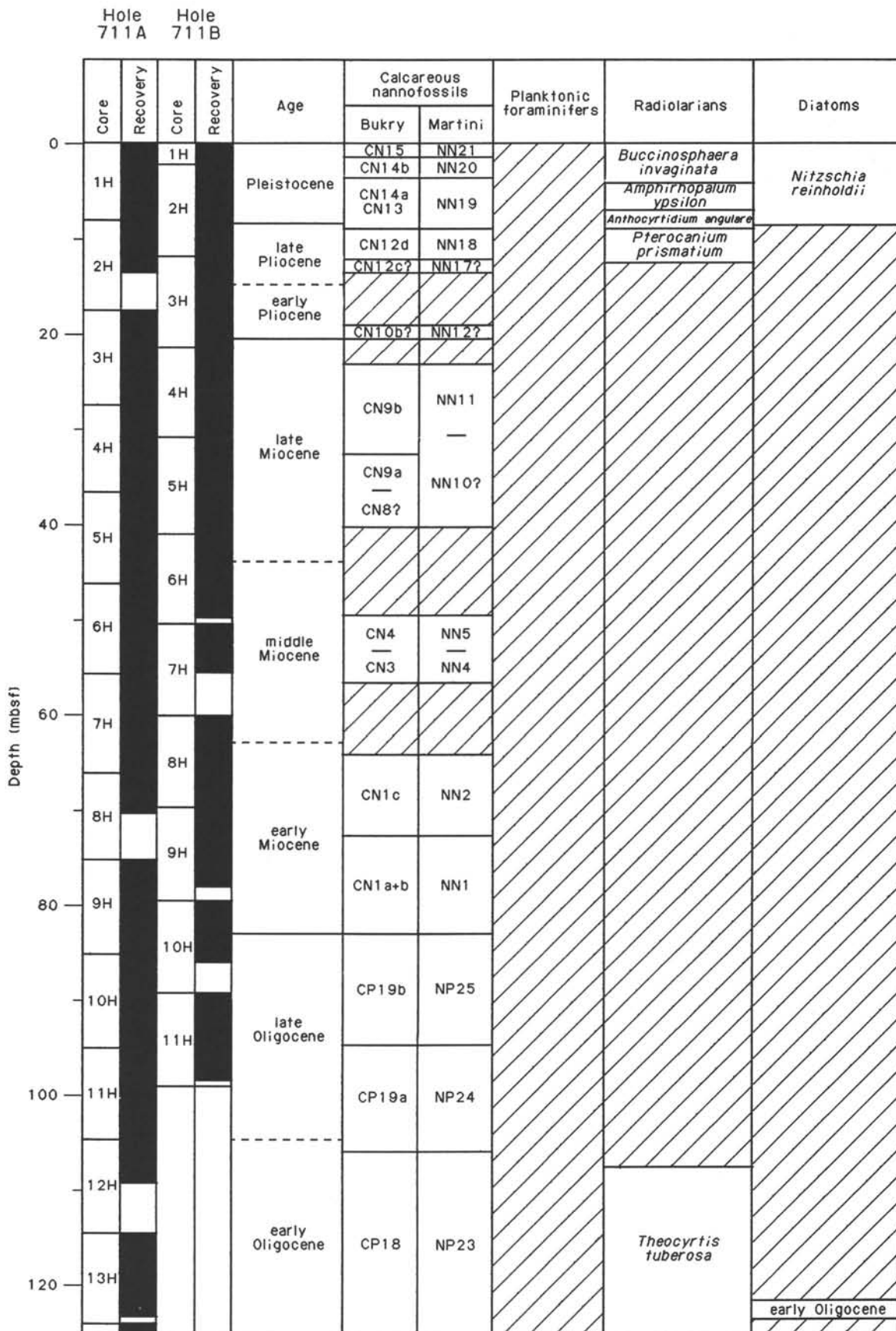


Figure 7. Biostratigraphic summary for Site 711. Black bars represent recovery in Hole 711A.

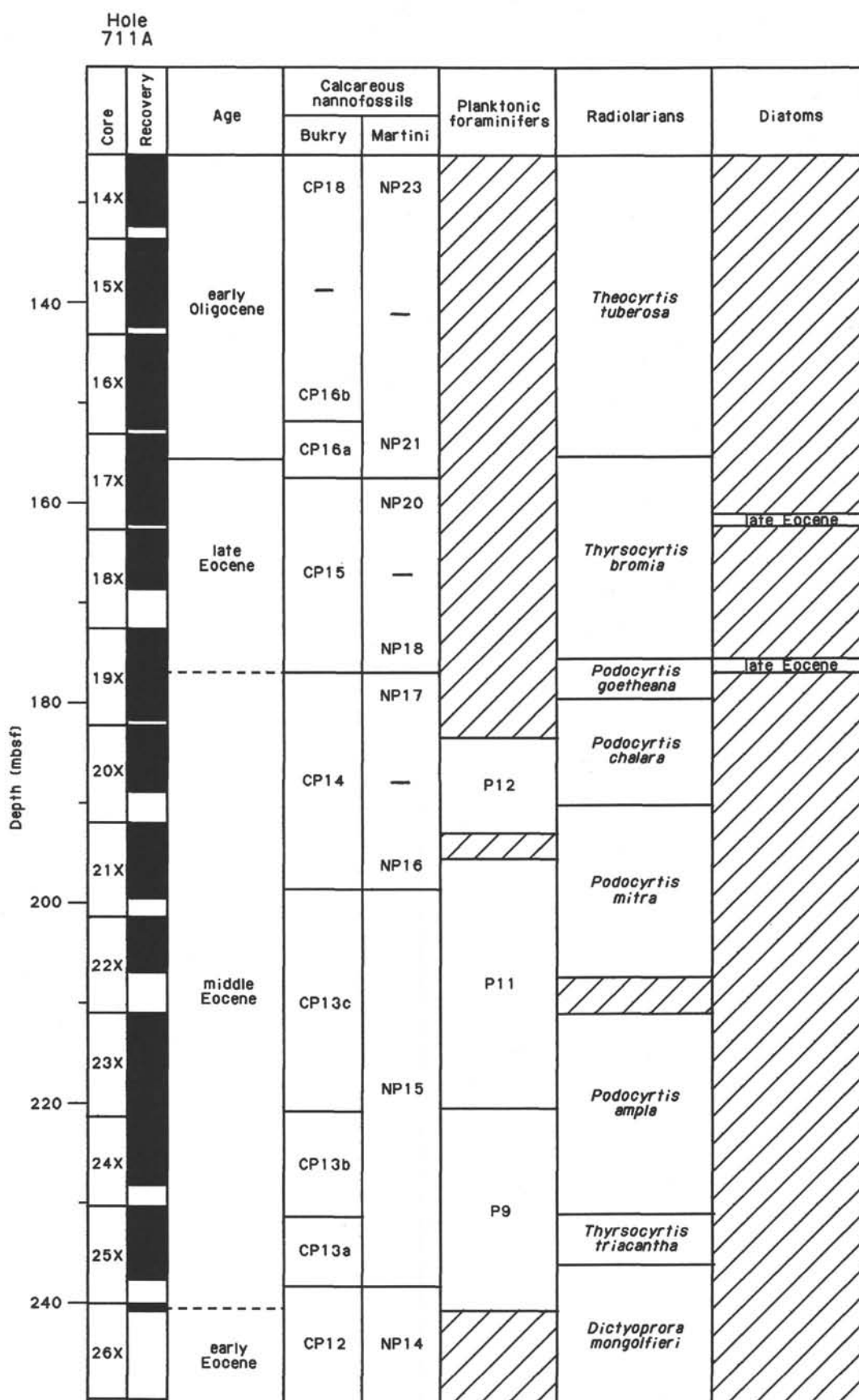


Figure 7 (continued).

contaminated by Eocene discoasters, including rare *Discoaster barbadiensis* and *Discoaster saipanensis*. Since the next underlying Sample 115-711A-17-3, 40–41 cm, yielded only *D. saipanensis*, which is the species having the latest LO age among Eocene discoasters, but no *D. barbadiensis*, the base of the lowest Oligocene Zone CP16 is likely to be located within Section 115-711A-17X-3. At Sample 115-711A-16X-6, 40–41 cm, the top of the acme of *Ericsonia subdisticha* was detected. We assigned the interval between this sample and Sample 115-711A-17X-3, 100 cm, to the lowest Oligocene Subzone CP16a. Rare specimens of *Isthmolithus recurvus* were observed in some samples of this subzone.

Eocene

Eocene assemblages occur from Section 115-711A-17X-4 through the bottom of the hole. The preservation of nannofossils is similar to that found in the overlying Oligocene sequence, but reworking is much less severe in the Eocene sequence.

The LO of *Chiasmolithus grandis* (base of CP15) was recognized in Sample 115-711A-19X-4, 38–39 cm, and the interval between Sections 115-711A-17X-4 and 115-711A-19X-3 was assigned to the uppermost Eocene Zone CP15. Overgrown specimens of rare *I. recurvus* were observed in some samples taken from the upper part of this sequence. Because of its rarity, however, the FO of *I. recurvus*, which defines the base of Subzone CP15b, was not determined by this preliminary investigation. The LO of *Criboecium reticulatum*, observed in Sample 115-711A-17X-5, 40–41 cm, precedes that of *D. barbadiensis*, which was recognized in Sample 115-711A-17X-4, 100 cm. Large specimens of *C. reticulatum* are the most conspicuous member of the CP15 flora.

The LO of *Chiasmolithus solitus* (base of Subzone CP14b) and the FO of *Reticulofenestra umbilica* (base of Subzone CP14a) were observed in Samples 115-711A-21X-5, 40–41 cm, and 115-711A-21X-5, 75 cm, respectively. The unusually thick CP14b sequence (from Sections 115-711A-19X-4 to 115-711A-21X-4) can be compared with the very thin CP14a sequence, which is represented only by Section 115-711A-19X-3. The relative thicknesses of these two subzones in Hole 711A are identical to those observed at Sites 707 and 709.

The interval between Sections 115-711A-21X, CC, and 115-711A-25X, CC, was assigned to the middle Eocene Zone CP13. Although *Nannotetrina alata* is rare, small *Nannotetrina* spp. commonly occur in this interval. The consistent occurrence of the large placolith *Cruciplacolithus staurion* is noteworthy in this assemblage. We observed *Chiasmolithus gigas*, whose range defines Subzone CP13b, in the interval from Sections 115-711A-21X, CC, to 115-711A-25X-1.

The last core (Core 115-711A-26X) recovered only 33 cm of sediment in the core catcher. Although most of the recovered material consists of chert, a small piece of calcareous siltstone and some soft sediment was found in the core catcher. The siltstone yielded abundant *Discoaster sublodoensis*, common *Rhabdosphaera inflata*, and *Discoaster lodoensis*. We assigned this assemblage to the lower middle Eocene Subzone CP12b. The soft sediment yielded an assemblage consisting of abundant *D. lodoensis*, common *Discoaster kuepperi*, *Toweius? gammation*, and a few *D. sublodoensis*, but no *R. inflata*. This assemblage is referred to the upper lower Eocene Subzone CP12a (52.0–52.6 Ma). Hole 711A thus ended in sediment of latest early Eocene age.

Planktonic Foraminifers

Paleogene planktonic foraminifers were found in only one core catcher of Oligocene age (Section 115-711A-10H, CC) and in upper lower to middle Eocene radiolarian-rich coarse fractions at the bottom of the hole (Sections 115-711A-20X, CC, to

115-711A-25X, CC). Site 711 apparently lay well below the foraminiferal lysocline through most of the Oligocene, the upper Eocene, and the upper middle Eocene. Only the Eocene planktonic foraminifers are considered to be in place.

Oligocene planktonic foraminifers consist of size-sorted, juvenile planktonic foraminifers and fine-fraction specimens dominated by *Streptochilus cubensis* and *Pseudohastigerina barbadoensis*, in a matrix of fine-fraction radiolarians and spicules. This fauna must be older than early Oligocene Zone P19. Section 115-711A-10H, CC, is considered a turbidite because it co-occurs with a mixed nannofossil assemblage that we can assign to late Oligocene Zone NP25.

Early to middle Eocene planktonic foraminifers become diverse and moderately well preserved, though they are beginning to recrystallize in Sections 115-711A-20X, CC, through 115-711A-25X, CC. The best preservation is seen in late middle Eocene Section 115-711A-24X, CC, where the residues consist of ~85% radiolarians and 15% planktonic foraminifers. Samples were assigned to the following zones:

1. Middle Eocene Zone P12 (Section 115-711A-20X, CC): on the presence of *Turborotalia pomeroli*, but the absence of *Morozovella aragonensis* and *Orbulinoides beckmanni*.
2. Middle Eocene Zone P11 (Sections 115-711A-21X, CC, through 115-711A-23X, CC): on the overlap of *M. aragonensis* and *Globigerinatheka mexicana* throughout the interval.
3. Upper lower Eocene Zone P9 (Sections 115-711A-24X, CC, through 115-711A-25X, CC): by the presence of *Turborotalia frontosa*, but the lack of any hantkeninids.

Benthic Foraminifers

Dissolution residues of benthic foraminifers were found in some of the Neogene core catchers from Site 711, but they were rarely found in Paleogene age samples. These faunas resembled the ones from Site 710 that occurred in the most dissolved samples. They were low in diversity, and small-sized individuals dominated below the Pleistocene.

Neogene

Each core-catcher fauna was different and demonstrated a different degree of dissolution. No benthic foraminifers were found in Sections 115-711A-2H, CC, 115-711A-3H, CC, 115-711A-5H, CC, or 115-711A-6H, CC, which suggests that at these times the site lay well below the CCD. As at Site 710, as dissolution diminished, new genera and species occurred in faunas in a predictable order, as follows:

1. Most dissolved (Sections 115-711A-1H, CC, and 115-711A-9H, CC): *Nuttalides umbonifera*, *Epistominella exigua*, juvenile *Globocassidulina subglobosa*, gyrogoninids, smooth lagenids, and three pullenids (*Pullenia quinqueloba*, *P. quadri-loba*, and *P. bulloides*). *Nuttalides umbonifera* dominated these faunas.
2. Less dissolved (Section 115-711A-4H, CC): add melonids, smooth planulinids, laticarininids, pleurostomellids, smooth cibicides, smooth *Orthomorphina*, and then the flat cassidulinid, *Cassidulina crassa*.
3. Slightly less dissolved (Section 115-711A-8H, CC): add striate chrysalogonium pieces, vulvulinids, *Eggerella bradyi*, ornamented and porous planulinids, textularids, and spinose stilostomellids such as *Stilostomella subspinosa*.

Paleogene

Benthic foraminifers were infrequently found in Oligocene samples, several of which came from turbidite layers. In upper Eocene coarse fractions, consisting primarily of radiolarians and pieces of micritized carbonate, we found an occasional benthic specimen. By the middle Eocene, planktonic foraminifers be-

came abundant in residues composed largely of radiolarians, but only one or two benthic specimens were found in each sample.

Oligocene Section 115-711A-10H, CC, contained size-sorted radiolarians, small spicules, and juvenile planktonic foraminifers. Benthic specimens were absent.

In Section 115-711A-11H, CC, preservation improved and faunas contained species from all three faunas listed above. In the Oligocene, however, the ornamented heterolepid, *Heterolepa grimsdalei*, occurs in most dissolution residues.

Oligocene and upper Eocene Sections 115-711A-12X, CC, through 115-711A-19X, CC, consisted mostly of radiolarians and occasional benthic specimens of *Oridorsalis umbonatus*, *Nuttalides truempyi*, or a cibicidid. In the middle Eocene radiolarian-planktonic foraminifer residues, only a few specimens of *N. truempyi*, *S. subspinosa*, and *Anomalinoides acuta* were observed.

Radiolarians

We examined radiolarian assemblages in four samples per core in Hole 711A (Sample 115-711A-1H-2, 70 cm, through Section 115-711A-25X, CC). Radiolarians are sufficiently well preserved to allow zonal age assignments in two stratigraphic intervals of Hole 711A: the Pleistocene and latest Pliocene, and the lower Oligocene through middle Eocene. Elsewhere at this site, radiolarians are absent entirely or are too poorly preserved to identify.

Sample 115-711A-1H-2, 70 cm, through Section 115-711A-1H, CC, are of Pleistocene age, associated with the *Amphirhopalum ypsilon* and *Anthocyrtdium angulare* Zones. Diagnostic taxa include *Anthocyrtdium angulare*, *A. ophirensis*, *A. michelinae*, *Theocorythium trachelium*, and *Amphirhopalum ypsilon*. Sample 115-711A-2H-2, 70 cm, is of late Pliocene age, associated with the *Pterocanium prismatium* Zone. Section 115-711A-2H, CC, through Sample 115-711A-12H-2, 70 cm (17.7–106.7 mbsf), are barren of radiolarians.

We assigned Sections 115-711A-12X, CC, through 115-711A-16X, CC (114.2–153.0 mbsf), to the *Theocyrtis tuberosa* Zone of early Oligocene age. Radiolarians are few and moderately preserved at the top of this interval, and preservation improves downward. Diagnostic Oligocene taxa include *Dorcadospyrus triceros*, *D. circulus*, *D. papilio*, *D. spinosa*, *Dictyoprora pirum*, *Artophormis gracilis*, and *T. tuberosa*. In many samples examined from this interval, however, reworked Eocene taxa are present in varying proportions, often exceeding 90% of the total radiolarian assemblage. This is especially true of core-catcher samples, and not of samples examined between the core catchers. Reworking in this stratigraphic interval may be summarized as shown in Table 2.

Table 2. Reworked radiolarians in the Oligocene stratigraphic interval, Hole 711A.

Sample interval (cm)	Radiolarian abundance ^a	Radiolarian preservation ^a	Zone	Reworked Eocene taxa (%)
115-711A-				
12X, CC	F	M	<i>Theocyrtis tuberosa</i>	20%
13X-4, 70	F	P	<i>T. tuberosa</i>	none
13X, CC	F	M	<i>T. tuberosa</i>	95%
14X-4, 70	R	VP	<i>T. tuberosa</i> (?)	none
14X, CC	F	M	<i>T. tuberosa</i>	none
15X-4, 70	F	P	<i>T. tuberosa</i>	none
15X, CC	F	M	Eocene, mixed	100%
16X-4, 70	F	P	<i>T. tuberosa</i>	none
16X, CC	C	G	<i>T. tuberosa</i>	none
17X-4, 70	C	G	<i>Thyrsoyrtis bromia</i>	—
17X, CC	C	G	<i>T. bromia</i>	—

^a See "Biostratigraphy" section, "Explanatory Notes," this volume, for the meaning of abbreviations.

Radiolarian assemblages throughout the late and middle Eocene intervals of this site are common and well preserved. Samples 115-711A-17X-4, 70–75 cm, through 115-711A-19X-2, 70 cm, are assigned to the *Thyrsoyrtis bromia* Zone of late Eocene age. Diagnostic radiolarian taxa in these two cores include *Cryptoprora ornata*, *Dictyoprora mongolfieri*, *D. pirum*, *D. armadillo*, *Lithocyclus aristotelis*, *Carpocanistrum azyx*, *Thyrsoyrtis bromia*, *T. tetracantha*, and *Calocyclus turris*.

Sample 115-711A-19X-4, 70 cm, is assigned to the *Podocyrtis goetheana* Zone of late Eocene age. Diagnostic taxa include *Calocyclus hispida*, *Thyrsoyrtis triacantha*, and *P. goetheana*.

We assigned Samples 115-711A-19X-6, 70 cm, through 115-711A-20X-4, 70 cm, to the *Podocyrtis chalara* Zone of middle Eocene age. Diagnostic taxa include *Calocyclus hispida*, *Thyrsoyrtis tetracantha*, *T. rhizodon*, *Podocyrtis chalara*, and *P. papalis*.

Section 115-711A-20X, CC, through Sample 115-711A-22X-4, 70 cm, may be assigned to the *Podocyrtis mitra* Zone of middle Eocene age. Diagnostic taxa include *P. mitra*, *Calocyclus hispida*, *Lithocyclus ocellus*, *Thyrsoyrtis triacantha*, and *Eusyringium fistuligerum*.

We assigned Sections 115-711A-22X, CC, through 115-711A-24X, CC, to the *Podocyrtis ampla* Zone of middle Eocene age. Diagnostic taxa include *Podocyrtis fasciolata*, *P. helenae*, *P. papalis*, *Dictyoprora mongolfieri*, *Eusyringium lagena*, *Calocyclus castum*, *Podocyrtis sinuosa*, and *Phormocyrtis striata striata*.

Samples 115-711A-25X-2, 70 cm, through 115-711A-25X-4, 70 cm, may be assigned to the *Thyrsoyrtis triacantha* Zone of middle Eocene age. Diagnostic taxa include *Podocyrtis sinuosa*, *Thyrsoyrtis triacantha*, and *Theocotyle venezuelensis*.

The *Dictyoprora mongolfieri* Zone of middle Eocene age occurs in Section 115-711A-25X, CC. Diagnostic taxa include *Podocyrtis sinuosa*, *P. diamesa*, *Thyrsoyrtis hirsuta*, and *Lamp-tonium fabaeforme fabaeforme*. *Thyrsoyrtis triacantha* s.s. is notably absent, and *Dictyoprora mongolfieri* is present.

Diatoms

The recovered sections of Site 711 are almost barren of diatoms. Only a few poorly preserved diatoms of late Pliocene–early Pleistocene age are present. Traces of diatom valves are further noted in the core-catcher samples of late Eocene and early Oligocene ages in Hole 711A.

Neogene

The Neogene of Site 711 gave a poor record of diatom events. Diatoms are present only in Sections 115-711A-1H, CC, and 115-711B-1H, CC. The silicoflagellate *Mesocena quadrangula* is recorded together with *Pseudoenotia doliolus*, which places these samples in the upper part of the *Nitzschia reinholdii* Zone.

The pre-Pleistocene section of the two holes is entirely depleted of opaline silica, except for a few radiolarian fragments in the core-catcher samples of late Miocene age.

Paleogene

The Paleogene section of Hole 711A has a high content of opaline silica. The siliceous microfossil assemblages are, however, totally dominated by radiolarians. Traces of presumably early Oligocene diatoms are found in Section 115-711A-13X, CC, and late Eocene diatom species of the genus *Hemiaulus* occur in upper Eocene Section 115-711A-17X, CC, and Sample 115-711A-19X-2, 79–80 cm.

PALEOMAGNETICS

Introduction

Paleomagnetic measurements of the sediments from Site 711 provide magnetostratigraphic data spanning part of the late Oli-

ocene, as well as much of the late Miocene to Pleistocene sections. In addition, we tentatively identified a reversal sequence from the highly compressed middle Miocene section in one core from Hole 711B. As with the results from Site 710, problems with the orienting device (see "Paleomagnetism" section, "Explanatory Notes" chapter, this volume) and with the core-barrel remagnetization effect (see "Paleomagnetism" section, "Site 709" chapter, this volume) complicate the interpretation of the magnetostratigraphy.

Results

All 22 APC cores recovered from Holes 711A and 711B were measured with the pass-through cryogenic magnetometer system before and after 5-mT demagnetization treatment. At least one discrete sample from each section was also analyzed with progressive alternating-field (AF) demagnetization. We identified 79 reversal boundaries in the two holes (Table 3). The pass-through declination log and a preliminary interpretation of polarity stratigraphy is shown in Figure 8. Generally, 180° shifts in declination have been indicated as magnetozone boundaries; however, many apparently spurious shifts occur. We have not interpreted these as indications of polarity reversals. As with the results from Site 710 (see "Paleomagnetism" section, "Site 710" chapter, this volume), inclination shifts at reversal boundaries are generally not well recovered by the pass-through magnetometer because the small inclination changes at this low-latitude site are usually masked by remagnetization effects. Nevertheless, the results of discrete sample analysis often determine the correct polarity sense.

Discussion

The paleomagnetic results, particularly those from Hole 711B, appear to show a nearly continuous reversal record in the uppermost four cores. We can easily correlate this reversal sequence with the latest Miocene to Recent portion of the magnetic polarity time scale. It is also consistent with the available biostratigraphic data (see "Biostratigraphy" section, this chapter).

Correlation of intervals of the relatively compressed early and middle Miocene section with the polarity time scale (shown in Fig. 8) is more problematic, as the paleomagnetic data covering this interval appear much less reliable. Nevertheless, the results from Core 115-711B-6H appear to show several distinct chronozones. The identification of the chron boundaries in this core agrees with the available biostratigraphy (see "Biostratigraphy" section, this chapter); however, these magnetostratigraphic correlations are considered only tentative.

We can correlate more easily the higher quality data from cores of late Oligocene age with the polarity time scale. In particular, Cores 115-711A-10H, 115-711A-11H, and 115-711B-11H show a clear reversal sequence which can be reasonably well correlated with Chrons C8 and C9. The correlations shown in Figure 8 with Chrons C6, C7, and C7A are probably less reliable, but they do represent the most consistent interpretation of the paleomagnetic and biostratigraphic data in this interval.

Magnetic Susceptibility

We performed whole-core magnetic susceptibility measurements on all sections of cores recovered from Hole 711A to a depth of 143 mbsf (Cores 115-711A-1H through -15X), and from Hole 711B to a depth of 31 mbsf (Cores 115-711B-1H through -4H). Measurements were made at intervals of 3 cm in the Quaternary horizons of each hole (Cores 115-711A-1H, 115-711B-1H, and 115-711B-2H), and thereafter at intervals of 5 cm. Magnetic susceptibility was measured with a Bartington Susceptibility Meter (Model MS1) and a whole-core, pass-through sen-

Table 3. Magnetic polarity reversal boundaries identified in APC cores from Site 711.

Sample interval (cm)	Depth (mbsf)	Sense	Chron	Age (Ma)
115-711A-				
1H-5, 0	6.0	R-N	Brunhes/Matuyama	0.73
1H-6, 20	7.7	N-R	Jaramillo (T)	0.91
3H-1, 70	18.4	R-N	Nunivak (O)	4.24
3H-1, 100	18.7	N-R	Sidufjall (T)	4.40
3H-1, 130	19.0	R-N	Sidufjall (O)	4.47
3H-2, 20	19.4	N-R	Thvera (T)	4.57
3H-2, 110	20.3	R-N	Thvera (O)	4.77
3H-5, 30	24.0	N-R	C3AN1 (T)	5.35
3H-6, 70	25.9	R-N	C3AN1 (O)	5.53
3H-7, 23	26.9	N-R	C3AN2 (T)	5.68
4H-2, 60	29.4	R-N	C3AN2 (O)	5.89
4H-3, 130	31.6	N-R	C3AN3 (T)	6.37
4H-4, 30	32.1	R-N	?	
4H-4, 50	32.3	N-R	?	
4H-4, 100	32.8	R-N	C3AN3 (O)	6.50
4H-5, 50	33.8	N-R	C4N1 (T)	6.70
9H-3, 130	79.9	N-R	C7N1 (T)	25.50
9H-5, 110	82.7	R-N	C7N2 (O)	25.97
11H-3, 100	98.8	N-R	C9N1 (T)	28.15
115-711B-				
2H-1, 110	3.2	R-N	Brunhes/Matuyama	0.73
2H-2, 100	4.6	N-R	Jaramillo (T)	0.91
2H-3, 10	5.2	R-N	Jaramillo (O)	0.98
2H-5, 100	9.1	N-R	Olduvai (T)	1.66
2H-6, 10	9.7	R-N	Olduvai (O)	1.88
3H-1, 20	11.9	N-R	Matuyama/Gauss	2.47
3H-2, 20	13.4	R-N	Kaena (T)	2.92
3H-2, 50	13.7	N-R	Kaena (O)	2.99
3H-2, 140	14.6	R-N	Gauss/Gilbert	3.40
3H-4, 30	16.5	N-R	Cochiti (T)	3.88
3H-4, 70	16.9	R-N	Cochiti (O)	3.97
3H-4, 120	17.4	N-R	Nunivak (T)	4.10
3H-5, 0	17.7	R-N	Nunivak (O)	4.24
3H-5, 20	17.9	N-R	Sidufjall (T)	4.40
3H-5, 40	18.1	R-N	Sidufjall (O)	4.47
3H-5, 100	18.7	N-R	Thvera (T)	4.57
3H-6, 60	19.8	R-N	Thvera (O)	4.77
4H-1, 90	22.3	N-R	C3AN1 (T)	5.35
4H-2, 120	24.1	R-N	C3AN1 (O)	5.53
4H-3, 80	25.2	N-R	C3AN2 (T)	5.68
4H-4, 120	27.1	R-N	C3AN2 (O)	5.89
4H-6, 50	29.4	N-R	C3AN3 (T)	6.37
5H-3, 50	34.5	R-N	C4N3 (T)	7.41
5H-5, 20	37.2	N-R	C4AN1 (T)	7.80
5H-5, 140	38.4	R-N	C4AN1 (O)	8.21
5H-6, 20	38.7	N-R	C4AN2 (T)	8.41
5H-6, 50	39.0	R-N	C4AN2 (O)	8.50
5H-6, 80	39.3	N-R	C4AN3 (T) ?	8.71
6H-1, 60	41.3	R-N ?	C5N2 (O) ?	10.58
6H-1, 120	41.9	N-R ?	C5AN1 (T) ?	11.55
6H-1, 140	42.1	R-N ?	C5AN1 (O) ?	11.73
6H-2, 10	42.3	N-R ?	C5AN2 (T) ?	11.86
6H-2, 20	42.4	R-N ?	C5AN2 (O) ?	12.12
6H-2, 80	43.0	N-R ?	C5AN3 (T) ?	12.46
6H-2, 110	43.3	R-N ?	C5AN4 (O) ?	12.62
6H-2, 130	43.5	N-R ?	C5AAN (T) ?	12.83
6H-3, 20	43.9	R-N ?	C5AAN (O) ?	13.01
6H-3, 70	44.4	N-R ?	C5ABN (T) ?	13.20
6H-3, 120	44.9	R-N ?	C5ABN (O) ?	13.46
6H-4, 0	45.2	N-R ?	C5ACN (T) ?	13.69
6H-4, 140	46.6	R-N ?	C5ACN (O) ?	14.08
6H-5, 20	46.9	N-R ?	C5ADN (T) ?	14.20
6H-5, 120	47.9	R-N ?	C5ADN (O) ?	14.66
8H-1, 60	60.6	N-R ?	?	
8H-1, 90	60.9	R-N ?	?	
8H-1, 110	61.1	N-R ?	?	
8H-2, 50	62.0	R-N ?	?	
8H-4, 10	64.6	N-R ?	C6BN (T) ?	22.57
8H-4, 50	65.0	R-N ?	?	
8H-4, 80	65.3	N-R ?	?	
8H-5, 40	66.4	R-N ?	C6BN (O) ?	22.97
8H-6, 20	67.7	N-R ?	C6CN1 (T) ?	23.27
8H-6, 80	68.3	R-N ?	C6CN1 (O) ?	23.44
8H-6, 130	68.8	N-R ?	C6CN2 (T) ?	23.55
9H-1, 90	70.8	N-R	C6CN3 (T)	24.04
9H-1, 120	71.1	R-N	C6CN3 (O)	24.21
10H-2, 130	82.1	N-R	C7AN (T)	26.38
10H-3, 100	83.3	R-N	C7AN (O)	26.56
11H-2, 100	91.4	N-R	C8N2 (O)	27.74
11H-6, 20	96.6	R-N	C9N1 (T)	28.15

Note: Depth values in columns 1 and 2 are determined from pass-through results and have an associated error of 10–20 cm. Sense = active sense of reversal; Chron = associated magnetic polarity chron boundary. (O) indicates onset of polarity chron, (T) indicates termination, and more tentative correlations are shown by "?".

sor coil of 80-mm inner diameter (Model MS2C). The results of these measurements are shown in Figures 9–11.

In general, with the exception of calc-turbidite horizons, modal susceptibility values are 4–5 times greater at this site than at Site 709, approximately 50% greater than at Site 710, and about the same or marginally greater than those at Site 708 (between turbidite horizons). The higher susceptibility values at this site are due to the generally lower proportion of biogenic silica and carbonate in the sediment than at Sites 709 and 710 (see “Geochemistry” and “Biostratigraphy” sections, this chapter). This is probably a function of the greater water depth of Site 711 and, thus, the intensified dissolution of biogenic constituents in the sediment relative to the shallower sites along the depth transect of the Madingley Rise. The dissolution of biogenic constituents effectively concentrates the lithogenic fraction of the sediment, within which most of the magnetizable components are located. Hence, in intervals free of volcanogenic material, turbidites, and/or high organic carbon concentrations (which lead to postdepositional reduction of iron oxides and oxyhydroxides—e.g., Froelich et al., 1979; Klinkhammer, 1980), susceptibility values may vary in relation to the extent of dissolution of carbonate and biogenic silica in the sediment.

The relationship between susceptibility values, carbonate content, and lithologic units (defined in the “Lithostratigraphy” section, this chapter) at Site 711, is generally good (see Figs. 9 and 17). The lithostratigraphic record of Hole 711A may be divided into four subsections according to its susceptibility profile, each subsection broadly correlating with a similar unit identified in Hole 710 (see “Paleomagnetism” section, “Site 710” chapter, this volume). The four intervals of distinct susceptibility and lithologic characteristics are as follows:

1. Between 0 and approximately 13 mbsf, turbidite-free susceptibility values oscillate between 1.2 and 2.5×10^{-5} cgs. This interval corresponds exactly to lithologic Unit I (Fig. 9), which consists of alternating horizons of clayey-nannofossil ooze, radiolarian-bearing nannofossil clay, and nannofossil-bearing clay of late Pliocene and Pleistocene age. The carbonate content of the sediment in this interval varies between 20% and 60% (see Fig. 17).

2. Between 13 and 39 mbsf, susceptibility values rise to between 2.0 and 3.5×10^{-5} cgs. We can correlate this interval with lithologic Subunit IB in Hole 710A (see Fig. 13, “Site 710” chapter, this volume) and, like Subunit IB in Hole 710A, is of late Miocene to late Pliocene age. At Site 711, however, this interval is classified as part of lithologic Unit II, which consists of three horizons of almost pure, carbonate-free clay or volcanic-glass-bearing clay, separated by two intervals of slightly higher carbonate content (between 20% and 40%). The uppermost horizon of clay-rich, carbonate-poor sediment, however, exhibits grayish brown, gray, and dark gray colors, which suggest that it has undergone postdepositional reduction (e.g., Lyle, 1983), possibly due to suboxic diagenesis of organic matter in the sediment (e.g., Froelich et al., 1979). The lower susceptibility values in this interval, relative to the two horizons of low carbonate content which precede it within lithologic Unit II, are therefore probably due to “dissolution” (i.e., bacterial dissociation or reduction) of the more strongly magnetic, natural remanent magnetization (NRM)-carrying iron oxides and oxyhydroxides originally in the sediment (e.g., Karlin and Levi, 1985). The same processes were thought to be responsible for the susceptibility characteristics of Subunit IB at Site 710 (see “Paleomagnetism” section, “Site 710” chapter, this volume).

3. Below 39 mbsf, to a depth of 68 mbsf, susceptibility values are generally much higher (i.e., between 4 and 8×10^{-5} cgs in the oxidized, clay-rich/carbonate-poor horizons at 39–51 mbsf and 57–68 mbsf), decreasing to minima of approximately $2 \times$

- 10⁻⁵ cgs in the intervening horizon of higher carbonate content (20%–40%). This interval (39–68 mbsf) corresponds to the oxidized portion of lithologic Unit II, consisting of lower to upper Miocene, yellowish-brown and brown clays and volcanic-glass-bearing clays, with light yellowish-brown nannofossil-bearing clay in the interval of slightly higher carbonate content between 51 and 57 mbsf. We tentatively related the higher susceptibility values, lower carbonate content, and high proportion of lithogenic clay in the sediment of Unit II to increased dissolution of biogenic constituents during early and middle Miocene times. The lower (oxidized) part of lithologic Unit II at Site 711 may be broadly correlated with lithologic Unit II at Site 710, both in terms of lithostratigraphic characteristics (including its susceptibility profile) and age relations.

4. Below a depth of 68 mbsf to the base of the measured section of Hole 711A, the general level of “background” values of magnetic susceptibility falls to below 1.5×10^{-5} cgs, corresponding to a large increase in the carbonate content of the sediment to between 80% and 90% (see Fig. 17). This interval corresponds to lithologic Unit III of late Eocene to late Oligocene age and comprises a sequence of clay-bearing nannofossil oozes that become increasingly indurated downhole (i.e., grading into clay-bearing nannofossil chalks), with occasional radiolarian-bearing intervals and volcanic-ash-rich horizons. Volcanic-ash horizons stand out as major peaks in the susceptibility profile of Hole 711A due to the high primary titanomagnetite content normally present in volcanic ash (Kennett, 1981). The large peak in susceptibility ($>1.2 \times 10^{-4}$ cgs) at a depth of 119 mbsf in Hole 711A (Sample 115-711A-13X-4, 15–35 cm), corresponds to a dark greenish-gray, degraded, volcanic-ash-rich interval (see “Lithostratigraphy” section). This may be correlated with volcanic-ash-rich horizons in Holes 708A (at 228 mbsf), 709B (at 236 mbsf), and 710A (at 183 mbsf), which also exhibit similar peaks in susceptibility values (see “Paleomagnetism” sections in previous site chapters).

Between-Hole Correlations at Site 711

At Site 711, as at Sites 709 and 710, the strong lithologic control of susceptibility variations again provides a reliable basis for interhole correlation (Fig. 10). Detailed correlation between the high-resolution (3 or 5 cm) magnetic susceptibility profiles of Holes 711A and 711B yields a complete lithostratigraphic record for this site to a depth of 31 mbsf, and also reveals the presence of four hiatuses in sedimentation: two in Hole 711A at 8.2 mbsf and 19.3 mbsf and two in Hole 711B at 2.3 mbsf and 22 mbsf. Figure 11 shows the proposed correlation between the uppermost 12 meters of Holes 711A and 711B, based on the whole-core susceptibility profile of each hole. On this enlarged scale, the cyclic nature of susceptibility variations within the Quaternary sections of Holes 711A and 711B is clearly revealed.

Carbonate content values for this interval in Holes 711A and 711B also exhibit high-frequency oscillations, within the constraints imposed by the much wider sampling interval used for carbonate content analyses, relative to the 3-cm-interval data points of the magnetic susceptibility profiles (see Fig. 17). If the covariance between magnetic susceptibility and carbonate content of the sediment is maintained at the fine scale of lithostratigraphic resolution seen in Figure 11, then it is feasible that the susceptibility oscillations values plotted in this figure possibly reflect “Milankovitch-type” (i.e., orbitally forced, climatically modulated) cycles of carbonate dissolution in the sediment (e.g., Volat et al., 1980; Dean and Gardner, 1986).

Using a crude estimate of sedimentation rate provided by the small number of nannofossil and paleomagnetic datums available for the Quaternary interval of Hole 711A (see “Sedimentation Rates” section, this chapter), it is possible to evaluate the

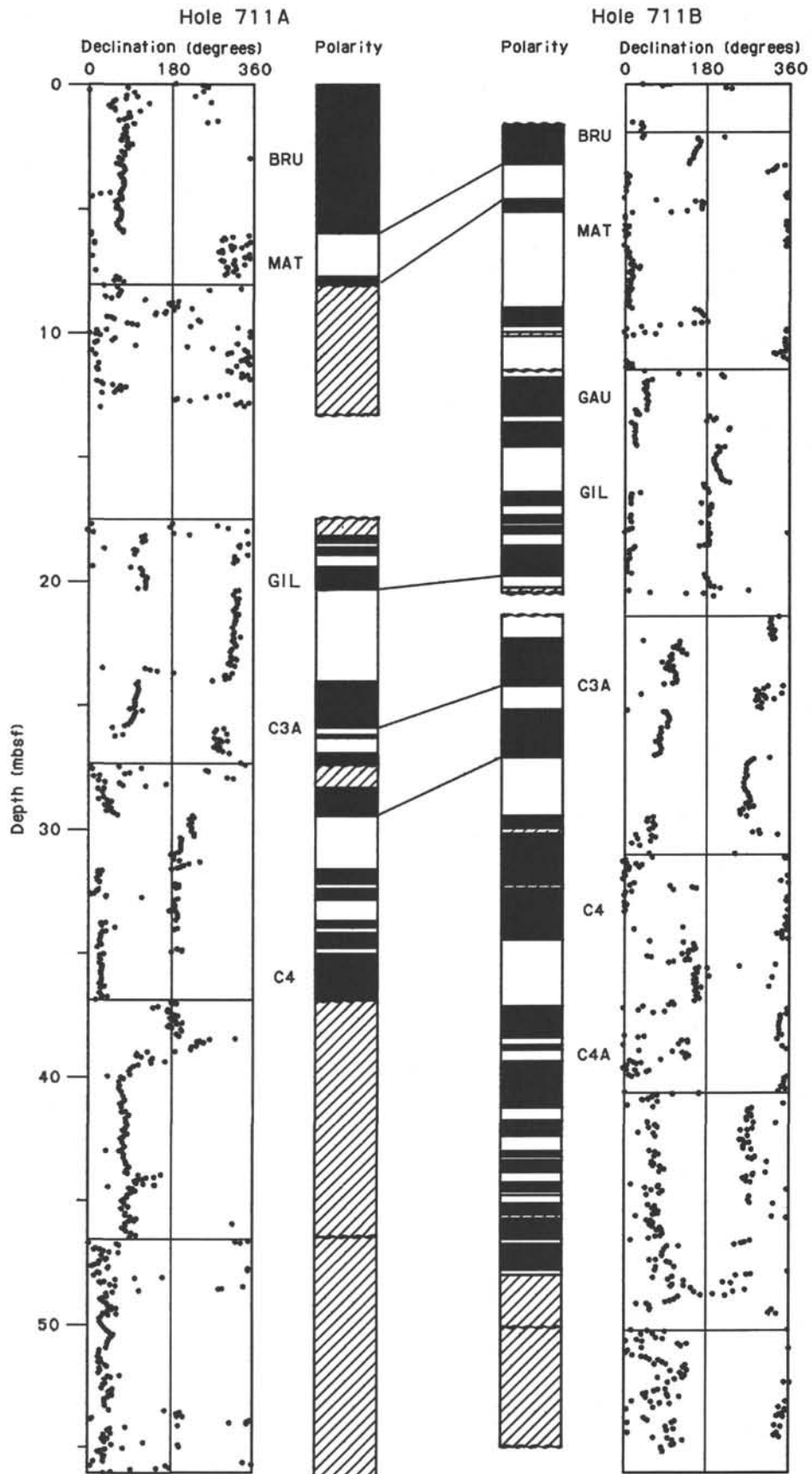


Figure 8. Declination records and magnetic polarity interpretation from APC cores for Holes 711A and 711B. Black indicates zones of presumed normal polarity, and white, reversed polarity. Diagonal line areas indicate disturbed zones of inconsistent magnetics. Horizontal lines on declination panel indicate core breaks; wavy lines on polarity panel indicate corresponding breaks in recovery.

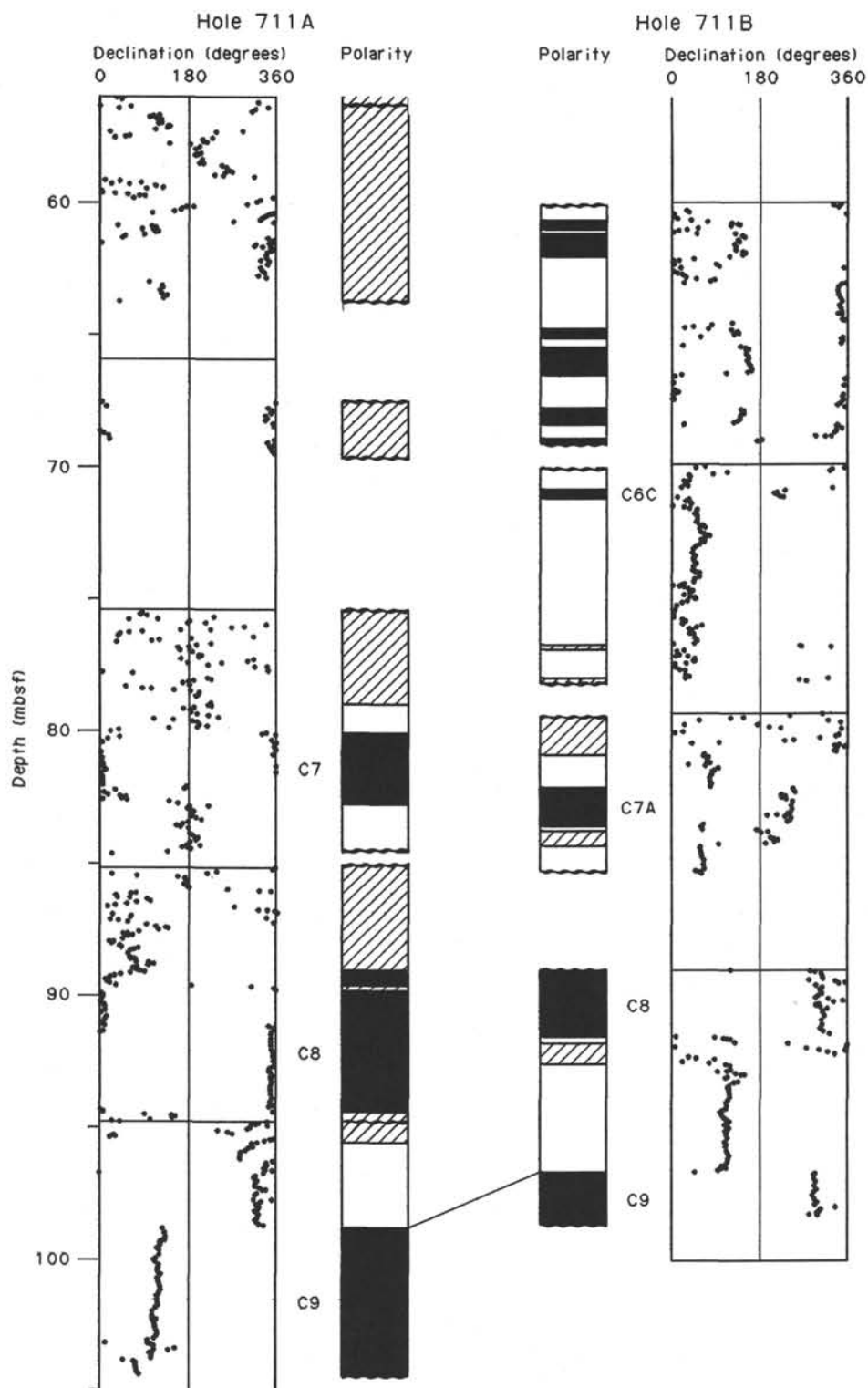


Figure 8 (continued).

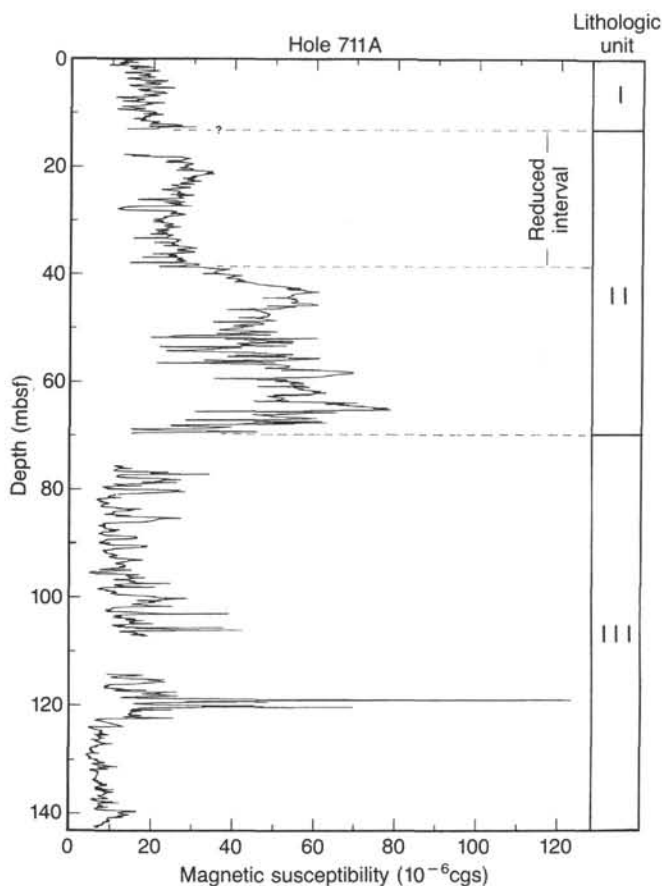


Figure 9. Whole-core magnetic susceptibility profile of Hole 711A to a depth of 143 mbsf. Lithologic units and their boundaries are the same as those defined in the "Lithostratigraphy" section, this chapter. The section of reduced sediment at the top of lithologic Unit II is not a recognized subunit at this site.

approximate periodicity of first-order cycles in the susceptibility profile of this hole (Fig. 11). The frequency of these cycles is about one per meter, corresponding to a periodicity of 104.5 k.y. This figure is remarkably close to the 100-k.y. periodicity in the record of the Earth's orbital eccentricity (e.g., Imbrie et al., 1984). It is reasonable to assume, therefore, that variations in magnetic susceptibility at Site 711A (clearly a proxy indicator of carbonate fluctuations at this site), are orbitally forced, possibly by way of the mechanism of climatically induced changes in the intensity of dissolution of biogenic constituents in the sediment.

Correlation between Sites 708, 709, 710, and 711

The principal objective of susceptibility measurements made during Leg 115 was to provide a simple, rapid, nondestructive, yet detailed and quantitative method of lithostratigraphic correlation between holes at a given site. However, the relatively close spacing of sites along the depth transect on the Madingley Rise (carbonate dissolution profile), suggests that an attempt to correlate between sites may be feasible, using the whole-core magnetic susceptibility profiles of individual holes. Figure 12 shows a preliminary estimate of possible lines of lithostratigraphic correlation between Sites 708, 709, 710, and 711, based on selected whole-core susceptibility profiles from one or more holes at each site. The reliability of the correlations suggested by Figure 12 is variable; thus, at this stage, all correlation lines should be regarded as tentative. To facilitate more accurate and precise correlation between holes and sites, use should be made of susceptibility profiles of selected subsections of individual holes, plot-

ted on scales such as those used in Figures 10 and 11. Each correlation line drawn in Figure 12, however, is based on comparisons made between the susceptibility profiles of the holes involved, plotted on much larger scales (as illustrated in the "Paleomagnetism" section of previous site chapters).

SEDIMENTATION RATES

We based the sedimentation rates calculated for Site 711 primarily on calcareous nannofossil datum levels and on magnetic polarity boundaries inferred from Hole 711A (Table 4; see "Paleomagnetism," this chapter, and Table 3 for depth positions of reversal boundaries). The magnetostratigraphic and biostratigraphic datum levels, and the inferred age-depth curve for Hole 711A, are plotted in Figure 13. We obtained a larger number of reversal boundaries from Hole 711B, and these are plotted separately in Figure 14. We identified these boundaries from biostratigraphic data not shown here.

The rates exhibited at Site 711 more or less mimic those obtained from Site 710, with higher rates in the Oligocene and the late Miocene through Pleistocene intervals, and a condensed middle through early Miocene section. The average sedimentation rate in the upper 40 m is about 4–5 m/m.y. The rate falls to about 1–2 m/m.y. in the condensed Miocene section and rises again to about 7–8 m/m.y. in the Oligocene.

GEOCHEMISTRY

Interstitial Water Studies

Interstitial water analyses were performed on 12 samples from Hole 711A, and the results are shown in Table 5 and Figure 15. Values for surface seawater are included and are listed at zero depth.

Calcium and Magnesium

The concentration of calcium increases from 10.67 mmol/L at 5.95 mbsf to 12.89 mmol/L at 225.10 mbsf, an overall gradient of 0.01 mmol/L/m. In contrast, the concentration of Mg^{2+} decreases rapidly from a surface seawater value of 55.56 to 52.24 mmol/L at 5.95 mbsf, but decreases only an additional 1.24 mmol/L by 225.10 mbsf, corresponding to a downhole gradient of -0.005 mmol/L/m. The behavior of Ca^{2+} and Mg^{2+} can therefore be described as nonconservative, suggesting that diagenetic reactions involving principally Mg^{2+} rather than Ca^{2+} ions are occurring in the sediment (Fig. 16). The upper 60 m of Hole 711A is characterized by an extremely low carbonate content (Fig. 17) and is consequently rich in clay minerals (see "Lithostratigraphy" section, this chapter). This suggests that diagenetic changes within this interval influence the Mg^{2+} concentration of the interstitial pore fluids while not significantly affecting their Ca^{2+} concentrations.

Sulfate, Ammonia, and Alkalinity

Alkalinity exhibits an increase from 3.26 mmol/L at 5.95 mbsf to 4.12 mmol/L at 197.60 mbsf. This increase is accompanied by a slight decrease in sulfate concentrations from 29.70 mmol/L in surface seawater to 26.74 mmol/L at 107.15 mbsf. No changes were observed in the concentration of ammonia, which remained below detection limits throughout the core. The absence of any increase in NH_4^+ suggests that it is removed from the pore waters as it is formed during the oxidation of organic material, perhaps by adsorption onto clay minerals.

Silica

The concentration of silica rapidly increases to over 700 $\mu\text{mol/L}$ by 5.95 mbsf and attains only marginally higher values than this by 225 mbsf. Between 44.35 and 53.75 mbsf, concentrations of silica fall to values as low as 370 $\mu\text{mol/L}$, suggesting local

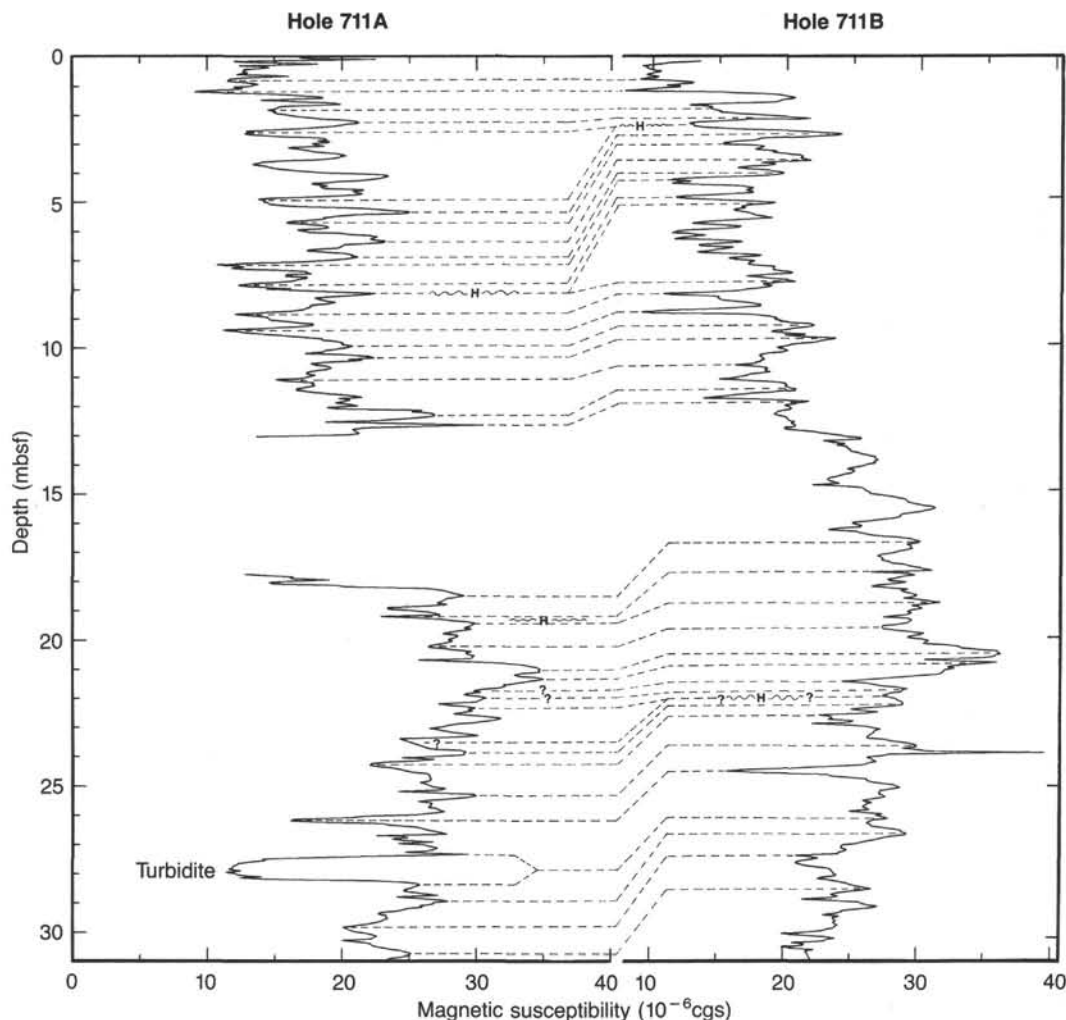


Figure 10. Lithostratigraphic correlation between the first 31 mbsf of Holes 711A and 711B, based on whole-core magnetic susceptibility profiles. H = hiatus.

precipitation, although no silicification was detected during the sedimentological observation (see "Lithostratigraphy" section, this chapter).

X-ray Diffraction, Carbonate, and Organic Carbon Content

The mineralogy of the sediments in the upper 50 mbsf of Hole 711A is dominated by clays, principally chlorite, smectite, illite-montmorillonite, and kaolinite. The abundance of these clays is reflected in the carbonate-content percentage, which falls to approximately 10 wt% during the middle Miocene minimum. The average carbonate content of the sediments analyzed from Hole 711A is 60.20% (± 32.57). We verified the occurrence of kaolinite by heating the sample at 550°C for 1 hour, after which time the kaolinite peak disappeared. Its presence in the sediments suggests that at least part of the clay minerals did not form from *in-situ* alteration of volcanic materials but are detrital in origin. However, the majority of the clays appear to be either illite or chlorite, which can easily form from the alteration of igneous minerals such as feldspars, pyroxenes, and olivines. The carbonate-soluble components are low-magnesium calcite.

The carbonate content at Site 711 exhibits many of the characteristic variations observed at previous CARB sites, in partic-

ular, a middle Miocene carbonate minimum and an upper Oligocene carbonate maximum (Table 6; Figs. 17 and 18). Sites 707 to 713 represent a transect of sites drilled in a range of water depths. In order to compare the various sites, we have calculated the mean carbonate content over the entire cored interval as well as for two specific time intervals, the middle Miocene carbonate minimum and the upper Oligocene carbonate maximum. These are listed in Table 7.

As one can see from this simple comparison, the mean carbonate percentage decreases with increasing water depth of the drilled hole, while the standard deviation around the mean increases, reflecting greater variability in the deeper sites. Future studies will examine changes within specific time periods in more detail; from this preliminary study, however, it is obvious that there was relatively little difference in carbonate content between the various sites during late Oligocene times. By the middle Miocene, moreover, bottom waters had become corrosive enough that the carbonate content was reduced to a mean of 15% at Site 711, compared with 92.5% at Site 707.

The amount of organic carbon measured at Site 711 was extremely low (Fig. 17 and Table 8), typical of the results seen at other sites examined during Leg 115. The low amount of organic carbon is reflected in the absence of detectable gaseous hydrocarbons at Site 711 and other sites.

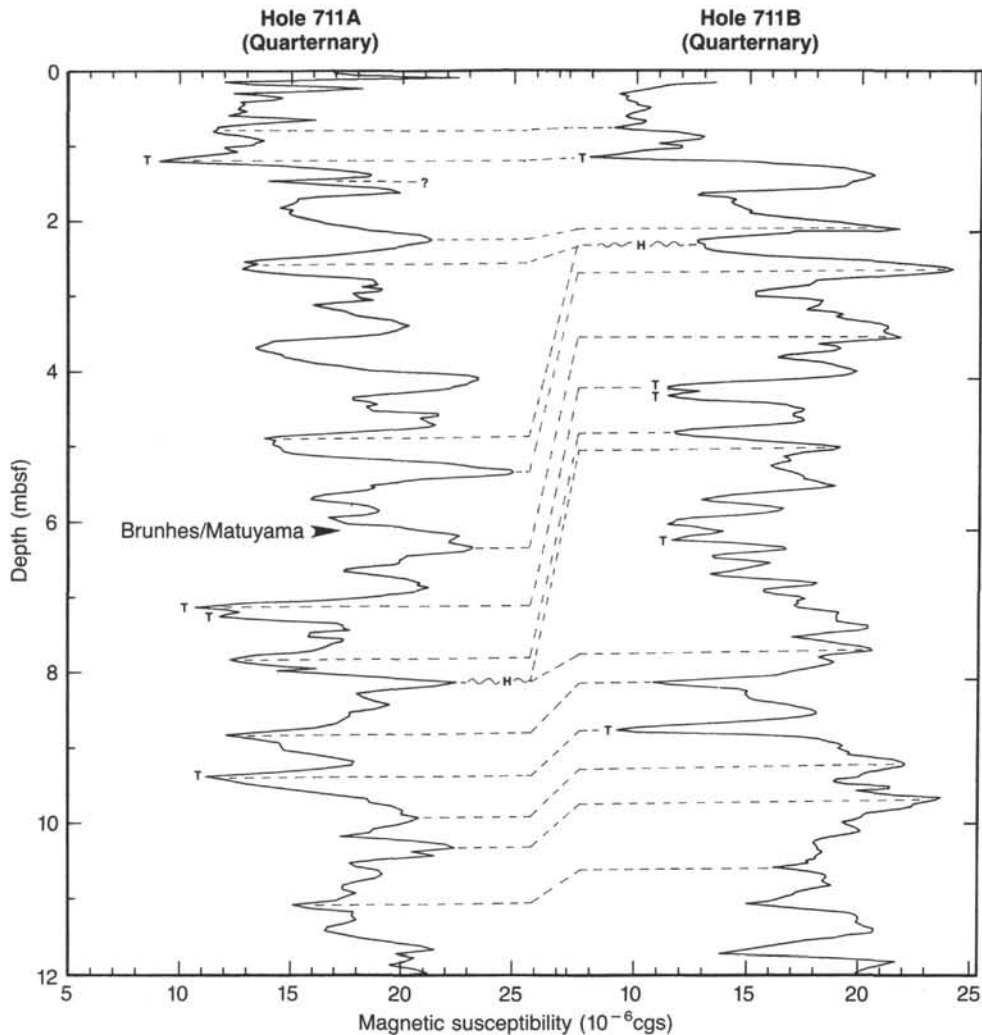


Figure 11. Lithostratigraphic correlation between the Quaternary sections of Holes 711A and 711B from 0 to 12 mbsf, based on whole-core magnetic susceptibility profiles. Note the cyclic nature of susceptibility variations corresponding to oscillations in the carbonate content of the sediment. First-order cycles recur with a frequency of 1 cycle per meter, which approximately corresponds to the 100-k.y. periodicity of the Earth's orbital eccentricity. The position of the Brunhes/Matuyama polarity reversal boundary (0.73 Ma.) is indicated. T = turbidite, H = hiatus.

PHYSICAL PROPERTIES

Introduction

Site 711 was located north of the Madingley Rise, about 140 km north of Site 710 at a water depth of 4428.2 m. We divided the recovered sediments into four major lithologic units (see "Lithostratigraphy" section, this chapter). Unit I (0–17.7 mbsf) consists of alternating radiolarian-bearing nannofossil clay and nannofossil-bearing clay. Unit II (17.7–68.0 mbsf) consists of three intervals of clay separated by two intervals of nannofossil clay. Unit III (68.0–173.0 mbsf) consists of nannofossil ooze and chalk, partly clay-bearing. Unit IV (173.0–249.6 mbsf) is characterized by the ubiquitous occurrence of radiolarians, with estimated concentrations occasionally reaching as high as 85%. These sediments consist of clay and radiolarian-bearing nannofossil chalk, clay-bearing radiolarian ooze, and, in a few cases, of radiolarite.

Index Properties

The index properties data for the sediments from Site 711 are shown in Figures 19 (Hole 711A) and 20 (Hole 711B), and in

Table 9. The large spread in these data is directly related to the varying carbonate content of the sediments (Fig. 21). Units I–III are defined on the basis of their carbonate content, while Unit IV is classified on the basis of induration in addition to sediment composition.

The wet-bulk densities of the sediments from Units I and II are low, averaging less than 1.4 g/cm^3 . This is due to the high water content of the clay-rich sediments. The porosities of these units are high, with an average greater than 80%. Porosity, water content, wet-bulk density, and carbonate content all remain approximately constant within Unit III. A closely spaced set of measurements was taken in a thin (0.5 m) nannofossil-ooze, turbidite bed within Unit III at 61 mbsf in Hole 711B (Fig. 20). There are only minor differences in the index properties between this layer and the surrounding nannofossil chalk. We observed a sharp drop in wet-bulk density and carbonate content within Unit IV at 174 mbsf (Fig. 19). The data points between 174 mbsf and 184 mbsf were obtained from two thin (1 m) beds of radiolarian ooze, which were interbedded with the nannofossil chalk of Unit IV. The measurements at 193 mbsf show an anomalously high wet-bulk density, which is probably due to experi-

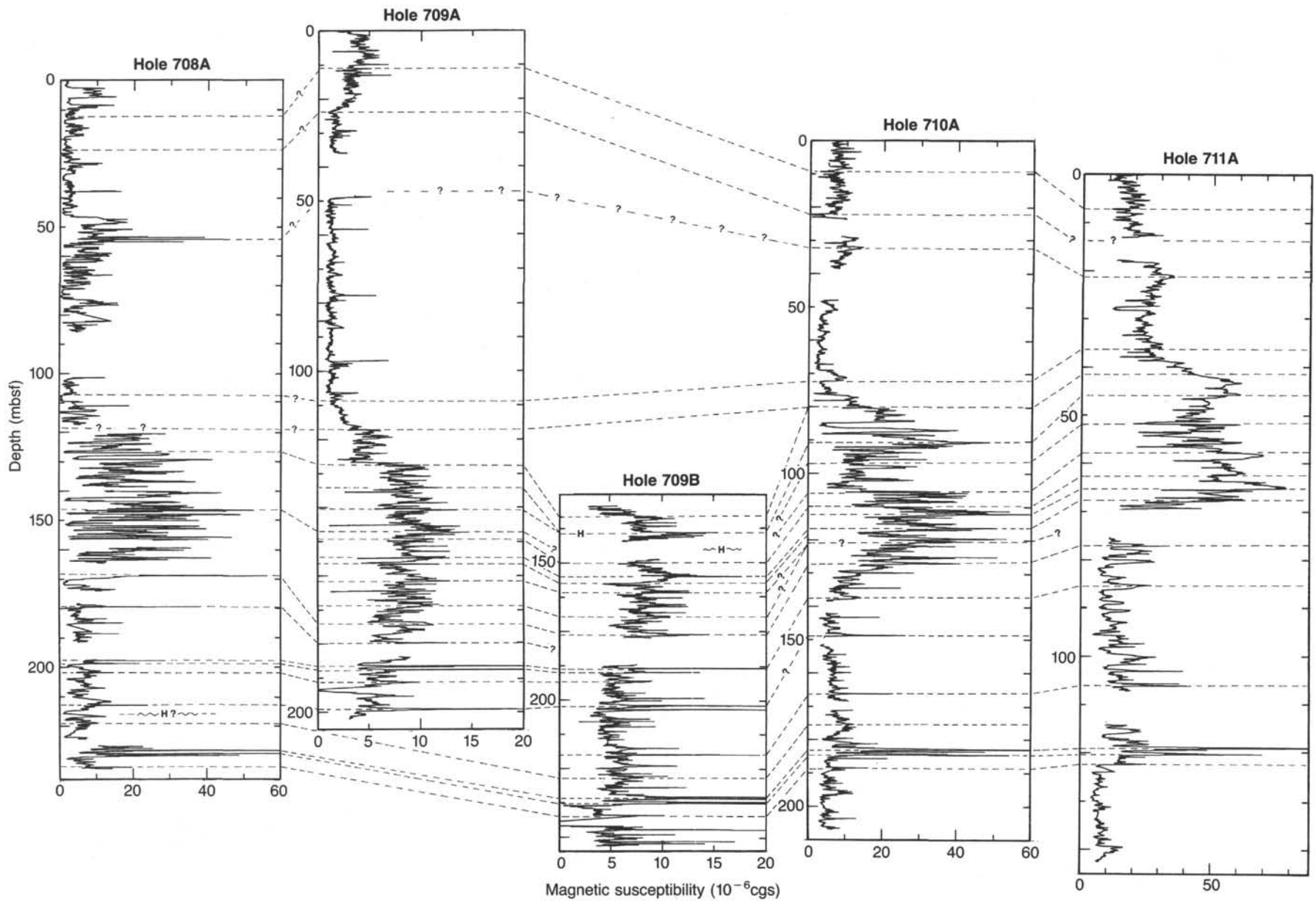


Figure 12. A tentative lithostratigraphic correlation between Sites 708, 709 (Holes 709A and 709B), 710, and 711, based on whole-core magnetic susceptibility records of one or more holes from each site. H = hiatus.

Table 4. Nannofossil datum events in Site 711.

	Species event	Depth (mbsf)	Age (Ma)
LO	<i>P. lacunosa</i>	1.9–4.9	0.46
LO	<i>C. macintyreii</i>	8.5–8.8	1.45
FO	<i>G. oceanica</i>	8.8–10.3	1.6
LO	<i>D. brouweri</i>	8.8–10.3	1.89
LO	<i>D. pentaradiatus</i>	11.8–12.8	2.35
LO	<i>R. pseudoumbilica</i>	17.7–19.8	3.56
LO	<i>D. quinqueringus</i>	17.7–19.8	5.6
FO	<i>C. acutus</i>	19.8–24.3	5.0
FO	<i>Amaurolithus</i> spp.	31.3–34.2	6.5
FO	<i>D. quinqueringus</i>	36.9–48.9	8.2
LO	<i>C. floridanus</i>	36.9–48.9	11.6
LO	<i>S. heteromorphus</i>	36.9–48.9	14.4
FO	<i>S. heteromorphus</i>	56.4–62.4	17.1
LO	<i>S. ciproensis</i>	76.0–77.5	25.2
FO	<i>S. ciproensis</i>	104.5–117.6	30.2
LO	<i>D. barbadiensis</i>	153.0–153.4	37.0
LO	<i>C. grandis</i>	175.8–178.8	40.0
LO	<i>C. solitus</i>	184.0–191.7	42.3
FO	<i>R. umbilica</i>	195.1–201.4	46.0
LO	<i>C. gigas</i>	214.5–220.7	47.0
FO	<i>C. gigas</i>	230.3–233.7	48.8
FO	<i>N. fulgens</i>	240.0–249.6	49.8

Note: FO = first occurrence and LO = last occurrence.

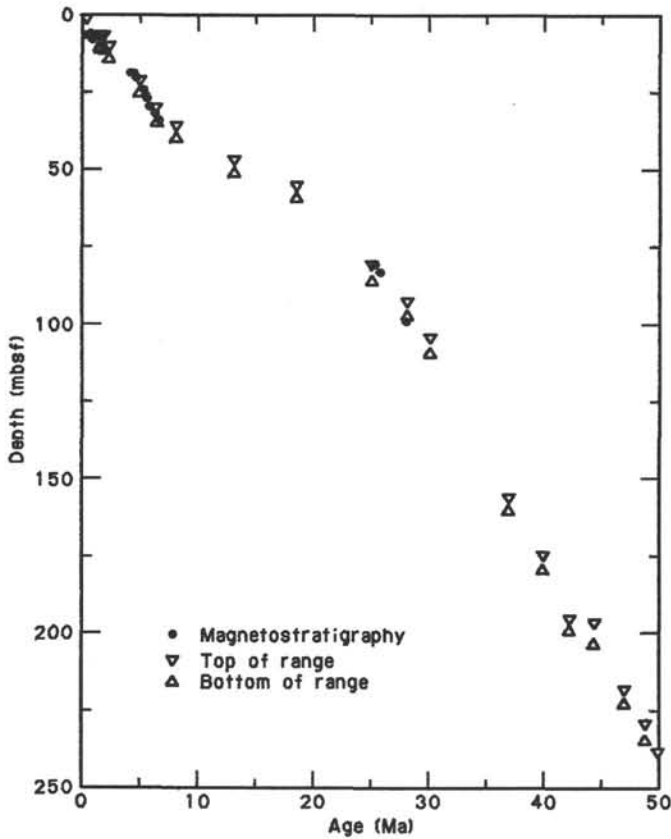


Figure 13. Age-depth plot for Hole 711A based on nannofossil datum events and magnetic reversal boundaries.

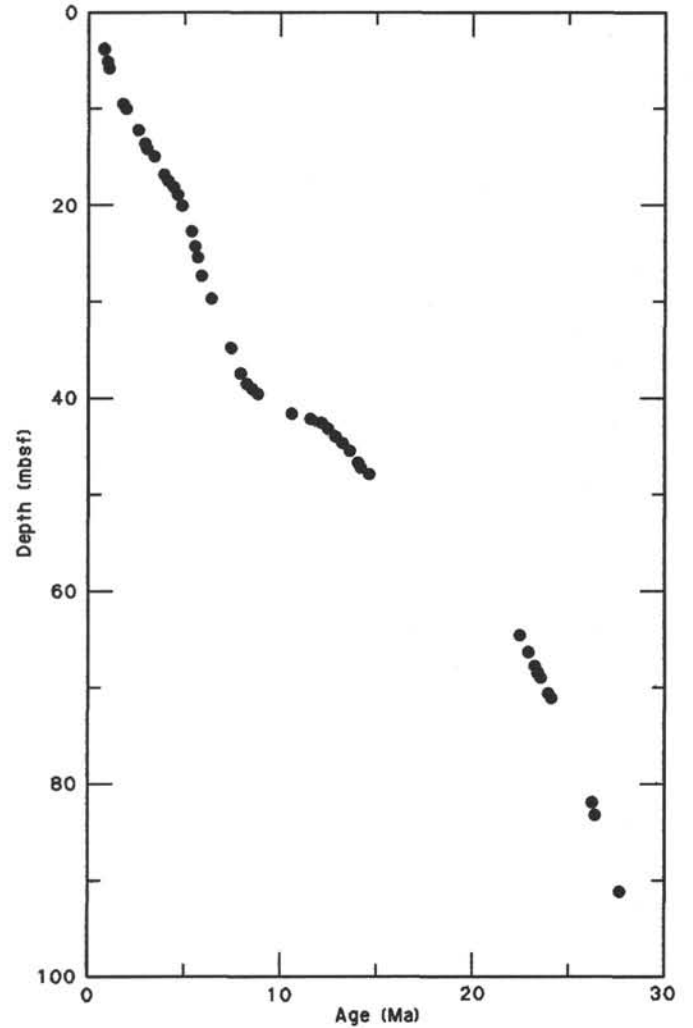


Figure 14. Magnetostratigraphic reversal boundaries plotted vs. depth for Hole 711B.

mental error. The measurements at 240 mbsf represent a chert layer from the base of Hole 711A.

There is a good match between Holes 711A and 711B regarding wet-bulk density, porosity, and water content data. In the upper two units all of these curves have the same sinuous character (Figs. 19 and 20). The grain densities are scattered between 2.0 and 3.25 g/cm³, but have little influence on the wet-bulk density. The grain densities of 2.0 g/cm³ between 39 and 60 mbsf (Fig. 19) in Hole 711A correspond to pure (volcanic-glass-rich) pelagic clay, with only a minor amount of carbonate. These grain density results suggest that the clay in this interval may be composed of smectites, which have a grain density as low as 2.0 g/cm³ (Rost, 1944). This is not, however, supported by the grain densities from Hole 711B. The low grain densities at 175 mbsf are due to the high abundance of radiolarians.

Compressional-Wave Velocity and Acoustic Impedance

The discrete data for compressional-wave velocity (V_p) for Site 711 are shown in Table 10 and Figure 22. These data show that V_p varies only slightly from an average of ~1500 m/s. There is a small amount of scatter in the data, and it is possible to observe a gradual increase of V_p with increasing depth within the pelagic clay. There is a slight drop in V_p at the boundary

Table 5. Interstitial water analyses, Hole 711A.

Sample interval (cm)	Depth (mbsf)	Ca (mmol/L)	Mg (mmol/L)	Cl (mmol/L)	Al (mmol/L)	pH	Salinity (%)	Si ($\mu\text{mol/L}$)	SO ₄ (mmol/L)	NH ₄ ($\mu\text{mol/L}$)
Seawater	0	10.54	55.56	567.53	2.51	8.47	35.5	3.5	29.70	0
115-711A-										
1H-4, 145-150	5.95	10.67	52.24	559.95	3.26	7.80	34.2	711.0	27.94	0
2H-3, 145-150	12.55	10.86	52.70	553.32	3.36	7.70	35.2	668.0	28.58	0
3H-4, 145-150	23.65	10.89	51.85	567.53	3.45	7.68	35.0	700.0	28.74	0
4H-5, 145-150	34.75	11.12	52.44	565.63	3.42	7.70	35.0	688.0	28.34	0
5H-5, 145-150	44.35	11.45	52.36	568.47	4.02	7.70	35.0	472.0	27.70	0
6H-5, 115-120	53.75	11.14	51.77	574.16	3.85	7.60	34.6	370.0	27.06	0
9H-5, 115-120	82.75	11.46	51.53	559.00	3.69	7.60	35.0	520.0	26.98	0
12X-2, 115-120	107.15	11.51	51.56	579.84	3.76	7.53	34.8	661.0	26.74	0
15X-5, 115-120	140.75	12.20	51.69	568.47	3.79	7.52	35.0	741.0	27.38	0
18X-3, 140-150	167.10	12.49	50.91	542.89	4.08	7.60	35.2	797.0	26.98	0
21X-4, 140-150	197.60	12.63	50.94	552.37	4.12	7.60	35.0	835.0	27.38	0
24X-3, 140-150	225.10	12.89	51.00	552.37	4.12	7.70	35.2	833.0	26.65	0

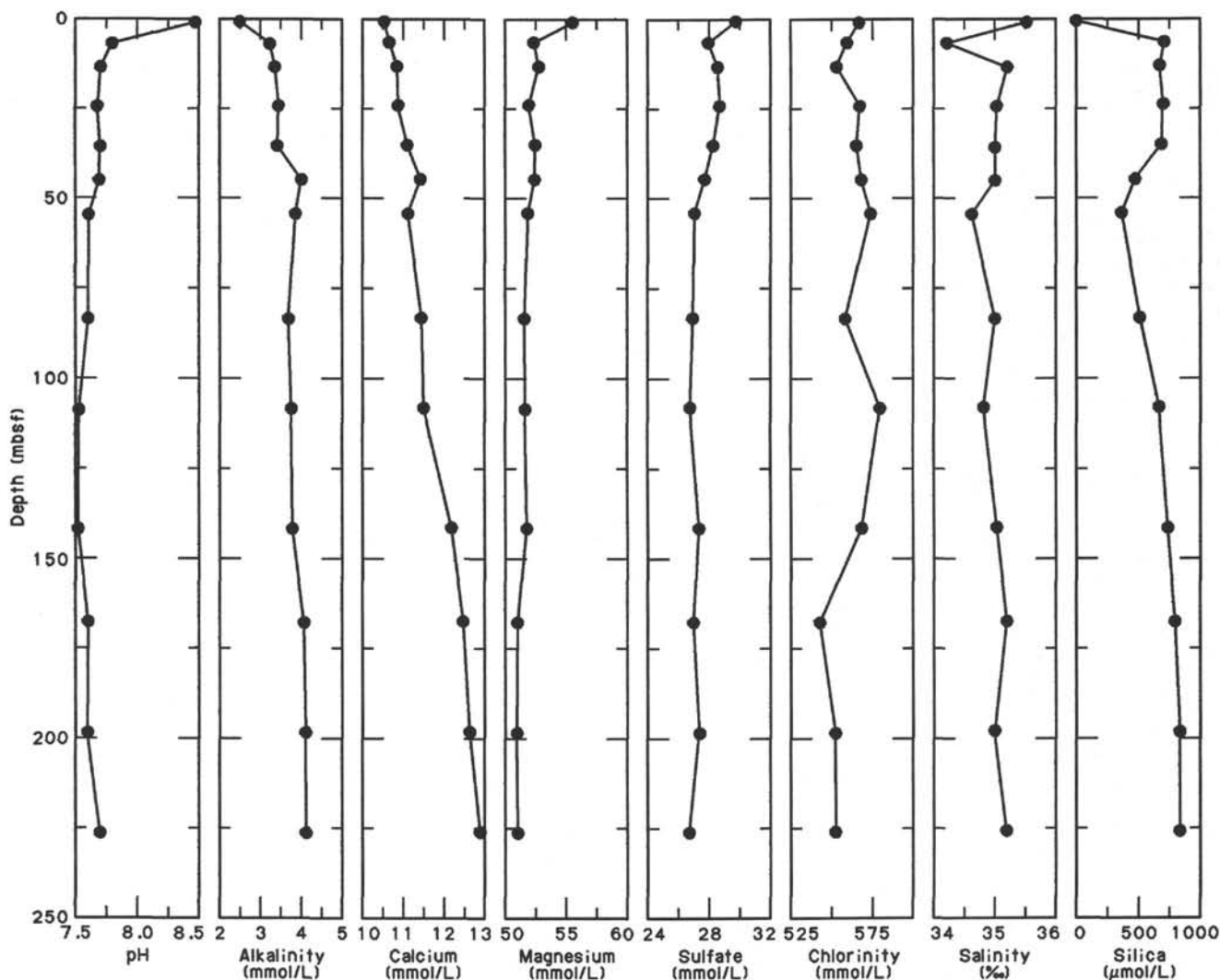


Figure 15. Summary of interstitial water analyses, Site 711, as a function of sub-bottom depth. Values for surface seawater are plotted at 0 m.

with the underlying nannofossil ooze and chalk at 73 mbsf. Only a few V_p measurements were possible on sediments from below 75 mbsf because they fractured very easily. Continuous V_p measurements vs. depth are shown in Figure 24. The V_p depth profile shows an almost constant velocity of 1500 m/s

over the entire site with a number of high-amplitude spikes; these spikes correlate with the basal layers of coarse-grained foraminiferal turbidites.

The calculated discrete and continuous acoustic impedances are shown in Figures 23 and 24. The discrete and continuous

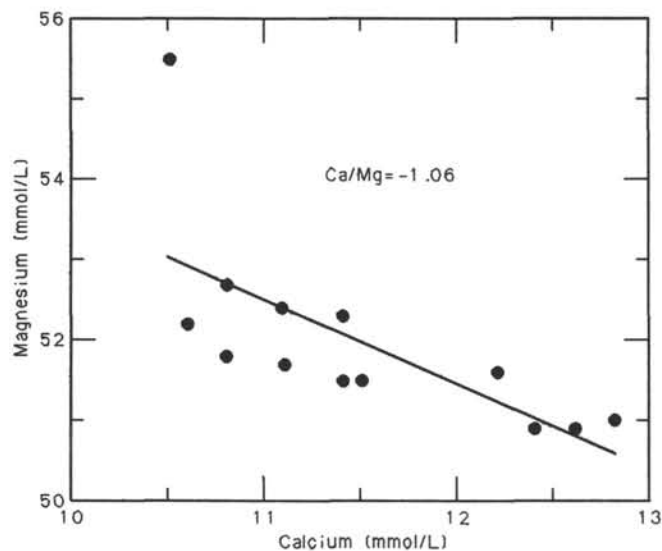


Figure 16. Calcium and magnesium concentrations, Site 711. The line represents a best fit to all the data. Surface seawater lies off the line in the upper left of the figure. The data for this site lie significantly below the relationships established for previous sites on Leg 115.

profiles match well: both show a gradual increase in impedance from $2000 \text{ g/cm}^2 \cdot \text{s} \cdot 10^2$ at 25 mbsf to $2500 \text{ g/cm}^2 \cdot \text{s} \cdot 10^2$ at 50 mbsf, followed by a relatively constant impedance signature for the remainder of the site. The spikes in the V_p data are suppressed in the impedance profile, while the high-frequency variations in wet-bulk density remain unaltered. These continuous profiles show the dominant influence of wet-bulk density on the calculated impedance.

Shear-Wave Velocity and Shear Strength

The shear-wave velocity (V_s) data from Site 711 are shown in Figure 25 and in Table 11. These data show a marked increase of V_s with depth, with a fair amount of experimental scatter. The soft radiolarian-bearing nannofossil clay (Unit I) has a shear velocity of less than 85 m/s. In the pelagic clay of Unit II, V_s increases from 83 to 186 m/s. There is then a drop in V_s to about 100 m/s, accompanied by an increased amount of experimental scatter for the underlying nannofossil ooze (Unit III). No reliable V_s measurements were possible in the clay-bearing nannofossil ooze and chalk recovered from below 85 mbsf, because the brittle chalk fractured when the shear transducers were inserted into it.

The shear strength measurements are shown in Figure 26 and are listed in Table 12. These data clearly show the increase in shear strength with depth within Units I and II. There is a significant increase in the amount of experimental scatter within Units III and IV, and we observed no depth dependence of shear strength from these data.

Thermal Conductivity

The results for thermal conductivity at Site 711 are listed in Table 13 and are shown in Figure 27. The thermal conductivity of the upper two units is about $0.9\text{--}0.95 \text{ W} \cdot \text{m}^{-1} \cdot \text{K}^{-1}$. These units are lower in carbonate and higher in clay content than Units III and IV. The higher carbonate contents of the lower units result in a higher and more variable thermal conductivity. Unit III has a mean conductivity of about $1.3 \text{ W} \cdot \text{m}^{-1} \cdot \text{K}^{-1}$, and Unit IV has a mean conductivity of about $1.1 \text{ W} \cdot \text{m}^{-1} \cdot \text{K}^{-1}$. Once again there are intervals of high variability in the conductivity. These intervals appear in sections of transition between entirely soft sediments and lithified sediments. We per-

formed several detailed studies of individual cores. They confirm that the wide variability is not simply scatter but, rather, a high-frequency signal that is not being sampled adequately at a one-measurement-per-section sample interval. The detailed studies are much smoother.

Summary

The physical properties results from Site 711 are mainly controlled by the carbonate content of the four lithologic units of sediment. For example, Units I and II have low carbonate contents and high amounts of clay, resulting in low wet-bulk densities. Wet-bulk density increases slightly with increasing depth. We observed similar increases for the shear strength, the compressional-wave velocity, and the shear-wave velocity. The transition from Unit II to Unit III at 75 mbsf was marked by a sharp increase in carbonate content, a decrease in shear strength, and a gradual leveling off of all other measured properties. Measurements throughout Unit III were relatively constant with varying amounts of experimental scatter. There was an increase in wet-bulk density and impedance at the boundary between Unit III and Unit IV, whereas V_p remained constant. The index properties remained constant within Unit IV, except for a significant reduction in the wet-bulk density, due to the low grain density of the radiolarian ooze.

SEISMIC STRATIGRAPHY

Site 711 is about 100 nmi north-northeast of Site 710, on the northern edge of the Madingley Rise at $2^\circ 44.56' \text{ S}$, $61^\circ 09.78' \text{ E}$ (Fig. 28) in water depths of 4428.2 m. We planned this site as the deepest end-point in a five-site depth transect to investigate the history of carbonate dissolution in the equatorial water column and circulation in the northwest Indian Ocean. Along a south to north line through Site 711, the Madingley Rise steps down to abyssal depths in a succession of offsets in the volcanic basement. Site 711 is located above the last of these steps (Fig. 29).

Several previous seismic reflection surveys (V34-06, RC17-07) permit examination of the structure of the region. Sediments in the vicinity of Site 711 are draped over the irregular volcanic basement or are folded from downslope transport. The site, however, is located in a 3-nmi-wide, sheltered basin between two local basement highs. The *JOIDES Resolution* survey of the site revealed approximately 300 m of sediments, and mostly flat-lying, parallel reflectors throughout the section. On the single-channel seismic (SCS) record, there appears to be some disturbance of the sediments just above the basement (Fig. 30).

REFERENCES

- Berger, W. H., 1975. Deep-sea carbonates: dissolution profiles from foraminiferal preservation. In Sliter, W. V., Bé, A.W.H., and Berger, W. H. (Eds.), *Dissolution of Deep-Sea Carbonates*, Cushman Found. Foram. Res. Spec. Publ., 13:82-86.
- Berggren, W. A., Kent, D. V., and Van Couvering, J. A., 1985. The Neogene: Part 2. Neogene geochronology and chronostratigraphy. In Snelling, N. J. (Ed.), *The Chronology of the Geological Record*, London Geol. Soc. Mem., 10:211-260.
- Broecker, W. S., and Peng, T.-H., 1982. *Tracers in the Sea*: Palisades, NY (Eldigio Press).
- Dean, W. E., and Gardner, J. V., 1986. Milankovitch cycles in Neogene deep-sea sediment. *Paleoceanography*, 1:539-553.
- Fisher, R. L., Bunce, E. T., et al., 1974. *Init. Repts. DSDP, 24*: Washington (U.S. Govt. Printing Office).
- Fisher, R. L., Sclater, J. G., and McKenzie, D. P., 1971. Evolution of the Central Indian Ridge, western Indian Ocean. *Geol. Soc. Am. Bull.*, 82:553-562.
- Froelich, P. N., Klinkhammer, G. P., Bender, M. L., Luedtke, N. A., Heath, G. R., Cullen, D., Dauphin, P., Hartman, B., Hammond, D., and Maynard, V. 1979. Early oxidation of organic matter in pelagic sediments of the eastern Equatorial Atlantic: suboxic diagenesis. *Geochim. Cosmochim. Acta*, 43:1075-1090.

- Imbrie, J., Hays, J. D., Martinson, D. G., McIntyre, A., Mix, A. C., Morley, J. J., Pisias, N. G., Prell, W. L., and Shackleton, N. J., 1984. The orbital theory of Pleistocene climate: support from a revised chronology of the marine ^{18}O record. In Berger, A., Imbrie, J., Hays, J., Kukla, G., and Saltzman, B. (Eds.), *Milankovitch and Climate* (Pt. 1): Hingham, MA (D. Reidel), 269-305.
- Karlin, R., and Levi, S., 1985. Geochemical and sedimentological control of the magnetic properties of hemipelagic sediments. *J. Geophys. Res.*, 90:10,373-10,392.
- Kennett, J. P., 1981. Marine tephrochronology. In Emiliani, C. (Ed.), *The Sea* (Vol. 7): New York (Wiley), 1373-1436.
- Klinkhammer, G. P., 1980. Early diagenesis in sediments from the eastern equatorial Pacific. II. Pore water metal results. *Earth Planet. Sci. Lett.*, 49:81-101.
- Lyle, M., 1983. The brown-green color transition in marine sediments: a marker of the Fe(III)-Fe(II) redox boundary. *Limnol. Oceanogr.*, 28: 1026-1033.
- Peterson, M.N.A., 1966. Calcite: rates of dissolution in a vertical profile in the central Pacific. *Science*, 154:1542-1544.
- Rost, R., 1944. Contribution to the knowledge of clay minerals. *Rozpravy Ceske Akad.*, 54:10-22.
- Volat, J.-L., Pastouret, L., and Vergnaud-Grazzini, C., 1980. Dissolution and carbonate fluctuations in Pleistocene deep-sea cores: a review. *Mar. Geol.*, 34:1-28.

Ms 115A-110

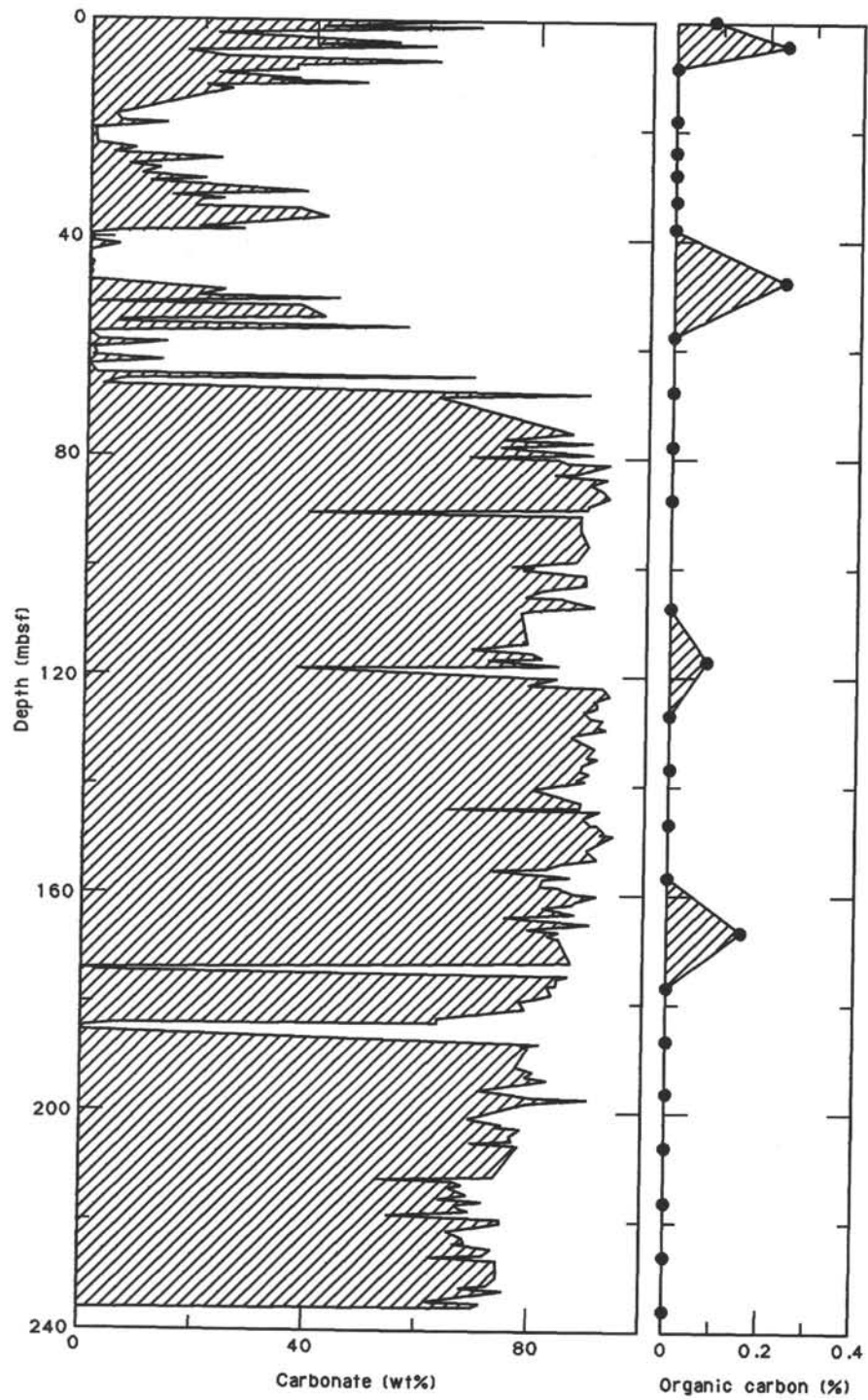


Figure 17. Carbonate and organic carbon content of samples from Hole 711A plotted against increasing sub-bottom depth.

Table 6. Carbonate content of samples from Hole 711A.

Sample interval (cm)	Depth (mbsf)	Carbonate content (wt%)
115-711A-		
1H-1, 25-26	0.25	75.73
1H-1, 135-136	1.35	40.81
1H-2, 25-26	1.75	69.54
1H-2, 62-64	2.12	48.24
1H-2, 135-136	2.85	22.22
1H-3, 25-26	3.25	36.20
1H-3, 135-136	4.35	54.96
1H-4, 25-26	4.75	39.79
1H-4, 62-64	5.12	61.41
1H-4, 135-136	5.85	18.46
1H-5, 25-26	6.25	16.62
1H-5, 135-136	7.35	26.96
1H-6, 38-40	7.88	62.31
2H-1, 25-26	8.35	43.11
2H-1, 60-63	8.70	36.49
2H-1, 136-137	9.46	36.43
2H-2, 25-26	9.85	22.36
2H-2, 136-137	10.96	37.11
2H-3, 25-26	11.35	31.85
2H-3, 60-63	11.70	49.21
2H-3, 136-137	12.46	19.90
2H-4, 25-26	12.85	25.36
3H-1, 25-26	17.95	4.30
3H-1, 135-136	19.05	5.32
3H-2, 25-26	19.45	13.88
3H-2, 60-63	19.80	10.15
3H-2, 135-136	20.55	0.79
3H-3, 25-26	20.95	0.87
3H-3, 135-136	22.05	0.89
3H-4, 25-26	22.45	1.27
3H-4, 60-63	22.80	1.04
3H-5, 25-26	23.95	8.25
3H-5, 135-136	25.05	4.12
3H-6, 25-26	25.45	14.17
3H-6, 60-63	25.80	23.52
3H-6, 135-136	26.55	8.10
3H-7, 25-26	26.92	6.64
4H-1, 25-26	27.55	12.65
4H-1, 135-136	28.65	9.31
4H-2, 60-63	29.40	20.50
4H-2, 135-136	30.15	10.68
4H-3, 25-26	30.55	13.01
4H-3, 135-136	31.65	38.66
4H-4, 25-26	32.05	19.88
4H-4, 60-63	32.40	14.22
4H-4, 135-136	33.15	23.90
4H-5, 25-26	33.55	19.78
4H-5, 135-136	34.65	18.35
4H-6, 25-26	35.05	37.94
4H-6, 135-136	36.15	42.06
4H-7, 25-26	36.55	42.06
5H-1, 25-26	37.15	33.26
5H-1, 135-136	38.25	19.08
5H-2, 25-26	38.65	27.34
5H-2, 60-63	39.00	6.64
5H-2, 135-136	39.75	0.02
5H-3, 25-26	40.15	0.51
5H-3, 135-136	41.25	0.98
5H-4, 25-26	41.65	5.60
5H-4, 135-136	42.75	0.12
5H-5, 135-136	44.25	0.02
5H-6, 60-63	45.00	0.84
5H-7, 25-26	46.15	0.22
6H-1, 25-26	46.85	0.48
6H-1, 135-136	47.95	0.15
6H-2, 25-26	48.35	0.29
6H-2, 135-136	49.45	19.51
6H-3, 25-26	49.85	24.08
6H-3, 135-136	50.95	19.51
6H-4, 25-26	51.35	44.78
6H-4, 135-136	52.45	1.16
6H-5, 25-26	52.85	38.33
6H-6, 25-26	54.35	41.88
6H-6, 60-63	54.70	42.17
6H-6, 135-136	55.45	5.91

Table 6 (Continued).

Sample interval (cm)	Depth (mbsf)	Carbonate content (wt%)
115-711A-		
6H-7, 25-26	55.85	5.24
7H-1, 25-25	56.55	57.00
7H-1, 135-136	57.65	1.28
7H-2, 25-26	58.05	0.48
7H-2, 60-63	58.40	0.59
7H-2, 135-136	59.15	2.39
7H-3, 25-26	59.55	14.09
7H-3, 135-136	60.65	0.89
7H-4, 25-26	61.05	1.15
7H-4, 60-63	61.40	1.50
7H-4, 135-136	62.15	0.24
7H-5, 25-26	62.55	13.44
7H-5, 135-136	63.65	0.39
7H-6, 25-26	64.05	0.34
7H-6, 135-136	65.15	1.88
7H-7, 25-26	65.55	69.15
8H-1, 25-26	66.25	6.58
8H-1, 135-136	67.35	2.68
8H-2, 25-26	67.75	54.64
8H-2, 135-136	68.85	89.63
8H-3, 25-26	69.25	62.66
9H-1, 25-26	75.85	86.70
9H-1, 135-136	76.95	74.64
9H-2, 25-26	77.35	84.94
9H-2, 58-60	77.68	90.03
9H-2, 135-136	78.45	73.67
9H-3, 25-26	78.85	79.71
9H-3, 135-136	79.95	90.20
9H-4, 25-26	80.35	68.32
9H-4, 54-56	80.64	84.03
9H-4, 135-136	81.45	86.26
9H-5, 25-26	81.85	93.12
9H-6, 25-26	83.35	87.51
9H-6, 49-51	83.59	83.46
9H-6, 135-136	84.45	92.93
10H-1, 25-26	85.45	89.70
10H-1, 135-136	86.55	92.13
10H-2, 12-14	86.82	91.81
10H-2, 25-26	86.95	92.47
10H-2, 135-136	88.05	93.27
10H-3, 25-26	88.45	92.47
10H-3, 135-136	89.55	89.48
10H-4, 25-26	89.95	89.50
10H-4, 96-98	90.66	39.58
10H-4, 135-135	91.05	88.48
10H-6, 96-98	93.66	88.05
11H-2, 46-48	96.76	89.52
11H-4, 25-26	99.55	87.46
11H-4, 100-103	100.30	76.17
11H-4, 135-136	100.65	80.20
11H-5, 25-26	101.05	78.14
11H-5, 135-136	102.15	89.14
11H-6, 25-26	102.55	89.20
11H-6, 135-136	103.65	89.31
11H-7, 25-26	104.05	87.08
12H-1, 25-26	104.75	81.52
12H-1, 135-136	105.85	78.42
12H-2, 25-26	106.25	85.20
12H-3, 25-26	107.75	90.68
12H-3, 82-83	108.32	79.07
12H-3, 135-136	108.85	77.77
13H-1, 25-26	114.45	78.95
13H-1, 135-136	115.55	69.03
13H-2, 25-26	115.95	77.72
13H-2, 34-36	116.04	79.98
13H-2, 135-136	117.05	81.60
13H-3, 25-26	117.45	71.40
13H-3, 135-136	118.55	84.69
13H-4, 25-26	118.95	37.89
13H-4, 135-136	120.05	61.19
13H-5, 25-26	120.45	76.18
13H-5, 71-73	120.91	84.27
13H-5, 135-136	121.55	80.75
13H-6, 25-26	121.95	78.95
13H-6, 110-111	122.80	92.35

Table 6 (Continued).

Sample interval (cm)	Depth (mbsf)	Carbonate content (wt%)
115-711A-		
14X-1, 25-26	124.15	93.36
14X-1, 135-136	125.25	90.31
14X-2, 25-26	125.65	91.40
14X-2, 84-86	126.24	91.2
14X-2, 135-136	126.75	90.31
14X-3, 25-26	127.15	88.71
14X-3, 135-136	128.25	90.10
14X-4, 25-26	128.65	92.40
14X-4, 135-136	129.75	91.11
14X-5, 25-26	130.15	92.63
14X-5, 56-58	130.46	92.78
14X-5, 135-136	131.25	87.22
14X-6, 25-26	131.65	86.81
15X-1, 25-26	133.85	91.05
15X-1, 135-136	134.95	89.85
15X-2, 25-26	135.35	88.99
15X-2, 53-54	135.63	91.53
15X-2, 135-136	136.45	89.89
15X-3, 25-26	136.85	88.72
15X-3, 135-136	137.95	88.42
15X-4, 25-26	138.35	90.01
15X-4, 135-136	139.45	87.45
15X-5, 25-26	139.85	89.54
15X-5, 76-78	140.36	84.25
15X-6, 25-26	141.35	80.26
16X-1, 25-26	143.55	88.82
16X-1, 135-136	144.65	88.49
16X-2, 25-26	145.05	64.77
16X-2, 45-47	145.25	92.09
16X-2, 135-136	146.15	89.41
16X-3, 25-26	146.55	88.90
16X-3, 135-136	147.65	90.08
16X-4, 25-26	148.05	91.43
16X-4, 135-136	149.15	92.87
16X-5, 25-26	149.55	91.84
16X-5, 47-49	149.77	94.63
16X-5, 135-136	150.65	92.87
16X-6, 25-26	151.05	92.20
16X-6, 135-136	152.15	89.82
16X-7, 25-26	152.55	89.38
17X-1, 25-26	153.25	90.18
17X-1, 135-136	154.35	91.41
17X-2, 25-26	154.75	85.67
17X-2, 135-136	155.85	82.67
17X-3, 25-26	156.25	72.89
17X-3, 135-136	157.35	86.84
17X-4, 25-26	157.75	81.99
17X-4, 135-136	158.85	81.45
17X-5, 25-26	159.25	84.80
17X-5, 65-66	159.65	85.69
17X-5, 135-136	160.35	88.11
17X-6, 25-26	160.75	91.63
17X-6, 135-136	161.85	87.58
17X-7, 25-26	162.25	87.19
18X-1, 25-26	162.95	82.15
18X-1, 135-136	164.05	87.75
18X-2, 25-26	164.45	79.59
18X-2, 60-63	164.80	75.33
18X-2, 135-136	165.55	80.30
18X-3, 25-26	165.95	90.41
18X-3, 108-109	166.78	79.28
18X-4, 25-26	167.45	85.07
18X-4, 60-63	167.80	82.84
18X-4, 135-136	168.55	84.82
19X-1, 25-26	172.65	87.30
19X-1, 135-136	173.75	65.97
19X-2, 13-16	174.03	2.64
19X-2, 24-25	174.14	0.29
19X-2, 46-48	174.36	3.23
19X-2, 74-76	174.64	2.13
19X-2, 135-136	175.25	86.63
19X-3, 26-27	175.66	84.65
19X-3, 135-136	176.75	84.64
19X-4, 26-27	177.16	83.27
19X-4, 135-136	178.25	83.83

Table 6 (Continued).

Sample interval (cm)	Depth (mbsf)	Carbonate content (wt%)
115-711A-		
19X-5, 26-27	178.66	83.90
19X-5, 135-136	179.75	80.55
19X-6, 26-27	180.16	78.22
19X-6, 135-136	181.25	79.37
20X-1, 25-26	182.35	72.74
20X-1, 135-136	183.45	63.44
20X-2, 25-26	183.85	63.57
20X-2, 60-62	184.20	7.86
20X-2, 135-136	184.95	0.17
20X-3, 25-26	185.35	0.20
20X-3, 50-51	185.60	0.13
20X-4, 25-26	186.85	26.84
20X-4, 135-136	187.95	81.99
20X-5, 25-26	188.35	78.41
20X-5, 44-45	188.55	79.93
21X-1, 25-26	191.95	77.25
21X-1, 135-136	193.05	80.74
21X-2, 25-26	193.45	80.17
21X-2, 60-63	193.80	79.09
21X-2, 135-136	194.55	83.30
21X-3, 25-26	194.95	79.29
21X-3, 135-136	196.05	73.89
21X-4, 25-26	196.45	71.36
21X-4, 111-112	197.31	77.30
21X-5, 25-26	197.95	81.31
21X-5, 60-63	198.30	90.71
21X-5, 111-112	198.81	78.93
22X-1, 25-25	201.65	69.21
22X-1, 135-136	202.75	75.53
22X-2, 25-26	203.15	74.06
22X-2, 60-63	203.50	78.38
22X-2, 135-136	204.25	76.82
22X-3, 25-26	204.65	76.37
22X-3, 135-136	205.75	77.19
22X-4, 25-26	206.15	69.58
22X-4, 60-63	206.50	78.38
23X-1, 25-26	211.35	74.63
23X-1, 135-136	212.45	73.69
23X-2, 25-26	212.85	52.94
23X-2, 60-63	213.20	66.81
23X-2, 135-136	213.95	68.56
23X-3, 25-26	214.35	65.64
23X-3, 135-136	215.45	69.55
23X-4, 25-26	215.85	68.23
23X-4, 60-63	216.20	64.31
23X-4, 135-136	216.95	72.03
23X-5, 25-26	217.35	66.86
23X-5, 135-136	218.45	68.08
23X-6, 25-26	218.85	69.67
23X-6, 52-54	219.12	54.95
23X-6, 135-136	219.95	75.22
24X-1, 20-25	220.90	74.97
24X-1, 60-63	221.30	71.46
24X-1, 135-136	222.05	69.07
24X-2, 20-25	222.40	65.55
24X-2, 135-136	223.55	68.70
24X-3, 20-25	223.90	68.48
24X-3, 60-63	224.30	69.04
24X-3, 97-98	224.67	66.86
24X-4, 20-25	225.40	73.63
24X-4, 135-136	226.55	71.73
24X-5, 25-26	226.95	62.04
24X-5, 60-63	227.30	65.65
24X-5, 97-98	227.67	74.52
25X-1, 25-26	230.55	74.53
25X-1, 135-136	231.65	73.11
25X-2, 25-26	232.05	72.84
25X-2, 60-63	232.40	67.72
25X-2, 135-136	233.15	75.79
25X-3, 25-26	233.55	73.02
25X-3, 135-136	234.65	67.13
25X-4, 25-26	235.05	61.54
25X-4, 60-63	235.40	71.59
25X-4, 135-136	236.15	69.70
25X-5, 25-26	236.55	64.60

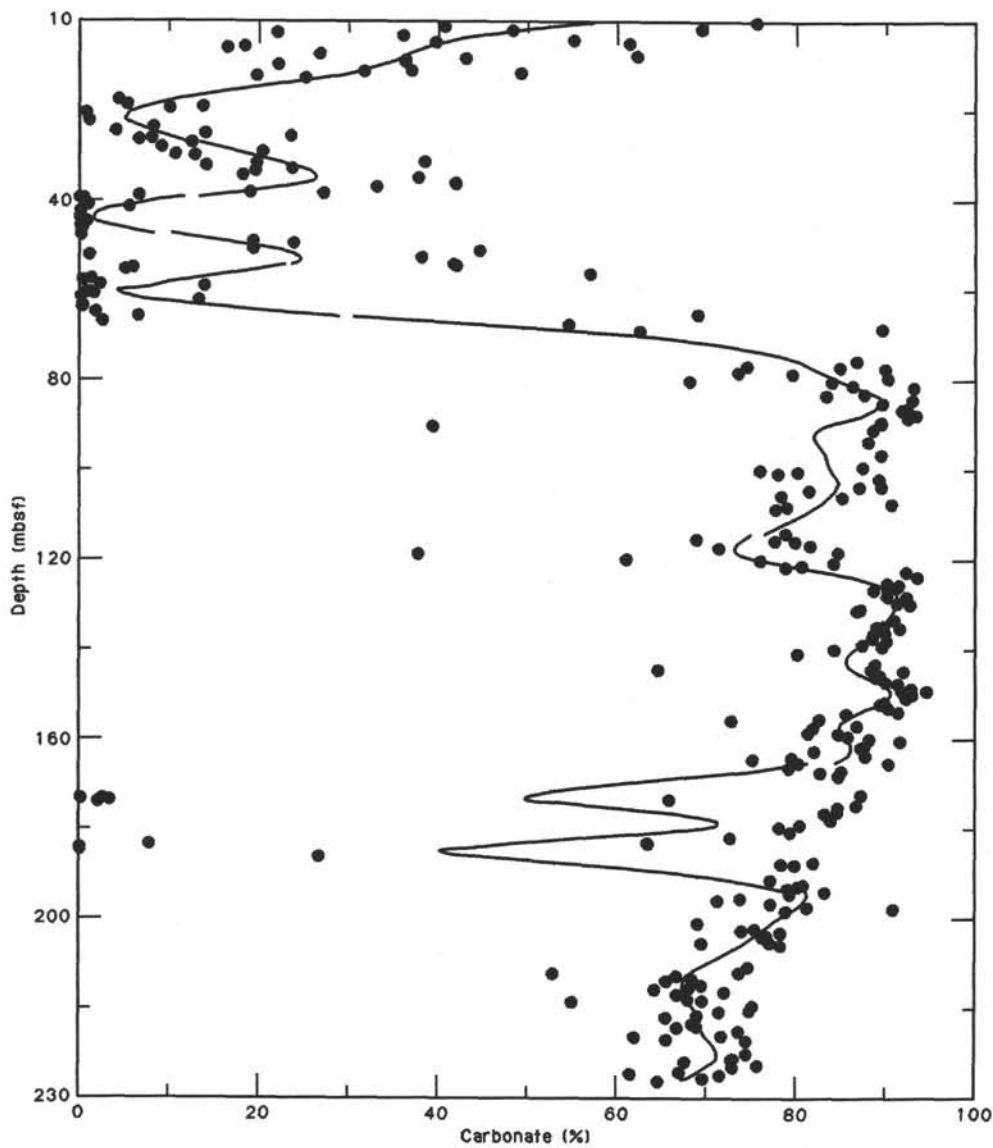


Figure 18. Low-resolution moving average of carbonate values shown in Figure 17.

Table 8. Organic carbon analyses, Hole 711A.

Sample interval (cm)	Depth (mbsf)	Organic carbon (%)
115-711A-		
1H-3, 25-26	3.25	0.13
1H-5, 135-136	7.35	0.36
2H-3, 25-26	11.35	0
3H-3, 25-26	20.95	0.07
3H-6, 135-136	26.55	0.07
4H-3, 25-26	30.55	0.04
4H-6, 25-26	35.05	0
5H-3, 25-26	40.15	0.08
6H-3, 25-26	49.85	0.32
7H-3, 25-26	59.55	0
8H-3, 25-26	69.25	0.01
9H-3, 25-26	78.85	0
10H-3, 25-26	88.45	0
12X-3, 25-26	107.75	0.07
13X-3, 25-26	117.45	0.10
14X-3, 25-26	127.15	0
15X-3, 25-26	136.85	0.06
16X-3, 25-26	146.55	0
17X-3, 25-26	156.25	0
18X-3, 25-26	165.95	0.22
19X-3, 26-27	175.66	0
20X-3, 25-26	185.35	0.01
21X-3, 25-26	194.95	0.06
22X-3, 25-26	204.65	0
23X-3, 25-26	214.35	0.03
24X-3, 25-26	223.95	0
25X-3, 25-26	233.55	0

Table 7. Comparison of the mean carbonate content of sediments from Sites 707, 708, 709, 710, and 711.

Site	Depth (mbsf)	Mean (wt%)	Standard deviation	Middle Miocene (wt%)	Upper Oligocene (wt%)
707	1541	92.90	3.17	92.50	94.00
708	4086	72.20	18.98	50.99	91.03
709	3038	89.72	3.56	85.00	90.38
710	3812	81.13	11.59	64.97	90.74
711	4428	60.20	32.57	15.01	83.34

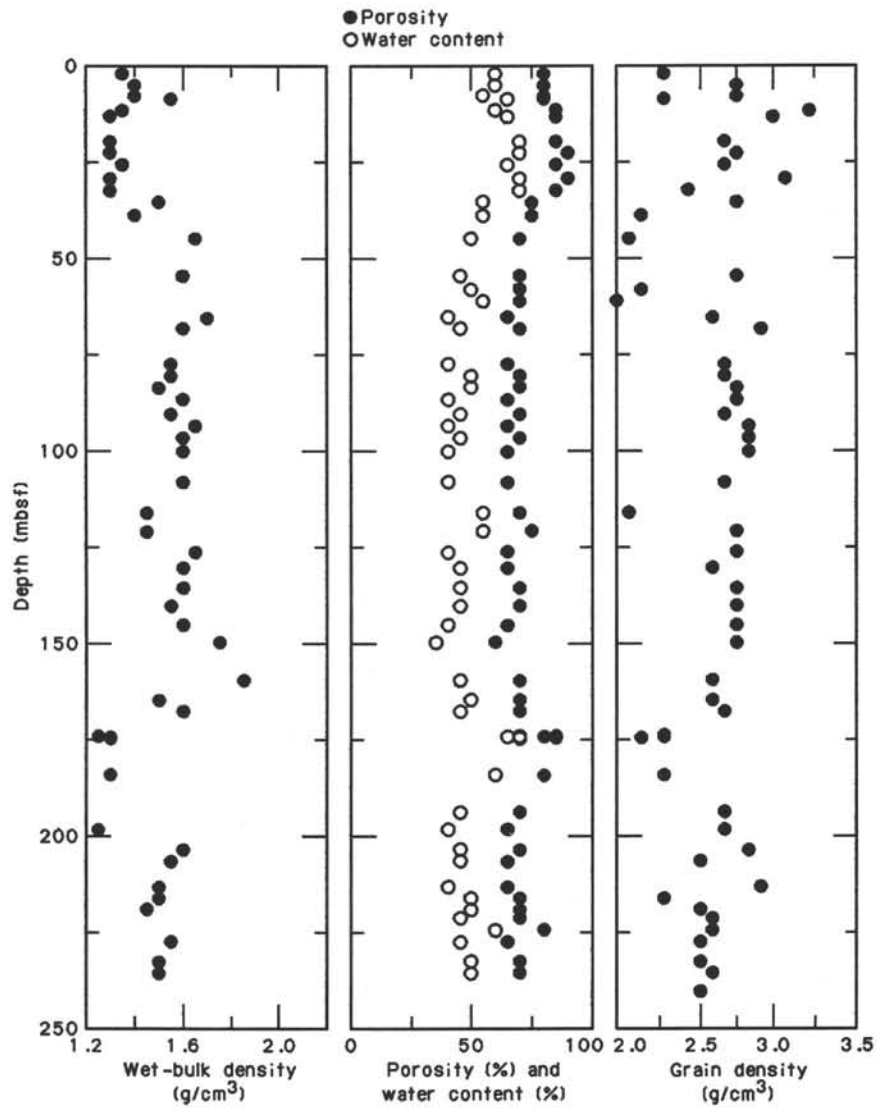


Figure 19. Index properties (wet-bulk density, water content, porosity, and grain density) at Hole 711A.

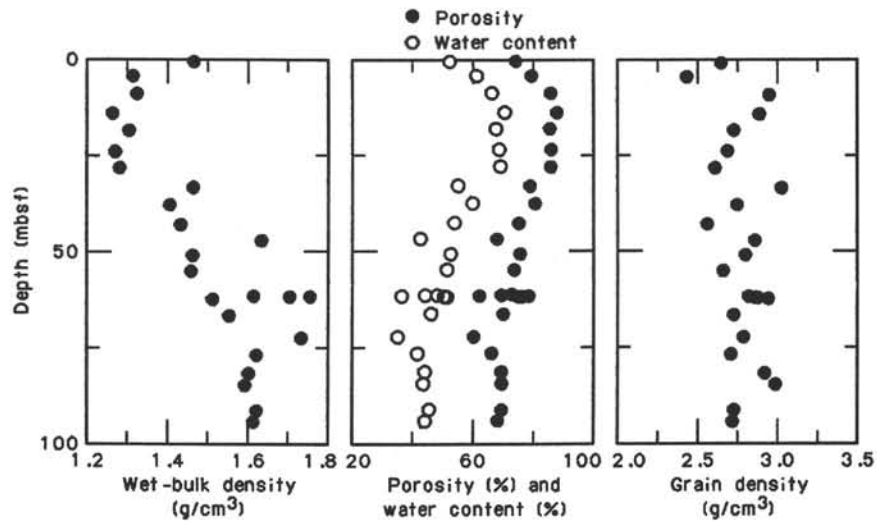


Figure 20. Index properties (wet-bulk density, water content, porosity, and grain density) at Hole 711B.

Table 9. Index-properties data and carbonate content of discrete samples from Site 711.

Section interval (cm)	Depth (mbsf)	Water content (%)	Porosity (%)	Wet-bulk density (g/cm ³)	Dry-bulk density (g/cm ³)	Grain density (g/cm ³)	Carbonate content (wt%)
115-711A-							
1H-2, 62	2.12	60.91	78.36	1.33	0.52	2.33	48.24
1H-4, 62	5.12	57.25	78.57	1.40	0.60	2.76	61.41
1H-6, 38	7.88	55.64	77.20	1.40	0.62	2.72	62.31
2H-1, 60	8.70	65.38	81.35	1.56	0.54	2.31	36.49
2H-3, 60	11.70	60.67	83.24	1.37	0.54	3.24	49.21
2H-5, 81	13.40	65.90	85.00	1.32	0.45	2.95	—
3H-2, 60	19.80	69.08	85.62	1.30	0.40	2.67	10.15
3H-4, 60	22.80	70.72	86.88	1.28	0.38	2.74	1.04
3H-6, 60	25.80	63.47	82.43	1.37	0.50	2.71	23.52
4H-2, 60	29.40	69.51	87.48	1.30	0.40	3.07	20.50
4H-4, 60	32.40	68.49	84.22	1.30	0.41	2.45	14.22
4H-6, 60	35.40	52.63	75.11	1.48	0.70	2.74	37.94
5H-2, 60	39.00	56.45	73.84	1.41	0.61	2.19	6.64
5H-6, 60	45.00	50.83	68.03	1.65	0.81	2.07	0.84
6H-6, 60	54.70	42.99	67.05	1.63	0.93	2.73	42.17
7H-2, 60	58.40	50.99	68.75	1.18	0.58	2.13	0.59
7H-4, 60	61.40	55.28	71.28	0.87	0.39	2.01	1.50
7H-7, 18	65.48	38.44	61.86	1.71	1.05	2.63	—
8H-2, 93	68.43	44.66	69.75	1.63	0.90	2.89	—
9H-2, 58	77.68	42.06	65.63	1.58	0.92	2.66	90.03
9H-4, 54	80.64	48.54	71.39	1.54	0.79	2.67	84.03
9H-6, 49	83.59	47.64	71.16	1.53	0.80	2.74	83.46
10H-2, 12	86.82	41.83	66.14	1.63	0.95	2.75	91.81
10H-4, 96	90.66	45.49	68.64	1.55	0.85	2.65	39.58
10H-6, 96	93.66	42.05	66.95	1.67	0.97	2.82	88.05
11H-2, 46	96.76	43.07	67.90	1.62	0.92	2.83	89.52
11H-4, 100	100.30	42.02	66.87	1.62	0.94	2.82	76.17
12X-3, 81	108.31	40.16	64.31	1.62	0.97	2.72	79.07
13X-2, 34	116.04	52.24	69.33	1.45	0.69	2.08	79.98
13X-5, 71	120.91	53.65	75.96	1.45	0.67	2.75	84.27
14X-2, 84	126.24	41.02	65.28	1.64	0.97	2.74	91.20
14X-5, 56	130.46	43.92	67.07	1.60	0.90	2.63	92.78
15X-2, 52	135.62	44.46	68.50	1.59	0.88	2.75	91.53
15X-5, 76	140.36	44.59	68.74	1.56	0.87	2.76	84.25
16X-2, 45	145.25	41.93	66.18	1.62	0.94	2.74	92.09
16X-5, 47	149.77	34.13	58.89	1.78	1.17	2.80	94.63
17X-5, 65	159.65	46.06	68.95	1.84	0.99	2.63	85.69
18X-2, 60	164.80	47.78	70.17	1.53	0.80	2.60	75.33
18X-4, 60	167.80	45.24	68.61	1.60	0.88	2.67	82.84
19X-2, 13	174.03	68.86	83.53	1.25	0.39	2.29	2.64
19X-2, 46	174.36	66.40	82.08	1.28	0.43	2.32	3.23
19X-2, 74	174.64	68.56	82.72	1.28	0.40	2.19	2.13
20X-2, 60	184.20	61.11	78.38	1.31	0.51	2.31	7.86
21X-2, 60	193.80	44.26	67.77	2.13	1.19	2.68	79.09
21X-5, 60	198.30	41.85	65.39	1.25	0.73	2.66	90.71
22X-2, 60	203.50	44.59	69.38	1.60	0.89	2.85	78.38
22X-4, 60	206.50	44.64	66.94	1.58	0.87	2.54	77.15
23X-2, 60	213.20	41.29	66.95	1.52	0.89	2.92	66.81
23X-4, 60	216.20	49.22	68.88	1.48	0.75	2.30	64.31
23X-6, 52	219.12	50.07	71.69	1.45	0.73	2.55	54.95
24X-1, 60	221.30	46.59	69.36	3.17	1.69	2.62	71.46
24X-3, 60	224.30	58.07	78.19	2.36	0.99	2.61	69.04
24X-5, 60	227.30	44.99	66.87	1.58	0.87	2.49	65.65
25X-2, 60	232.40	47.96	70.03	1.52	0.79	2.56	67.71
25X-4, 60	235.40	48.17	70.26	1.52	0.79	2.57	71.59
26X, CC, 1	240.01	—	—	2.13	—	2.51	—
115-711B-							
1H-1, 60	0.60	52.05	74.02	1.46	0.70	2.65	73.09
2H-2, 87	4.47	60.83	78.98	1.31	0.51	2.43	34.09
2H-5, 81	8.91	65.92	85.05	1.32	0.45	2.95	27.25
3H-2, 77	13.97	70.16	87.17	1.26	0.38	2.89	12.4
3H-5, 65	18.35	67.41	84.94	1.30	0.42	2.73	5.6
4H-2, 78	23.68	68.53	85.40	1.27	0.40	2.69	10.2
4H-5, 62	28.02	68.82	85.18	1.28	0.40	2.61	11.97
5H-2, 64	33.14	54.75	78.43	1.46	0.66	3.03	41.58
5H-5, 62	37.62	59.55	80.12	1.40	0.56	2.75	0.56
6H-2, 51	42.71	53.68	74.67	1.43	0.66	2.56	0.8
6H-5, 31	47.01	42.60	67.72	1.63	0.93	2.86	52.08
7H-1, 63	50.93	52.39	75.32	1.46	0.69	2.80	1.36
7H-4, 24	55.04	51.15	73.42	1.46	0.71	2.66	1.38
8H-2, 6	61.56	48.52	72.48	1.61	0.83	2.82	10.08
8H-2, 16	61.66	44.32	69.20	1.70	0.95	2.86	37.36

Table 9 (continued).

Section interval (cm)	Depth (mbsf)	Water content (%)	Porosity (%)	Wet-bulk density (g/cm ³)	Dry-bulk density (g/cm ³)	Grain density (g/cm ³)	Carbonate content (wt%)
115-711B-							
8H-2, 31	61.81	36.68	61.93	1.75	1.11	2.84	71.72
8H-2, 36	61.86	50.39	78.05	0.58	0.29	3.54	14.87
8H-2, 42	61.92	50.58	74.48	0.49	0.24	2.88	7.4
8H-2, 56	62.06	51.59	75.63	1.51	0.73	2.94	10.93
8H-5, 52	66.52	46.09	69.81	1.55	0.84	2.73	63.86
9H-2, 90	72.30	35.17	59.91	1.73	1.12	2.79	90.87
9H-5, 72	76.62	41.83	65.80	1.62	0.94	2.71	78.98
10H-2, 60	81.40	44.07	69.46	1.60	0.89	2.92	87.44
10H-4, 60	84.40	43.67	69.64	1.59	0.90	2.99	86.68
11H-2, 60	91.00	45.53	69.32	1.62	0.88	2.73	86.06
11H-4, 60	94.00	44.20	68.04	1.61	0.90	2.72	85.99

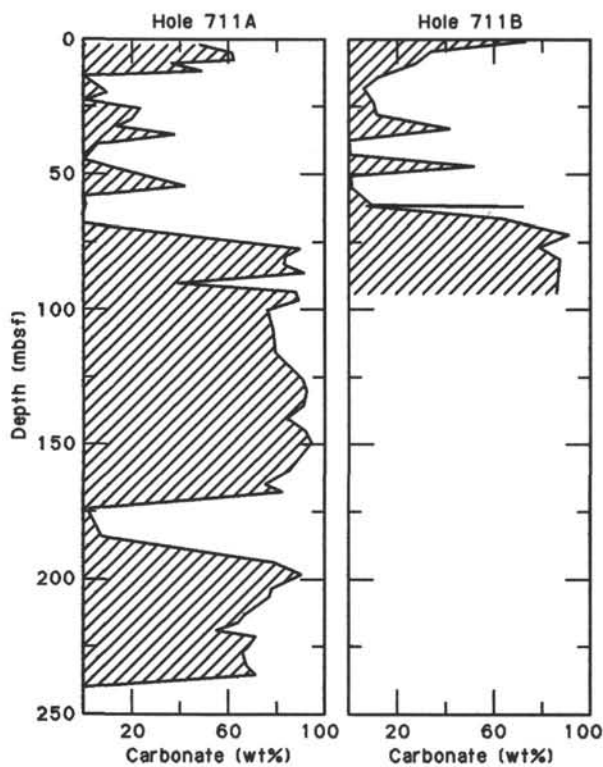


Figure 21. Carbonate content of samples for which the index properties were measured at Holes 711A and 711B.

Table 10. Compressional-wave velocity and impedance data, Site 711.

Section interval (cm)	Depth (mbsf)	V _p (m/s)	Impedance (g/cm ² ·s·10 ⁴)
115-711A-			
1H-2, 62	2.12	1499	19.93
1H-4, 62	5.12	1518	21.25
1H-6, 38	7.88	1502	21.02
2H-3, 60	11.70	1519	23.69
3H-2, 60	19.80	1519	19.74
3H-4, 60	22.80	1544	19.76
3H-6, 60	25.80	1518	20.79
4H-2, 60	29.40	1506	19.57
4H-4, 60	32.40	1517	19.72
4H-6, 60	35.40	1493	22.09
5H-2, 60	39.00	1484	20.92
5H-4, 60	42.00	1493	22.82
5H-6, 60	45.00	1498	24.71
6H-6, 60	54.70	1514	24.67
7H-2, 60	58.40	1510	17.81
7H-4, 60	61.40	1530	—
7H-7, 18	65.48	1543	26.38
8H-2, 107	68.57	1494	24.35
9H-2, 58	77.68	1539	24.32
10H-2, 12	86.82	1504	24.52
11H-2, 46	96.76	1500	24.30
13X-2, 34	116.04	1506	21.84
14X-5, 56	130.46	1496	23.94
26X, CC, 1	249.71	4167	—
26X, CC, 18	249.78	4207	—
115-711B-			
1H-1, 60	0.60	1474	21.52
2H-5, 81	8.91	1511	19.79
4H-2, 78	23.68	1478	18.87
5H-2, 64	33.14	1488	21.72
5H-5, 62	37.62	1480	20.72
6H-2, 51	42.71	1492	21.33
6H-5, 31	47.01	1503	24.50
7H-1, 63	50.93	1495	21.83
7H-4, 24	55.04	1495	21.83
8H-2, 56	62.06	1504	22.71
8H-5, 52	66.52	1507	23.25
9H-2, 90	72.30	1535	26.56
9H-5, 72	76.62	1494	24.21

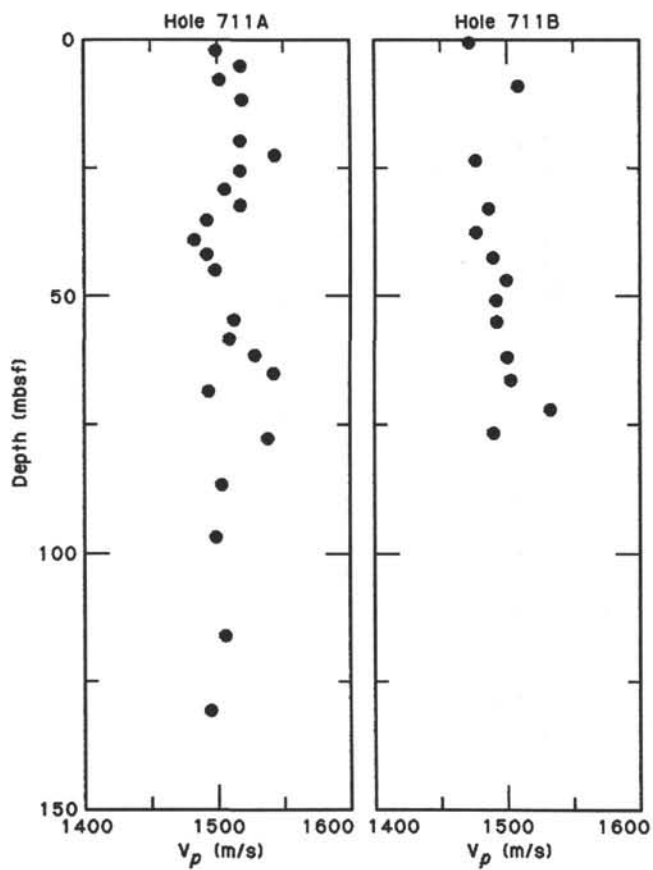


Figure 22. Compressional-wave velocity at Holes 711A and 711B.

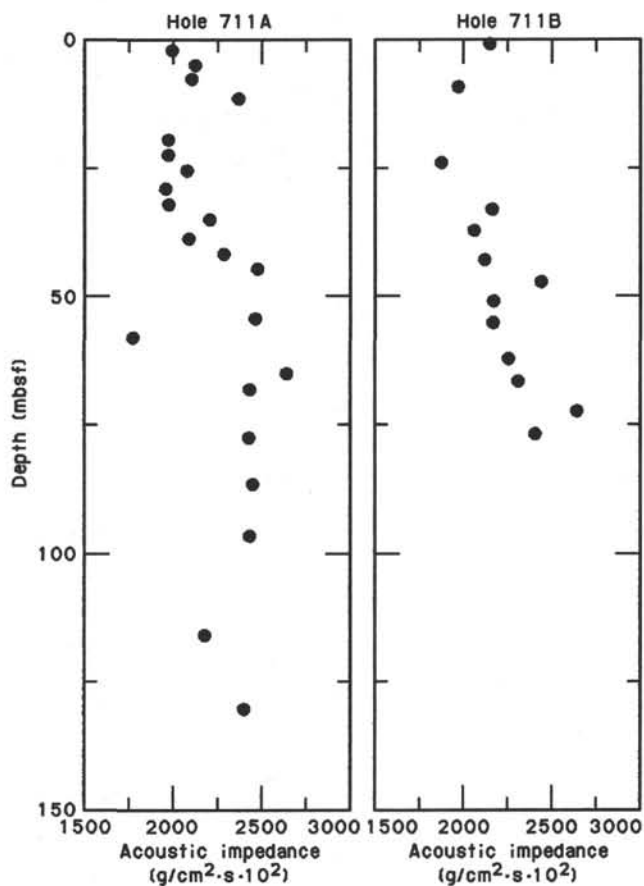


Figure 23. Acoustic impedance calculated from wet-bulk density and compressional-wave velocity of discrete samples at Hole 711A and 711B.

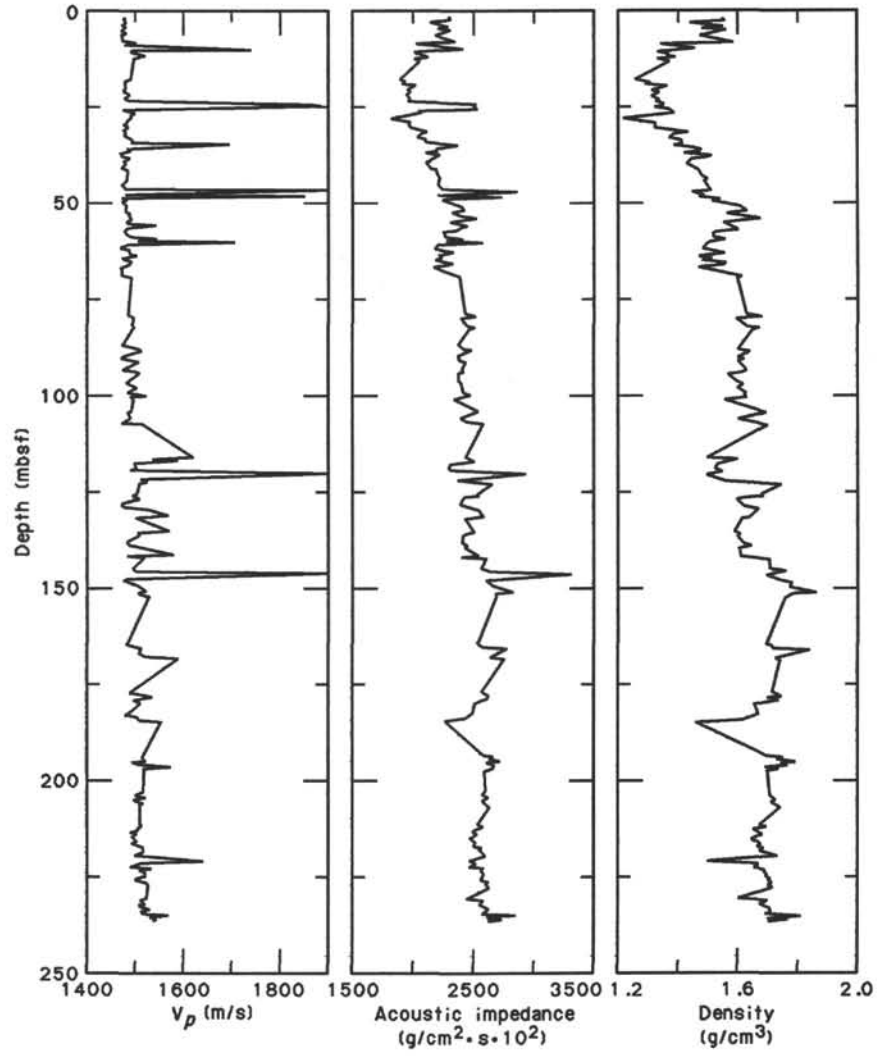


Figure 24. Continuous P -wave logger, computed acoustic impedance, and GRAPE wet-bulk density records (left to right) for Site 711.

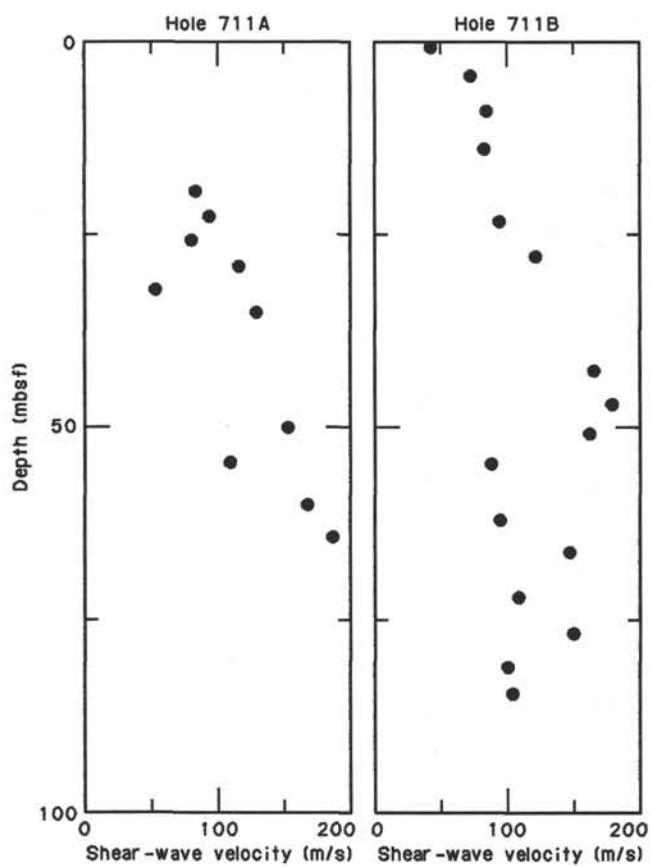


Figure 25. Shear-wave velocity at Site 711 for Holes 711A and 711B.

Table 11. Shear-wave velocity data, Site 711.

Section interval (cm)	Depth (mbsf)	V_s (m/s)
115-711A-		
3H-2, 34	19.54	83
3H-4, 52	22.72	93
3H-6, 53	25.73	80
4H-2, 52	29.32	115
4H-4, 52	32.32	53
4H-6, 48	35.28	128
6H-3, 67	50.27	152
6H-6, 65	54.75	109
7H-3, 74	60.04	167
7H-6, 53	64.33	186
115-711B-		
1H-1, 71	0.71	43
2H-2, 95	4.55	73
2H-5, 94	9.04	85
3H-2, 70	13.90	83
4H-2, 63	23.53	95
4H-5, 56	27.96	122
5H-2, 58	33.08	246
5H-5, 59	37.59	338
6H-2, 59	42.79	166
6H-5, 39	47.09	179
7H-1, 58	50.88	163
7H-4, 15	54.95	89
8H-2, 59	62.09	96
8H-5, 58	66.58	148
9H-2, 83	72.23	110
9H-5, 86	76.76	151
10H-2, 50	81.30	102
10H-4, 70	84.50	106

Table 12. Motorized shear strength data, Site 711.

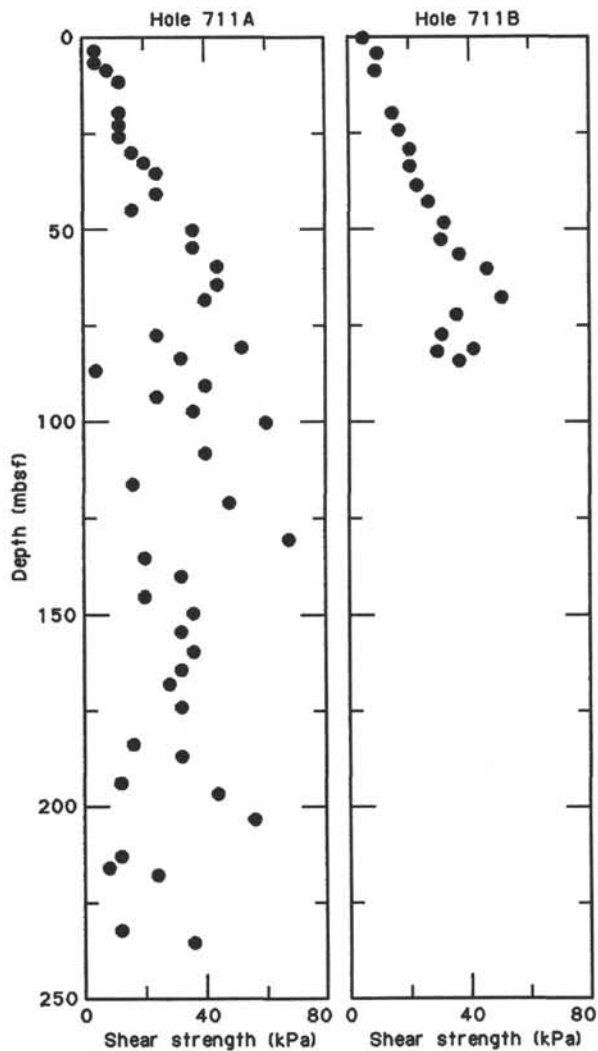


Figure 26. Measured shear strength on discrete samples from Holes 711A and 711B.

Section interval (cm)	Depth (mbsf)	Peak (kPa)
115-711A-		
1H-3, 70	3.70	5.3
1H-5, 73	6.73	5.9
2H-1, 50	8.60	8.3
2H-3, 50	11.60	10.6
3H-2, 58	19.58	14.2
3H-4, 74	22.94	13.1
3H-6, 74	25.94	13.1
4H-2, 120	30.00	17.8
4H-4, 82	32.62	22.0
4H-6, 70	35.50	24.3
5H-3, 100	40.90	24.4
5H-6, 75	45.15	17.2
6H-3, 80	50.40	35.0
6H-6, 90	55.00	35.5
7H-3, 62	59.92	45.7
7H-6, 74	64.54	42.7
8H-2, 103	68.53	40.3
9H-2, 54	77.64	23.1
9H-4, 62	80.72	54.5
9H-6, 55	83.65	33.2
10H-2, 17	86.87	5.9
10H-4, 101	90.71	38.5
10H-6, 100	93.70	23.7
11H-2, 106	97.36	35.0
11H-4, 106	100.36	59.3
12H-3, 57	108.07	39.1
13H-2, 43	116.13	17.8
13H-5, 75	120.95	48.6
14H-5, 64	130.54	67.6
15H-2, 611	135.71	19.0
15H-5, 70	140.30	32.3
16H-2, 74	145.54	22.5
16H-5, 64	149.94	38.0
17H-2, 14	154.64	30.8
17H-5, 70	159.70	35.9
18H-2, 47	164.67	34.4
18H-4, 108	168.28	27.9
19H-2, 34	174.24	30.8
20H-2, 48	184.08	16.6
20H-4, 43	187.03	32.0
21H-2, 75	193.95	13.1
21H-4, 45	196.65	45.0
22H-2, 45	203.35	55.7
23H-2, 35	212.95	13.1
23X-4, 40	216.00	8.3
23X-5, 45	217.55	23.7
25H-2, 50	232.30	11.9
25X-4, 50	235.30	35.5
115-711B-		
1H-1, 48	0.48	4.8
2H-2, 83	4.43	8.9
2H-5, 87	8.97	8.3
3H-2, 64	19.84	14.2
3H-5, 70	24.40	16.6
4H-2, 70	29.50	20.1
4H-5, 46	33.76	20.1
5H-2, 51	38.91	22.5
5H-5, 41	43.31	26.1
6H-2, 67	48.77	31.4
6H-5, 47	53.07	30.3
7H-1, 45	56.75	36.8
7H-4, 22	61.02	46.3
8H-2, 64	68.14	51.0
8H-5, 67	72.67	35.5
9H-2, 76	77.86	30.8
9H-5, 77	82.37	29.0
10H-2, 75	81.55	41.5
10H-4, 75	84.55	36.8

Table 13. Thermal conductivity data, Hole 711A.

Section interval (cm)	Depth (mbsf)	Thermal conductivity ($W \cdot m^{-1} \cdot K^{-1}$)
115-711A-		
1H-1, 100	1.00	1.357
1H-2, 70	2.20	0.940
1H-3, 70	3.70	1.029
1H-4, 70	5.20	0.906
1H-5, 70	6.70	1.001
1H-6, 30	7.80	1.043
2H-1, 70	8.80	1.130
2H-3, 70	11.80	0.926
2H-4, 30	12.90	0.919
3H-1, 70	18.40	0.778
3H-2, 10	19.30	0.929
3H-2, 20	19.40	0.940
3H-2, 30	19.50	0.871
3H-2, 40	19.60	0.951
3H-2, 50	19.70	0.894
3H-2, 60	19.80	0.871
3H-2, 70	19.90	0.899
3H-2, 80	20.00	0.880
3H-2, 90	20.10	0.846
3H-2, 100	20.20	0.803
3H-2, 110	20.30	0.782
3H-2, 120	20.40	0.869
3H-2, 130	20.50	0.859
3H-2, 140	20.60	0.795
3H-3, 70	21.40	0.858
3H-4, 70	22.90	0.884
3H-5, 70	24.40	0.921
3H-6, 80	26.00	0.943
3H-7, 40	27.00	0.745
5H-1, 70	37.60	1.061
5H-2, 70	39.10	0.928
5H-3, 70	40.60	0.963
5H-4, 70	42.10	1.007
5H-5, 70	43.60	0.971
5H-6, 70	45.10	0.968
5H-7, 30	46.20	0.973
6H-1, 70	47.30	0.952
6H-2, 70	48.80	1.118
6H-3, 70	50.30	1.214
6H-4, 70	51.80	1.151
6H-5, 70	53.30	0.988
6H-6, 70	54.80	1.021
6H-7, 40	56.00	1.338
7H-1, 80	57.10	0.980
7H-2, 80	58.60	0.901
7H-3, 80	60.10	0.962
7H-4, 80	61.60	0.933
7H-5, 80	63.10	0.955
7H-6, 80	64.60	0.920
7H-7, 30	65.60	0.964
8H-1, 80	66.80	0.968
8H-2, 80	68.30	1.014
8H-3, 40	69.40	1.151
9H-1, 80	76.40	1.318
9H-2, 80	77.90	1.273
9H-3, 10	78.70	1.259
9H-3, 20	78.80	1.191
9H-3, 30	78.90	1.172
9H-3, 40	79.00	1.164
9H-3, 50	79.10	1.313
9H-3, 60	79.20	1.318
9H-3, 70	79.30	1.333
9H-3, 80	79.40	1.398
9H-3, 90	79.50	1.523
9H-3, 100	79.60	1.297
9H-3, 110	79.70	1.317
9H-3, 120	79.80	1.255
9H-3, 130	79.90	1.298
9H-3, 140	80.00	1.097
9H-4, 80	80.90	1.199
9H-5, 80	82.40	1.329
9H-6, 80	83.90	1.222
10H-1, 80	86.00	1.238
10H-2, 80	87.50	1.231

Table 13 (continued).

Section interval (cm)	Depth (mbsf)	Thermal conductivity ($W \cdot m^{-1} \cdot K^{-1}$)
115-711A-		
10H-3, 80	89.00	1.206
10H-4, 80	90.50	1.222
10H-5, 80	92.00	1.234
10H-6, 80	93.50	1.390
10H-7, 40	94.60	1.252
11H-1, 80	95.60	1.403
11H-2, 80	97.10	1.458
11H-3, 80	98.60	1.503
11H-4, 80	100.10	1.369
11H-5, 80	101.60	1.278
11H-6, 110	103.40	1.352
11H-7, 40	104.20	1.331
12X-1, 80	105.30	1.436
12X-2, 80	106.80	1.317
12X-3, 80	108.30	1.295
13X-1, 80	115.00	1.188
13X-2, 80	116.50	1.357
13X-3, 80	118.00	1.108
13X-4, 80	119.50	1.725
13X-5, 80	121.00	1.116
13X-6, 80	122.50	1.424
14X-1, 80	124.70	1.330
14X-2, 80	126.20	1.293
14X-3, 80	127.70	1.223
14X-4, 80	129.20	1.444
14X-5, 80	130.70	1.272
14X-6, 40	131.80	1.301
15X-1, 80	134.40	1.065
15X-2, 80	135.90	1.290
15X-3, 80	137.40	1.342
15X-4, 80	138.90	1.324
15X-5, 80	140.40	1.200
15X-6, 80	141.90	1.255
16X-1, 80	144.10	1.344
16X-2, 80	145.60	1.283
16X-3, 80	147.10	1.291
16X-4, 80	148.60	1.349
16X-5, 80	150.10	1.334
16X-6, 80	151.60	1.363
16X-7, 17	152.47	1.364
17X-1, 80	153.80	1.239
17X-2, 80	155.30	1.272
17X-3, 70	156.70	1.177
17X-4, 80	158.30	1.042
17X-5, 80	159.80	1.113
17X-6, 80	161.30	1.369
17X-7, 20	162.20	1.359
18X-1, 81	163.51	1.291
18X-2, 81	165.01	1.252
18X-3, 82	166.52	1.115
18X-4, 81	168.01	0.857
19X-1, 80	173.20	1.401
19X-2, 80	174.70	0.857
19X-4, 80	177.70	1.289
19X-5, 80	179.20	1.156
19X-6, 80	180.70	1.163
20X-1, 80	182.90	1.139
20X-2, 80	184.40	0.678
20X-3, 80	185.90	0.867
20X-4, 80	187.40	1.225
20X-5, 25	188.35	1.232
21X-1, 80	192.50	1.173
21X-2, 80	194.00	1.128
21X-3, 80	195.50	1.210
21X-4, 80	197.00	1.353
21X-5, 80	198.50	1.216
22X-1, 80	202.20	1.159
22X-2, 80	203.70	1.159
22X-3, 80	205.20	1.131
22X-4, 40	206.30	1.161
23X-1, 10	211.20	1.068
23X-1, 20	211.30	0.884
23X-1, 30	211.40	0.730
23X-1, 40	211.50	0.865

Table 13 (Continued)

Section interval (cm)	Depth (mbsf)	Thermal conductivity ($W \cdot m^{-1} \cdot K^{-1}$)
115-711A-		
23X-1, 50	211.60	0.875
23X-1, 60	211.70	1.028
23X-1, 70	211.80	0.961
23X-1, 80	211.90	1.072
23X-1, 90	212.00	0.870
23X-1, 100	212.10	0.942
23X-1, 110	212.20	0.723
23X-1, 120	212.30	1.102
23X-1, 130	212.40	1.073
23X-1, 140	212.50	1.006
23X-2, 80	213.40	1.136
23X-3, 80	214.90	0.949
23X-4, 80	216.40	1.102
23X-5, 80	217.90	1.112
23X-6, 80	219.40	1.278
24X-1, 80	221.50	1.224
24X-2, 80	223.00	1.149
24X-3, 80	224.50	1.155
24X-4, 80	226.00	1.098
24X-5, 80	227.50	1.192
25X-1, 80	231.10	1.085
25X-2, 80	232.60	1.110
25X-3, 80	234.10	1.093
25X-4, 80	235.60	1.014
25X-5, 40	236.70	1.171

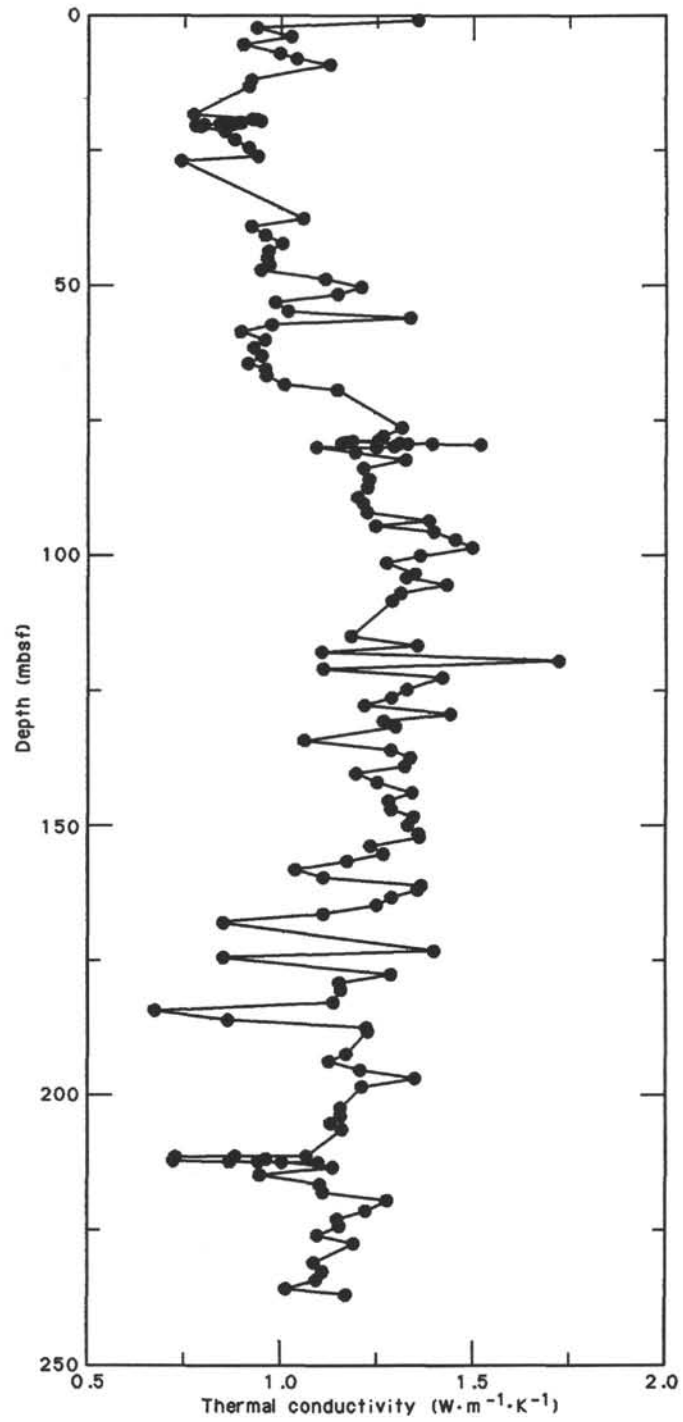


Figure 27. Thermal conductivity at Site 711.

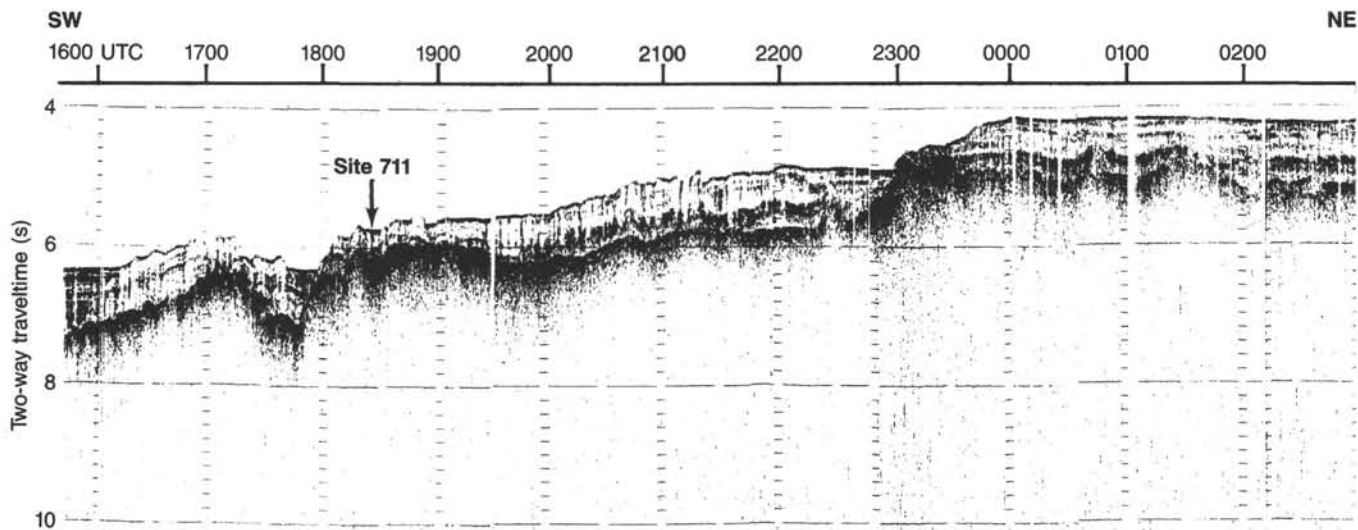


Figure 29. The V34-06 cruise SCS line (9–10 August 1977) which shows the stepped nature of the northern flank of the Madingley Rise. Site 711 is located 25 nmi north-northwest of this line at the approximate depth indicated.

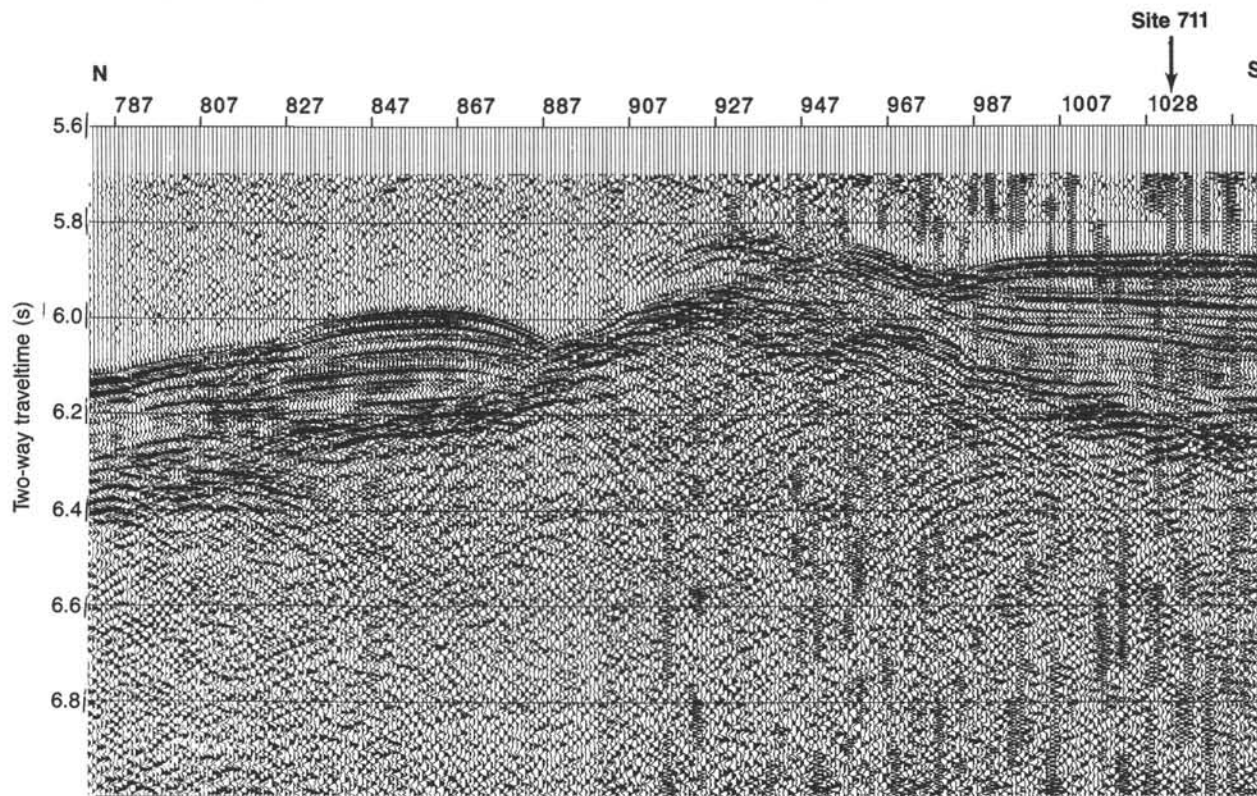
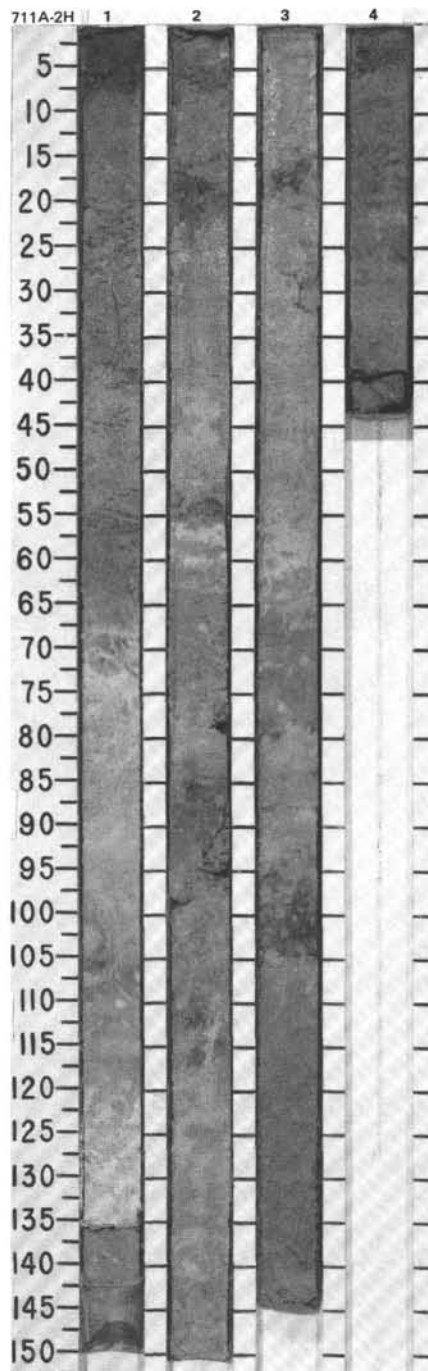


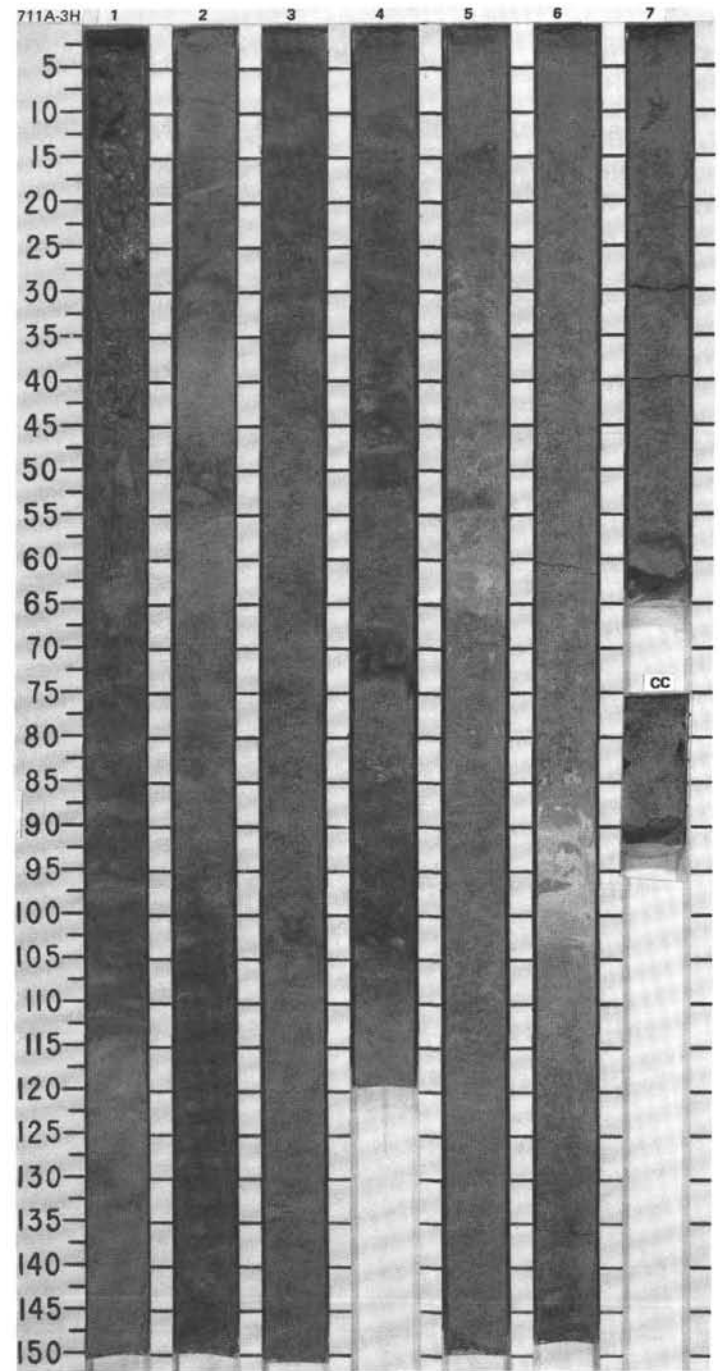
Figure 30. The *JOIDES Resolution* single-channel seismic (SCS), water-gun reflection profile recorded 10 June 1987 over Site 711.

SITE 711 HOLE A CORE 2H CORED INTERVAL 4436.3-4445.9 mbsf; 8.1-17.7 mbsf

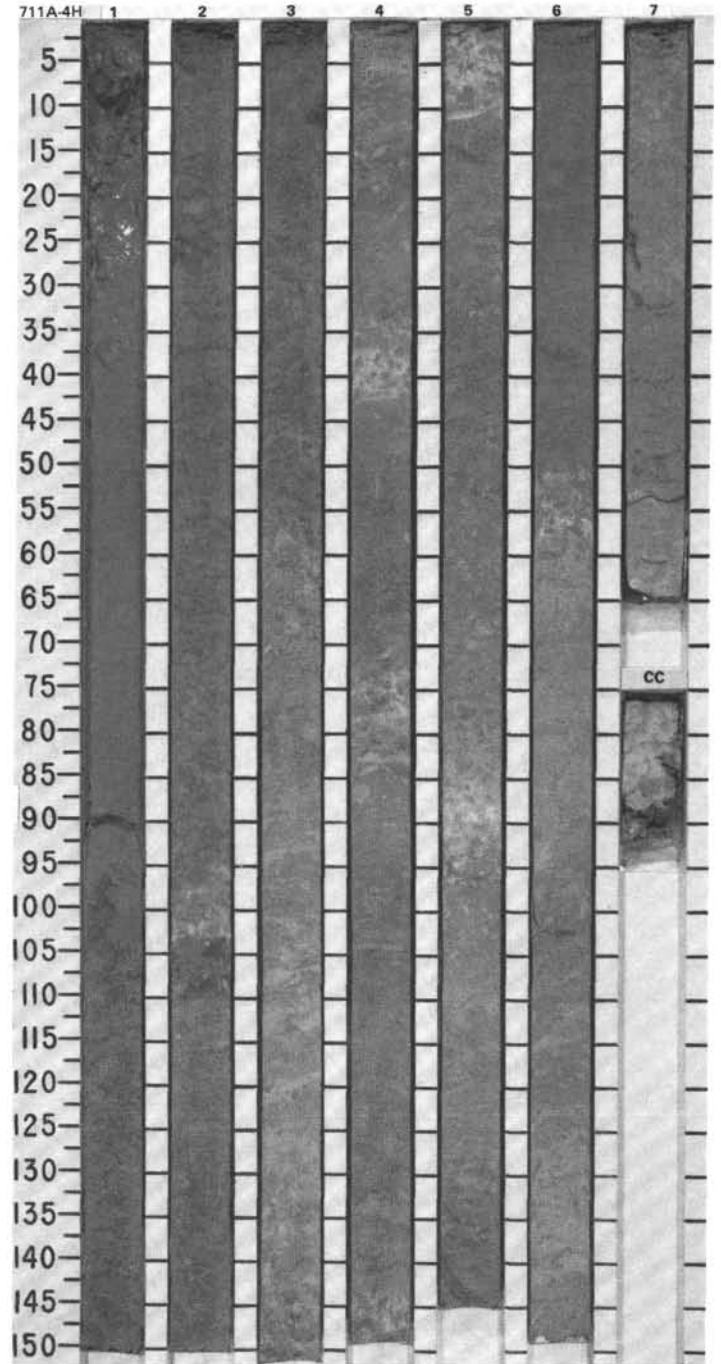
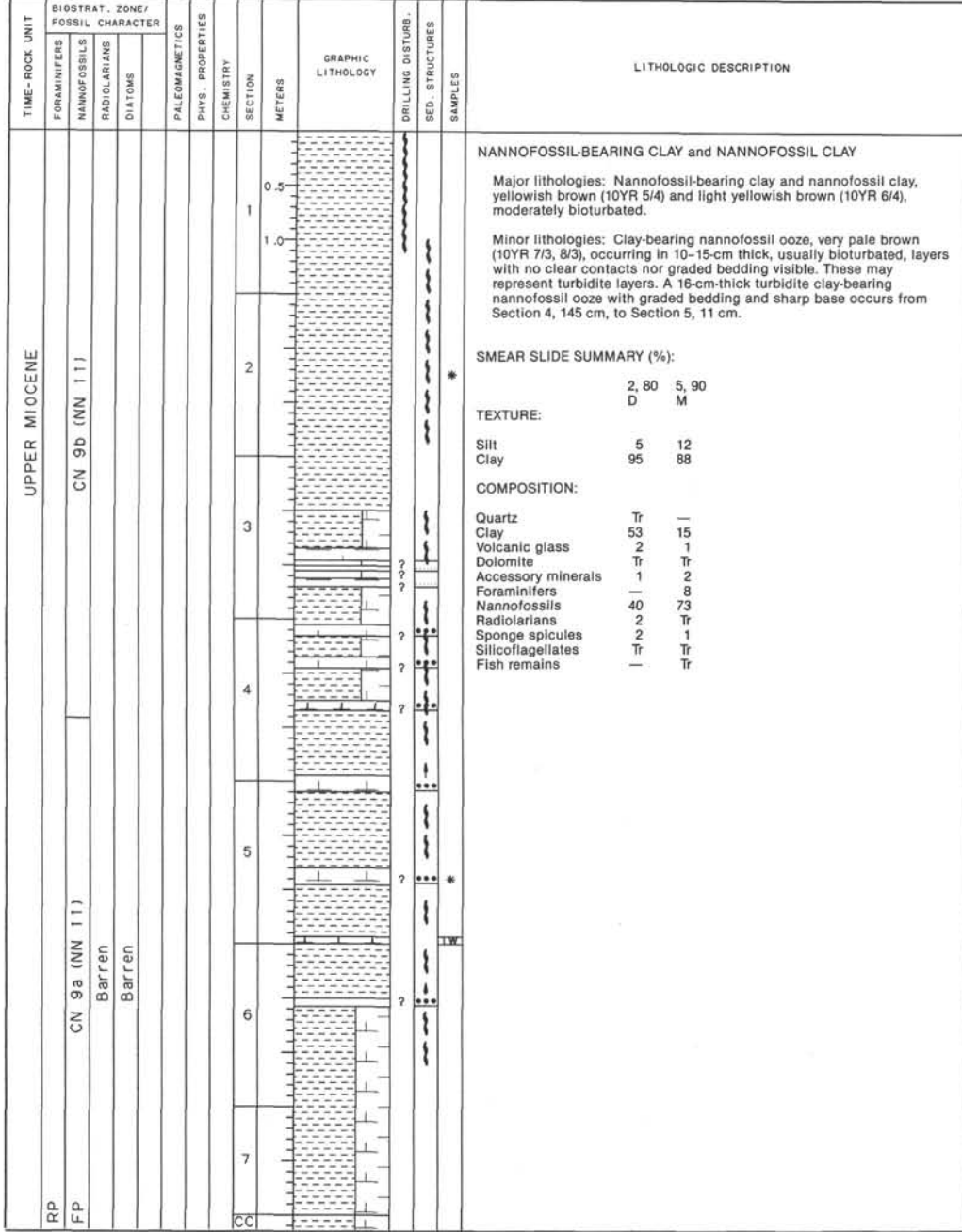
TIME-ROCK UNIT		BIOSTRAT. ZONE/ FOSSIL CHARACTER				PALEOMAGNETICS	PHYS. PROPERTIES	CHEMISTRY	SECTION METERS	GRAPHIC LITHOLOGY	DRILLING DISTURB. SED. STRUCTURES	SAMPLES	LITHOLOGIC DESCRIPTION																																													
UPPER PLIOCENE	PLEISTOCENE	FORAMINIFERS	NANNOFOSSILS	RADIOLARIANS	DIATOMS																																																					
RP													<p>NANNOFOSSIL CLAY and NANNOFOSSIL-BEARING CLAY</p> <p>Major lithology: Nannofossil clay and nannofossil-bearing clay, yellowish brown (10YR 6/4) and light yellowish brown (10YR 6/4) to very pale brown (10YR 7/4, 7/3). All color contacts are gradational, and mottling is common due to bioturbation.</p> <p>Minor lithology: One turbidite layer, 15 cm thick, white (10YR 8/2) consisting of foraminifer-nannofossil ooze, with sharp basal contact, coarse-sized particles at the base, and general grading, in Section 1, 121-136 cm.</p> <p>SMEAR SLIDE SUMMARY (%):</p> <table border="0"> <tr> <td></td> <td>1, 75</td> <td>4, 18</td> </tr> <tr> <td></td> <td>D</td> <td>D</td> </tr> </table> <p>TEXTURE:</p> <table border="0"> <tr> <td>Silt</td> <td>7</td> <td>7</td> </tr> <tr> <td>Clay</td> <td>93</td> <td>93</td> </tr> </table> <p>COMPOSITION:</p> <table border="0"> <tr> <td>Quartz</td> <td>—</td> <td>Tr</td> </tr> <tr> <td>Clay</td> <td>15</td> <td>50</td> </tr> <tr> <td>Volcanic glass</td> <td>—</td> <td>1</td> </tr> <tr> <td>Accessory minerals</td> <td>—</td> <td>2</td> </tr> <tr> <td>Foraminifers</td> <td>5</td> <td>1</td> </tr> <tr> <td>Nannofossils</td> <td>78</td> <td>43</td> </tr> <tr> <td>Radiolarians</td> <td>1</td> <td>Tr</td> </tr> <tr> <td>Sponge spicules</td> <td>Tr</td> <td>Tr</td> </tr> <tr> <td>Silicoflagellates</td> <td>Tr</td> <td>Tr</td> </tr> <tr> <td>Fish remains</td> <td>—</td> <td>Tr</td> </tr> <tr> <td>Mollusk fragments</td> <td>1</td> <td>3</td> </tr> </table>		1, 75	4, 18		D	D	Silt	7	7	Clay	93	93	Quartz	—	Tr	Clay	15	50	Volcanic glass	—	1	Accessory minerals	—	2	Foraminifers	5	1	Nannofossils	78	43	Radiolarians	1	Tr	Sponge spicules	Tr	Tr	Silicoflagellates	Tr	Tr	Fish remains	—	Tr	Mollusk fragments	1	3
	1, 75	4, 18																																																								
	D	D																																																								
Silt	7	7																																																								
Clay	93	93																																																								
Quartz	—	Tr																																																								
Clay	15	50																																																								
Volcanic glass	—	1																																																								
Accessory minerals	—	2																																																								
Foraminifers	5	1																																																								
Nannofossils	78	43																																																								
Radiolarians	1	Tr																																																								
Sponge spicules	Tr	Tr																																																								
Silicoflagellates	Tr	Tr																																																								
Fish remains	—	Tr																																																								
Mollusk fragments	1	3																																																								
AM		CN 12d (NN 18)	CN 13 - 14a					1																																																		
	Barren	<i>P. prismatum</i>						2																																																		
		Barren						3																																																		
								4																																																		



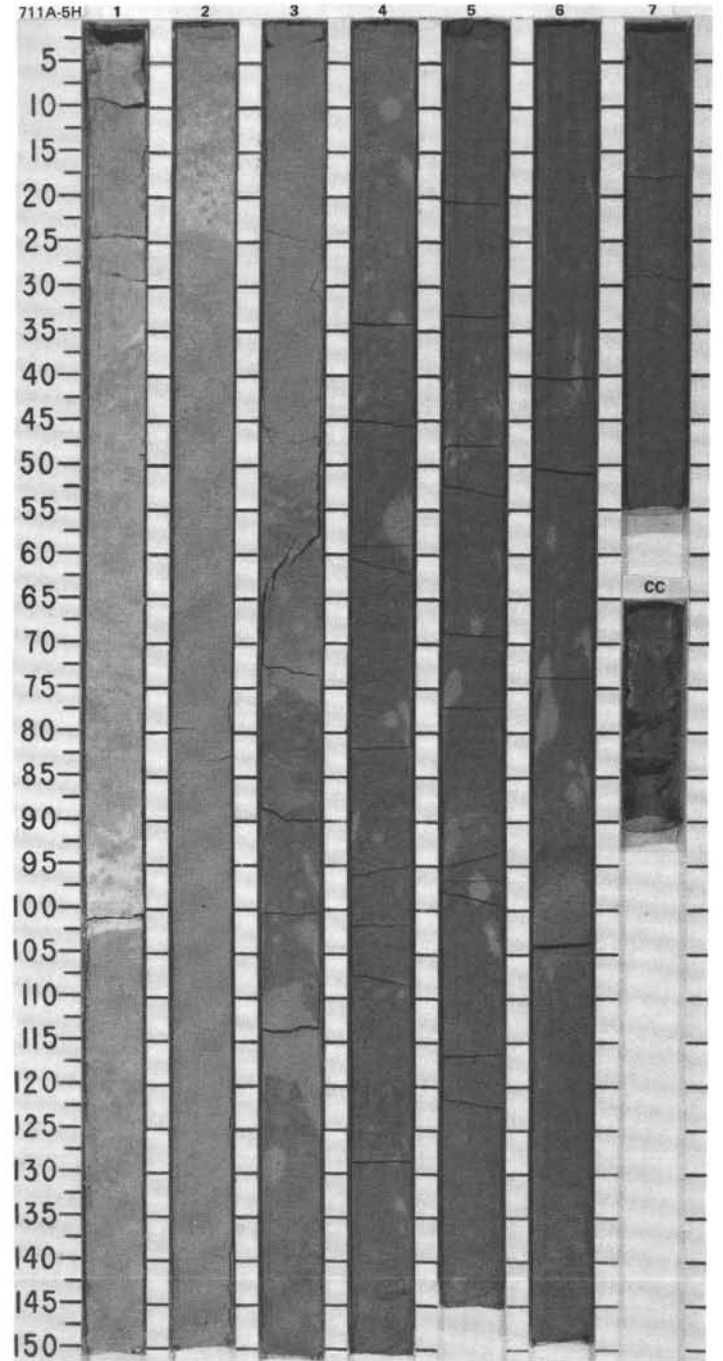
TIME-ROCK UNIT	BIOSTRAT. ZONE/ FOSSIL CHARACTER				PALEOMAGNETICS	PHYS. PROPERTIES	CHEMISTRY	SECTION	METERS	GRAPHIC LITHOLOGY	DRILLING DISTURB. SED. STRUCTURES SAMPLES	LITHOLOGIC DESCRIPTION																																																						
	FORAMINIFERS	NANNOFOSSILS	RADIOLARIANS	DIATOMS																																																														
LOWER PLIOCENE		Barren	CN 10b	Barren				1	0.5 1.0			<p>CLAY</p> <p>Major lithology: Clay, with alternating color cycles of light yellowish brown (10YR 6/4) to yellowish brown (10YR 5/4), and gray (10YR 5/1), grayish brown (10YR 5/2), and brown (10YR 5/3) to dark gray (10YR 4/1). Moderately bioturbated throughout.</p> <p>Minor lithology: One turbidite layer, graded, 13-cm-thick, consisting of foraminifer-nannofossil ooze, very pale brown (10YR 8/3), in Section 6, 90-103 cm.</p> <p>SMEAR SLIDE SUMMARY (%):</p> <table border="0"> <tr> <td></td> <td>3, 90</td> <td>6, 96</td> </tr> <tr> <td></td> <td>D</td> <td>M</td> </tr> </table> <p>TEXTURE:</p> <table border="0"> <tr> <td>Sand</td> <td>—</td> <td>32</td> </tr> <tr> <td>Silt</td> <td>5</td> <td>—</td> </tr> <tr> <td>Clay</td> <td>95</td> <td>68</td> </tr> </table> <p>COMPOSITION:</p> <table border="0"> <tr> <td>Quartz</td> <td>Tr</td> <td>—</td> </tr> <tr> <td>Feldspar</td> <td>Tr</td> <td>—</td> </tr> <tr> <td>Mica</td> <td>Tr</td> <td>—</td> </tr> <tr> <td>Clay</td> <td>90</td> <td>—</td> </tr> <tr> <td>Volcanic glass</td> <td>—</td> <td>Tr</td> </tr> <tr> <td>Dolomite</td> <td>Tr</td> <td>—</td> </tr> <tr> <td>Accessory minerals</td> <td>Tr</td> <td>1</td> </tr> <tr> <td>Foraminifers</td> <td>—</td> <td>30</td> </tr> <tr> <td>Nannofossils</td> <td>—</td> <td>68</td> </tr> <tr> <td>Radiolarians</td> <td>1</td> <td>Tr</td> </tr> <tr> <td>Sponge spicules</td> <td>4</td> <td>1</td> </tr> <tr> <td>Silicoflagellates</td> <td>—</td> <td>Tr</td> </tr> <tr> <td>Micrite</td> <td>5</td> <td>—</td> </tr> </table>		3, 90	6, 96		D	M	Sand	—	32	Silt	5	—	Clay	95	68	Quartz	Tr	—	Feldspar	Tr	—	Mica	Tr	—	Clay	90	—	Volcanic glass	—	Tr	Dolomite	Tr	—	Accessory minerals	Tr	1	Foraminifers	—	30	Nannofossils	—	68	Radiolarians	1	Tr	Sponge spicules	4	1	Silicoflagellates	—	Tr	Micrite	5	—
	3, 90	6, 96																																																																
	D	M																																																																
Sand	—	32																																																																
Silt	5	—																																																																
Clay	95	68																																																																
Quartz	Tr	—																																																																
Feldspar	Tr	—																																																																
Mica	Tr	—																																																																
Clay	90	—																																																																
Volcanic glass	—	Tr																																																																
Dolomite	Tr	—																																																																
Accessory minerals	Tr	1																																																																
Foraminifers	—	30																																																																
Nannofossils	—	68																																																																
Radiolarians	1	Tr																																																																
Sponge spicules	4	1																																																																
Silicoflagellates	—	Tr																																																																
Micrite	5	—																																																																
UPPER MIOCENE		Barren		Barren			2																																																											
							3																																																											
							4																																																											
	CN 9b (NN 11)						5																																																											
							6																																																											
							7																																																											
RP							CC																																																											



SITE 711 HOLE A CORE 4H CORED INTERVAL 4455.5-4465.1 mbsl; 27.3-36.9 mbsf

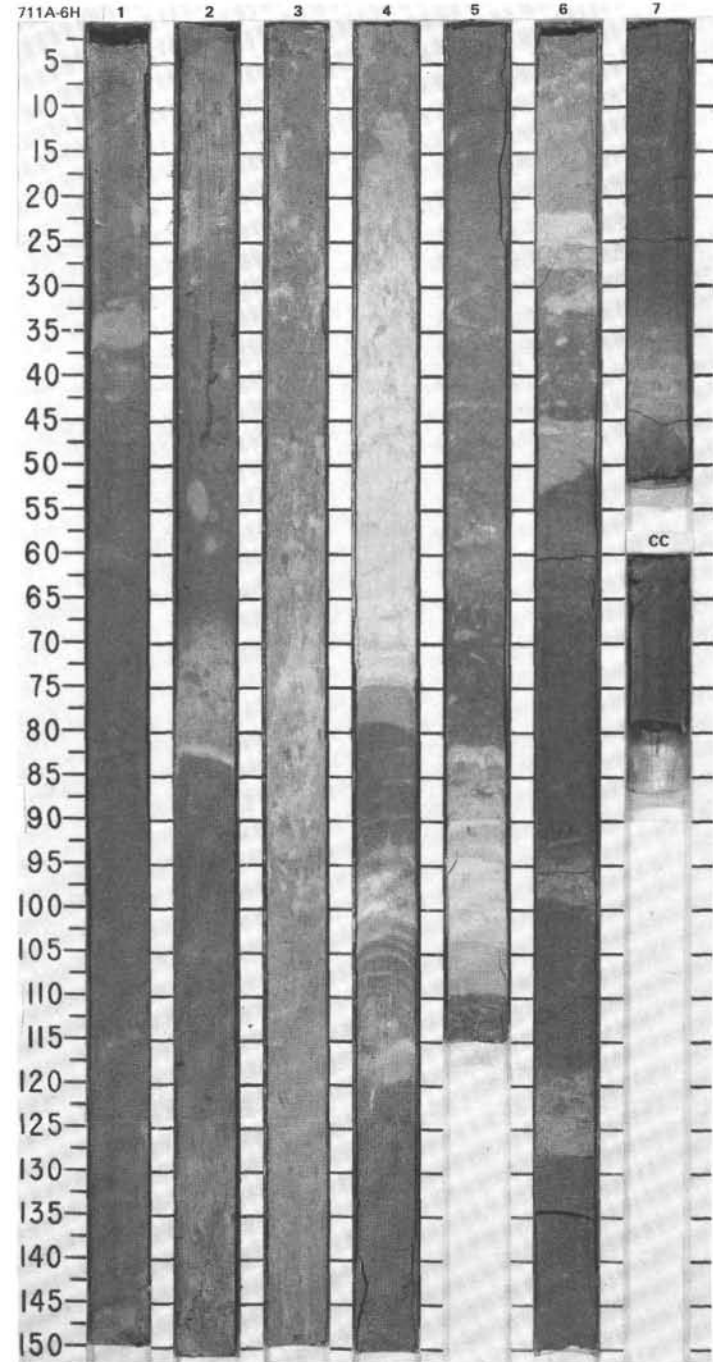


TIME-ROCK UNIT	BIOSTRAT. ZONE/ FOSSIL CHARACTER				PALEOMAGNETICS	PHYS. PROPERTIES	CHEMISTRY	SECTION	METERS	GRAPHIC LITHOLOGY	DRILLING DISTURB.	SED. STRUCTURES	SAMPLES	LITHOLOGIC DESCRIPTION																																								
	FORAMINIFERS	NANNOFOSSILS	RADIOLARIANS	DIAZONES																																																		
UPPER MIOCENE	CN 8 - CN 9a (NN 10 - NN 11)							1	0.5					<p>NANNOFOSSIL CLAY and VOLCANIC GLASS-BEARING CLAY</p> <p>Major lithologies: Nannofossil clay at top of the core, Section 1, 0 cm, to Section 2, 55 cm, very pale brown (10YR 7/3) to light yellowish brown (10YR 8/4), bioturbated and mottled, grades downcore to volcanic glass-bearing clay, homogeneous, light yellowish brown (10YR 5/2), and slightly bioturbated.</p> <p>Minor lithologies:</p> <p>a. One, possibly two, turbidite layers, 8-10 cm thick, very pale brown (10YR 7/3, 8/3), with sharp base, consisting of clay-bearing nannofossil ooze; in Section 1, 96-103 cm, and Section 2, 12-22 cm.</p> <p>b. Within the volcanic glass-bearing clay, a few scattered several-cm-thick in diameter, light yellowish brown (10YR 6/4) blebs, interpreted as either large infilled burrows(?) or diagenetic in origin.</p> <p>* SMEAR SLIDE SUMMARY (%):</p> <table border="0"> <tr> <td></td> <td>2</td> <td>100</td> <td>5</td> <td>117</td> </tr> <tr> <td></td> <td>D</td> <td></td> <td>D</td> <td></td> </tr> </table> <p>TEXTURE:</p> <table border="0"> <tr> <td>Silt</td> <td>32</td> <td>33</td> </tr> <tr> <td>Clay</td> <td>68</td> <td>67</td> </tr> </table> <p>COMPOSITION:</p> <table border="0"> <tr> <td>Feldspar</td> <td>Tr</td> <td>—</td> </tr> <tr> <td>Clay</td> <td>77</td> <td>65</td> </tr> <tr> <td>Volcanic glass</td> <td>20</td> <td>30</td> </tr> <tr> <td>Dolomite</td> <td>Tr</td> <td>—</td> </tr> <tr> <td>Accessory minerals</td> <td>—</td> <td>3</td> </tr> <tr> <td>Nannofossils</td> <td>1</td> <td>2</td> </tr> <tr> <td>Fish remains</td> <td>Tr</td> <td>—</td> </tr> <tr> <td>Bioclasts</td> <td>2</td> <td>—</td> </tr> </table>		2	100	5	117		D		D		Silt	32	33	Clay	68	67	Feldspar	Tr	—	Clay	77	65	Volcanic glass	20	30	Dolomite	Tr	—	Accessory minerals	—	3	Nannofossils	1	2	Fish remains	Tr	—	Bioclasts	2	—
		2	100	5	117																																																	
	D		D																																																			
Silt	32	33																																																				
Clay	68	67																																																				
Feldspar	Tr	—																																																				
Clay	77	65																																																				
Volcanic glass	20	30																																																				
Dolomite	Tr	—																																																				
Accessory minerals	—	3																																																				
Nannofossils	1	2																																																				
Fish remains	Tr	—																																																				
Bioclasts	2	—																																																				
MIDDLE - UPPER	Barren	Barren	Barren	Barren			2	1.0																																														
							3																																															
							4																																															
							5																																															
							6																																															
							7																																															
							CC																																															



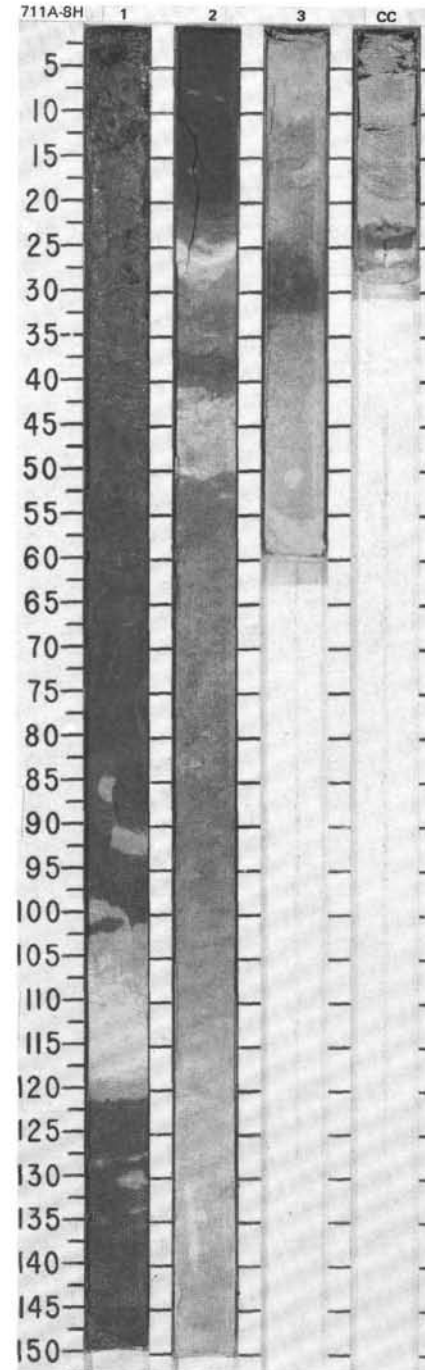
SITE 711 HOLE A CORE 6H CORED INTERVAL 4474.8-4484.5 mbsf; 46.6-56.3 mbsf

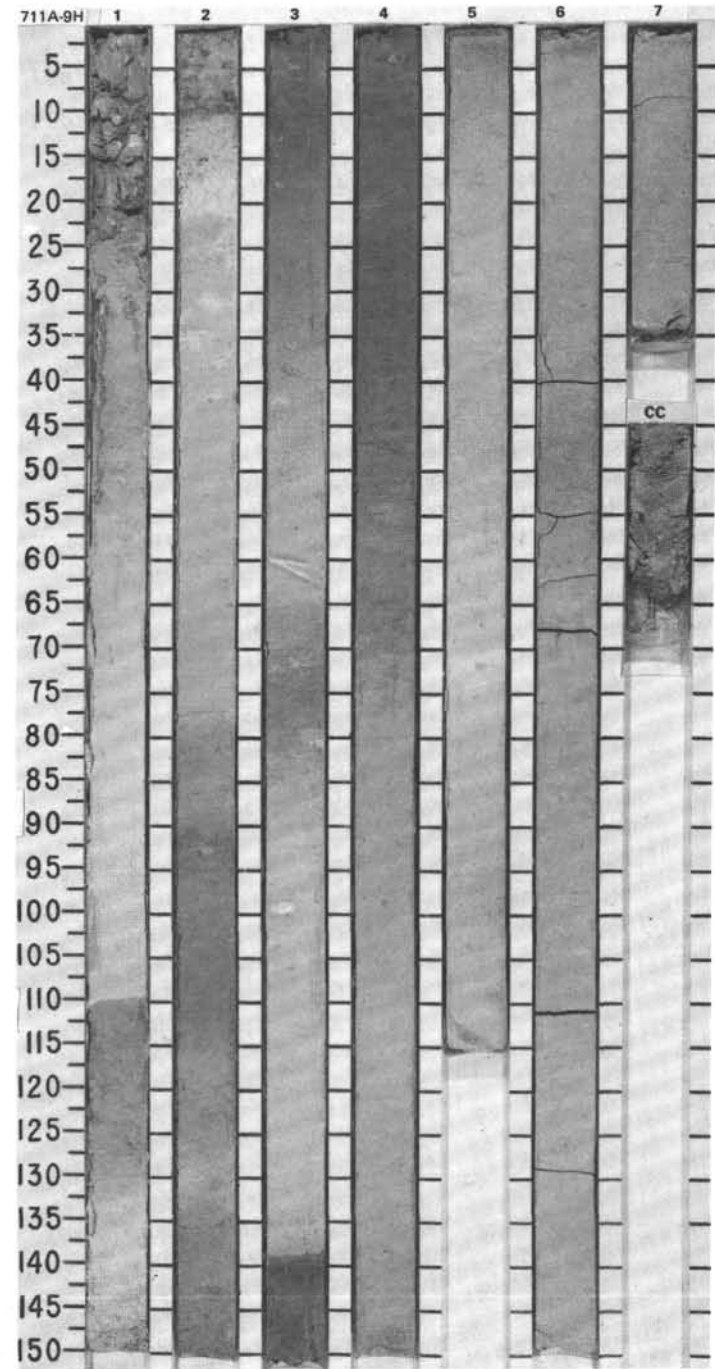
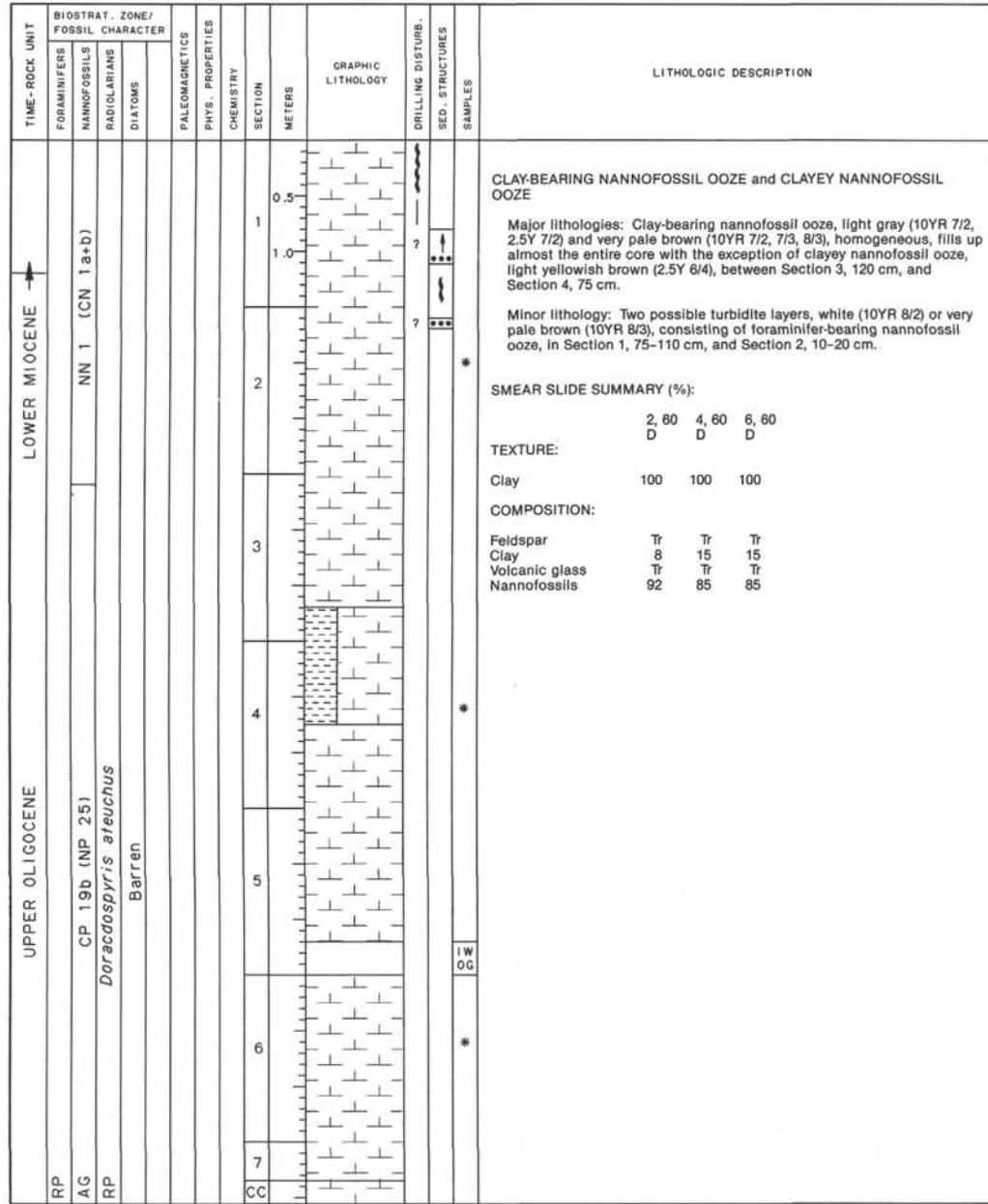
TIME-ROCK UNIT	BIOSTRAT. ZONE/ FOSSIL CHARACTER				PALEOMAGNETICS	PHYS. PROPERTIES	CHEMISTRY	SECTION	METERS	GRAPHIC LITHOLOGY	DRILLING DISTURB.	SED. STRUCTURES	SAMPLES	LITHOLOGIC DESCRIPTION																																	
	FORAMINIFERS	NANNOFOSSILS	RADIOLARIANS	DIAZOOMS																																											
LOWER MIDDLE MIOCENE	Barren							0.5						<p>VOLCANIC GLASS-BEARING CLAY and NANNOFOSSIL CLAY</p> <p>Major lithologies: Volcanic glass-bearing clay, dark grayish brown (10YR 4/2) and grayish brown (10YR 5/2), alternating with nannofossil clay, light yellowish brown (10YR 6/4), brown (10YR 5/3), pale brown (10YR 6/3), and very pale brown (10YR 7/3), with considerable mottling.</p> <p>Minor lithologies: Five, possibly six, turbidite layers, 4-15 cm thick, very pale brown (10YR 8/3), with sharp base and gradational top, consisting of foraminifer-nannofossil ooze, in Section 2, 70-82 cm; Section 4, 60-75 and 95-102 cm; Section 5, 93-103 cm; and Section 6, 21-25 cm. Possible 30-cm-thick turbidite layer in Section 3, 60-90 cm. The few cm just below turbidite layers usually have a characteristic light yellowish brown color (10YR 6/4) similar to the color of blebs scattered within the clay (see 115-711A-5H), both may be diagenetic in origin.</p> <p>SMEAR SLIDE SUMMARY (%):</p> <table border="1"> <tr> <td></td> <td>1, 80</td> <td>3, 80</td> </tr> <tr> <td></td> <td>D</td> <td>M</td> </tr> </table> <p>TEXTURE:</p> <table border="1"> <tr> <td>Silt</td> <td>41</td> <td>3</td> </tr> <tr> <td>Clay</td> <td>59</td> <td>97</td> </tr> </table> <p>COMPOSITION:</p> <table border="1"> <tr> <td>Feldspar</td> <td>1</td> <td>—</td> </tr> <tr> <td>Clay</td> <td>59</td> <td>—</td> </tr> <tr> <td>Volcanic glass</td> <td>30</td> <td>2</td> </tr> <tr> <td>Dolomite</td> <td>—</td> <td>1</td> </tr> <tr> <td>Accessory minerals:</td> <td></td> <td></td> </tr> <tr> <td> Opales</td> <td>10</td> <td>—</td> </tr> <tr> <td> Nannofossils</td> <td>—</td> <td>97</td> </tr> </table>		1, 80	3, 80		D	M	Silt	41	3	Clay	59	97	Feldspar	1	—	Clay	59	—	Volcanic glass	30	2	Dolomite	—	1	Accessory minerals:			Opales	10	—	Nannofossils	—	97
		1, 80	3, 80																																												
		D	M																																												
	Silt	41	3																																												
	Clay	59	97																																												
	Feldspar	1	—																																												
	Clay	59	—																																												
Volcanic glass	30	2																																													
Dolomite	—	1																																													
Accessory minerals:																																															
Opales	10	—																																													
Nannofossils	—	97																																													
Barren							1.0																																								
CN 3 - CN 4 (NN 4 - NN 5)							2																																								
Barren							3																																								
Barren							4																																								
Barren							5																																								
							6																																								
							7																																								
							CC																																								



SITE 711 HOLE A CORE 8H CORED INTERVAL 4494.2-4503.8 mbsf: 66.0-75.6 mbsf

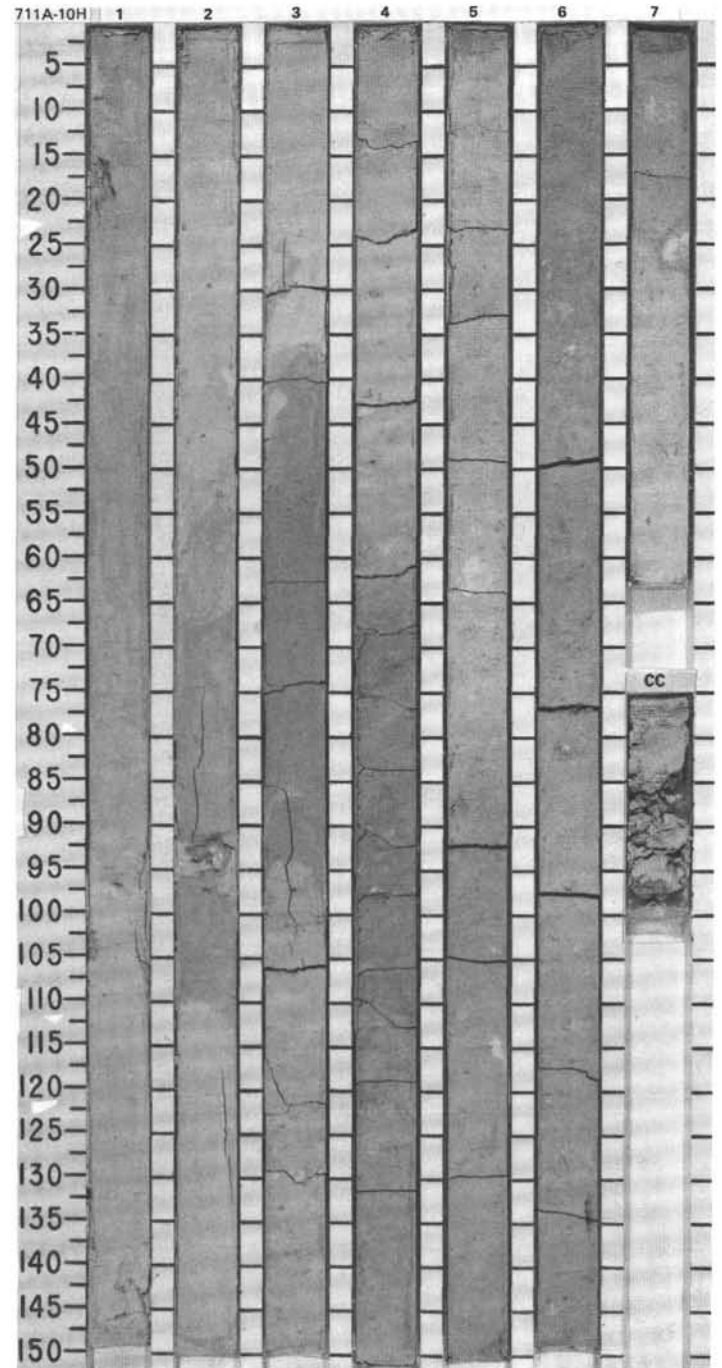
TIME-ROCK UNIT	BIOSTRAT. ZONE/ FOSSIL CHARACTER				PALEOMAGNETICS	PHYS. PROPERTIES CHEMISTRY	SECTION	METERS	GRAPHIC LITHOLOGY	DRILLING DISTURB.	SED. STRUCTURES	SAMPLES	LITHOLOGIC DESCRIPTION																														
	FORAMINIFERS	NANNOFOSSILS	RADIOLARIANS	DIATOMS																																							
LOWER MIOCENE	RP	AM	CN 1c (NN 2)	Barren			1	0.5 1.0					VOLCANIC GLASS-BEARING CLAY and CLAYEY NANNOFOSSIL OOZE Major lithologies: Volcanic glass-bearing clay, dark grayish brown (10YR 4/2), with scattered blebs, light yellowish brown (10YR 6/4), in Section 1, 0-150 cm, and Section 2, 0-20 cm. Rest of the core consists of clayey nannofossil ooze, pale yellow (2.5Y 7/4) and very pale brown (10YR 8/2), slightly bioturbated. Minor lithology: Three 2-10-cm-thick turbidite layers, very pale brown (10YR 8/3), consisting of foraminifer-bearing nannofossil ooze, in Section 1, 107-117 cm, and Section 2, 20-22 and 40-48 cm. SMEAR SLIDE SUMMARY (%): <table style="margin-left: 40px;"> <tr> <td></td> <td>1, 125</td> <td>2, 89</td> </tr> <tr> <td>D</td> <td></td> <td>D</td> </tr> </table> TEXTURE: <table style="margin-left: 40px;"> <tr> <td>Silt</td> <td>30</td> <td>10</td> </tr> <tr> <td>Clay</td> <td>70</td> <td>90</td> </tr> </table> COMPOSITION: <table style="margin-left: 40px;"> <tr> <td>Quartz</td> <td>Tr</td> <td>—</td> </tr> <tr> <td>Feldspar</td> <td>2</td> <td>2</td> </tr> <tr> <td>Clay</td> <td>50</td> <td>30</td> </tr> <tr> <td>Volcanic glass</td> <td>40</td> <td>8</td> </tr> </table> Accessory minerals: <table style="margin-left: 40px;"> <tr> <td>Opauques</td> <td>Tr</td> <td>—</td> </tr> <tr> <td>Nannofossils</td> <td>8</td> <td>60</td> </tr> </table>		1, 125	2, 89	D		D	Silt	30	10	Clay	70	90	Quartz	Tr	—	Feldspar	2	2	Clay	50	30	Volcanic glass	40	8	Opauques	Tr	—	Nannofossils	8	60
	1, 125	2, 89																																									
D		D																																									
Silt	30	10																																									
Clay	70	90																																									
Quartz	Tr	—																																									
Feldspar	2	2																																									
Clay	50	30																																									
Volcanic glass	40	8																																									
Opauques	Tr	—																																									
Nannofossils	8	60																																									
			Barren			2																																					
						3																																					
						CC																																					



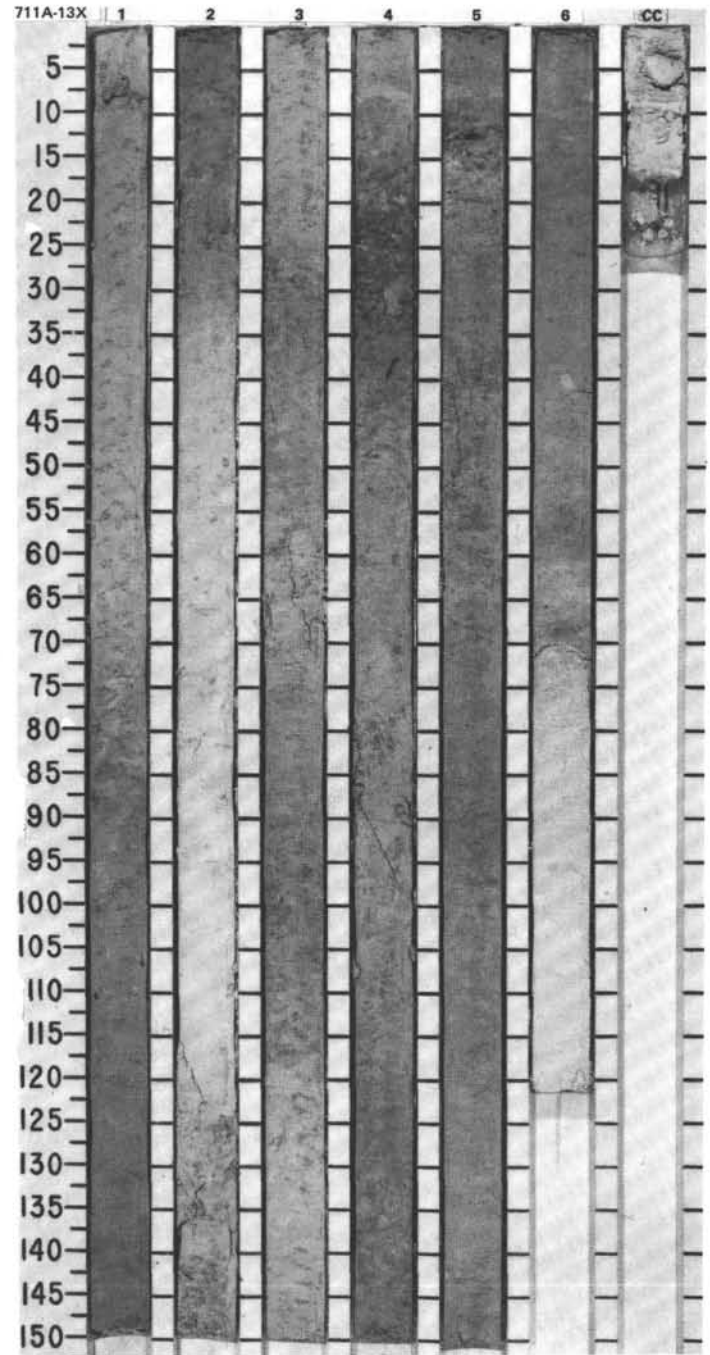


SITE 711 HOLE A CORE 10H CORED INTERVAL 4513.4-4523.0 mbsf: 85.2-94.8 mbsf

TIME-ROCK UNIT	BIOSTRAT. ZONE/ FOSSIL CHARACTER				PALEOMAGNETICS	PHYS. PROPERTIES	CHEMISTRY	SECTION	METERS	GRAPHIC LITHOLOGY	DRILLING DISTURB.	SED. STRUCTURES	SAMPLES	LITHOLOGIC DESCRIPTION																																																												
	FORAMINIFERS	NANNOFOSSILS	RADIOLARIANS	DIATOMS																																																																						
UPPER OLIGOCENE																																																																										
CM	P 19 (turbidite ?)													<p>NANNOFOSSIL OOZE and CLAY-BEARING NANNOFOSSIL OOZE</p> <p>Major lithologies: Nannofossil ooze, white (2.5Y 8/2) and light gray (10YR 7/2, 2.5Y 7/2) to light yellowish brown (2.5Y 6/4), in Section 1, 0 cm, to Section 4, 60 cm; gradually becoming clay-bearing nannofossil ooze, light brownish gray (2.5Y 6/2) to light gray (10YR 7/2, 2.5Y 7/2). The entire core is homogeneous and displays no clear evidence of bioturbation. The top of the core may be flow-in.</p> <p>SMEAR SLIDE SUMMARY (%):</p> <table border="1"> <thead> <tr> <th></th> <th>2, 47 D</th> <th>3, 70 D</th> <th>4, 42 D</th> </tr> </thead> <tbody> <tr> <td>TEXTURE:</td> <td></td> <td></td> <td></td> </tr> <tr> <td>Sand</td> <td>2</td> <td>—</td> <td>—</td> </tr> <tr> <td>Silt</td> <td>20</td> <td>20</td> <td>20</td> </tr> <tr> <td>Clay</td> <td>78</td> <td>80</td> <td>80</td> </tr> </tbody> </table> <p>COMPOSITION:</p> <table border="1"> <thead> <tr> <th></th> <th>2</th> <th>3</th> <th>4</th> </tr> </thead> <tbody> <tr> <td>Quartz</td> <td>—</td> <td>—</td> <td>Tr</td> </tr> <tr> <td>Clay</td> <td>12</td> <td>15</td> <td>15</td> </tr> <tr> <td>Volcanic glass</td> <td>Tr</td> <td>—</td> <td>—</td> </tr> <tr> <td>Accessory minerals:</td> <td></td> <td></td> <td></td> </tr> <tr> <td> Opales</td> <td>—</td> <td>Tr</td> <td>Tr</td> </tr> <tr> <td>Foraminifers</td> <td>2</td> <td>—</td> <td>—</td> </tr> <tr> <td>Nannofossils</td> <td>86</td> <td>85</td> <td>85</td> </tr> <tr> <td>Radiolarians</td> <td>—</td> <td>Tr</td> <td>—</td> </tr> <tr> <td>Sponge spicules</td> <td>Tr</td> <td>Tr</td> <td>—</td> </tr> </tbody> </table>		2, 47 D	3, 70 D	4, 42 D	TEXTURE:				Sand	2	—	—	Silt	20	20	20	Clay	78	80	80		2	3	4	Quartz	—	—	Tr	Clay	12	15	15	Volcanic glass	Tr	—	—	Accessory minerals:				Opales	—	Tr	Tr	Foraminifers	2	—	—	Nannofossils	86	85	85	Radiolarians	—	Tr	—	Sponge spicules	Tr	Tr	—
	2, 47 D	3, 70 D	4, 42 D																																																																							
TEXTURE:																																																																										
Sand	2	—	—																																																																							
Silt	20	20	20																																																																							
Clay	78	80	80																																																																							
	2	3	4																																																																							
Quartz	—	—	Tr																																																																							
Clay	12	15	15																																																																							
Volcanic glass	Tr	—	—																																																																							
Accessory minerals:																																																																										
Opales	—	Tr	Tr																																																																							
Foraminifers	2	—	—																																																																							
Nannofossils	86	85	85																																																																							
Radiolarians	—	Tr	—																																																																							
Sponge spicules	Tr	Tr	—																																																																							
AM	CP 19b (NP 25)																																																																									
RM	<i>Dorcatospyris atouchus</i>																																																																									
	Barren																																																																									
CC																																																																										

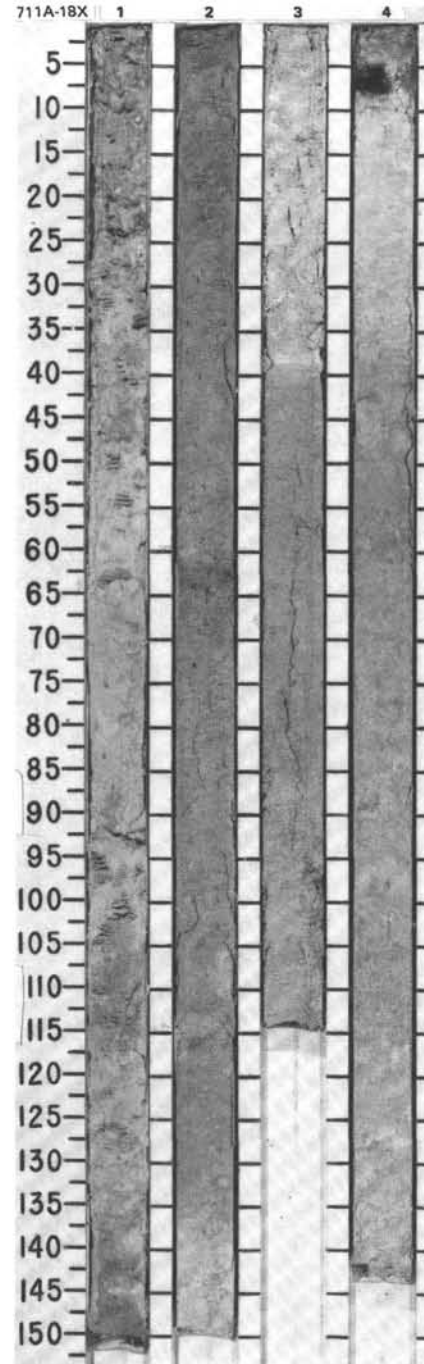


TIME-ROCK UNIT	BIOSTRAT. ZONE/ FOSSIL CHARACTER				PALEOMAGNETICS	PHYS. PROPERTIES	CHEMISTRY	SECTION	METERS	GRAPHIC LITHOLOGY	DRILLING DISTURB.	SED. STRUCTURES	SAMPLES	LITHOLOGIC DESCRIPTION																																																																	
	FORAMINIFERS	NANNOFOSSILS	RADIOLARIANS	DIATOMS																																																																											
LOWER OLIGOCENE														<p>CLAY-BEARING NANNOFOSSIL OOZE and CLAYEY NANNOFOSSIL OOZE</p> <p>Major lithologies: Clay-bearing nannofossil ooze, white (2.5Y 8/2), very pale brown (10YR 7/3, 7/4), light gray (2.5Y 7/2), and light yellowish brown (2.5Y 6/4), homogeneous, interlayered with clayey nannofossil ooze, light yellowish brown (10YR 6/2). No clear bioturbation, and only a few levels with color mottling.</p> <p>Minor lithologies:</p> <p>a. Two possible white (N9) turbidite layers consisting of nannofossil ooze, sharp base, gradational upper boundary, in Section 2, 75-120 cm; and Section 6, 115 cm, to CC, 15 cm. Two volcanic ash layers, mottled grayish brown (10YR 7/3) and very dark grayish brown (2.5Y 3/2).</p> <p>b. Clay-bearing volcanic ash with as much as 80% glass in Section 4, around 30 cm. Clay-bearing volcanic ash with 80% fresh, unaltered, sand-sized glass grains in Section 5, around 12 cm.</p> <p>c. First level of partial chalk in the turbidite layer, in Section 6, 133-135 cm.</p> <p>SMEAR SLIDE SUMMARY (%):</p> <table border="1"> <tr> <td></td> <td>2, 80</td> <td>4, 32</td> <td>5, 12</td> <td>5, 80</td> </tr> <tr> <td></td> <td>D</td> <td>D</td> <td>M</td> <td>D</td> </tr> </table> <p>TEXTURE:</p> <table border="1"> <tr> <td>Sand</td> <td>—</td> <td>60</td> <td>50</td> <td>—</td> </tr> <tr> <td>Silt</td> <td>20</td> <td>20</td> <td>30</td> <td>20</td> </tr> <tr> <td>Clay</td> <td>80</td> <td>20</td> <td>20</td> <td>80</td> </tr> </table> <p>COMPOSITION:</p> <table border="1"> <tr> <td>Quartz</td> <td>—</td> <td>1</td> <td>1</td> <td>—</td> </tr> <tr> <td>Clay</td> <td>9</td> <td>12</td> <td>12</td> <td>10</td> </tr> <tr> <td>Volcanic glass</td> <td>Tr</td> <td>80</td> <td>80</td> <td>Tr</td> </tr> </table> <p>Accessory minerals:</p> <table border="1"> <tr> <td>Opaques</td> <td>—</td> <td>5</td> <td>5</td> <td>—</td> </tr> <tr> <td>Foraminifers</td> <td>1</td> <td>—</td> <td>—</td> <td>—</td> </tr> <tr> <td>Nannofossils</td> <td>90</td> <td>1</td> <td>1</td> <td>90</td> </tr> <tr> <td>Radiolarians</td> <td>—</td> <td>1</td> <td>1</td> <td>Tr</td> </tr> <tr> <td>Sponge spicules</td> <td>Tr</td> <td>Tr</td> <td>Tr</td> <td>—</td> </tr> </table>		2, 80	4, 32	5, 12	5, 80		D	D	M	D	Sand	—	60	50	—	Silt	20	20	30	20	Clay	80	20	20	80	Quartz	—	1	1	—	Clay	9	12	12	10	Volcanic glass	Tr	80	80	Tr	Opaques	—	5	5	—	Foraminifers	1	—	—	—	Nannofossils	90	1	1	90	Radiolarians	—	1	1	Tr	Sponge spicules	Tr	Tr	Tr	—
	2, 80	4, 32	5, 12	5, 80																																																																											
	D	D	M	D																																																																											
Sand	—	60	50	—																																																																											
Silt	20	20	30	20																																																																											
Clay	80	20	20	80																																																																											
Quartz	—	1	1	—																																																																											
Clay	9	12	12	10																																																																											
Volcanic glass	Tr	80	80	Tr																																																																											
Opaques	—	5	5	—																																																																											
Foraminifers	1	—	—	—																																																																											
Nannofossils	90	1	1	90																																																																											
Radiolarians	—	1	1	Tr																																																																											
Sponge spicules	Tr	Tr	Tr	—																																																																											
B																																																																															
AM	CP 16b - CP 18 (NP 21 - NP 23)																																																																														
FM	<i>Theocyrtis tuberosa</i>																																																																														
RP	LOWER OLIGOCENE																																																																														
CC																																																																															

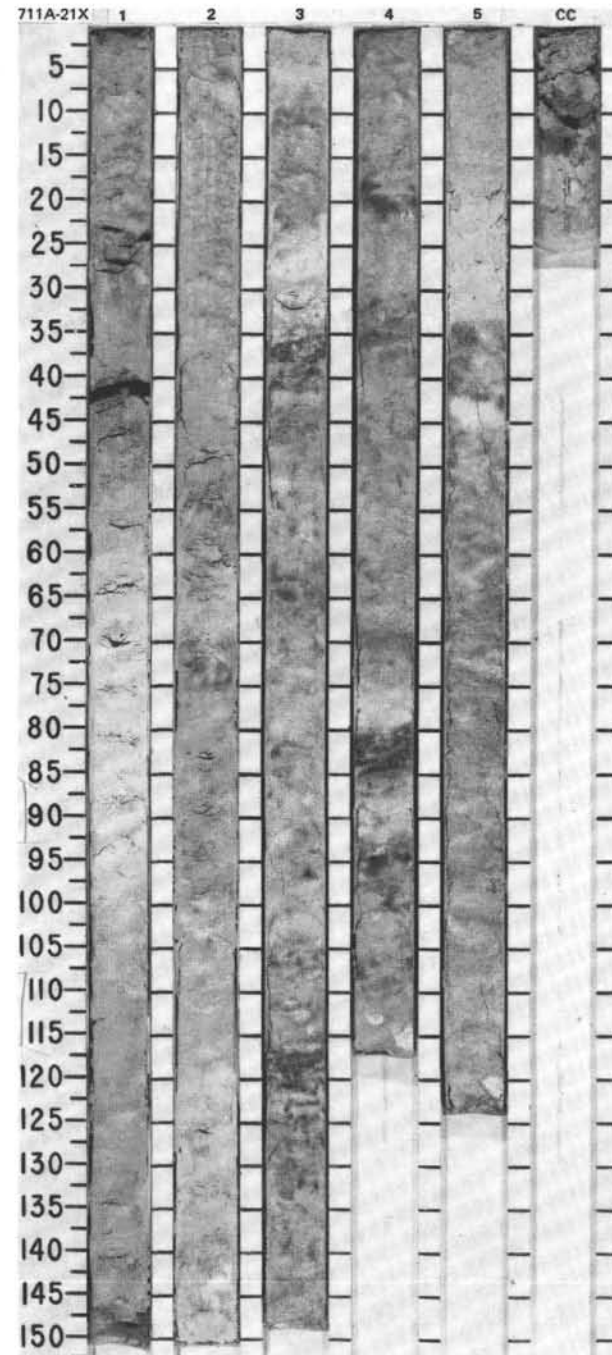


SITE 711 HOLE A CORE 18X CORED INTERVAL 4590.8-4600.5 mbsl; 162.7-172.4 mbsf

TIME-ROCK UNIT	BIOSTRAT. ZONE/ FOSSIL CHARACTER			PALEOMAGNETICS	PHYS. PROPERTIES	CHEMISTRY	SECTION	METERS	GRAPHIC LITHOLOGY	DRILLING DISTURB.	SED. STRUCTURES	SAMPLES	LITHOLOGIC DESCRIPTION																																										
	FORAMINIFERS	NANNOFOSSILS	RADIOLARIANS																																																				
UPPER EOCENE																																																							
B								0.5					<p>CLAY-BEARING NANNOFOSSIL CHALK</p> <p>Major lithology: Clay-bearing nannofossil chalk, very pale brown (10YR 7/4, 8/3) to white (10YR 8/2), homogeneous, slightly bioturbated.</p> <p>Minor lithology: Very pale brown layer, Section 3, 39-40 cm, can be interpreted as a turbidite, but upper color boundary is very sharp, whereas lower contact is gradational.</p> <p>SMEAR SLIDE SUMMARY (%):</p> <table border="0"> <tr> <td></td> <td>2, 80</td> <td>4, 6</td> </tr> <tr> <td></td> <td>D</td> <td>M</td> </tr> </table> <p>TEXTURE:</p> <table border="0"> <tr> <td>Sand</td> <td>3</td> <td>2</td> </tr> <tr> <td>Silt</td> <td>12</td> <td>8</td> </tr> <tr> <td>Clay</td> <td>85</td> <td>90</td> </tr> </table> <p>COMPOSITION:</p> <table border="0"> <tr> <td>Feldspar</td> <td>Tr</td> <td>—</td> </tr> <tr> <td>Clay</td> <td>5</td> <td>5</td> </tr> <tr> <td>Volcanic glass</td> <td>Tr</td> <td>1</td> </tr> <tr> <td>Dolomite</td> <td>—</td> <td>Tr</td> </tr> </table> <p>Accessory minerals:</p> <table border="0"> <tr> <td>Black MnO₂?</td> <td>—</td> <td>48</td> </tr> <tr> <td>Nannofossils</td> <td>83</td> <td>40</td> </tr> <tr> <td>Radiolarians</td> <td>8</td> <td>4</td> </tr> <tr> <td>Sponge spicules</td> <td>4</td> <td>2</td> </tr> <tr> <td>Silicoflagellates</td> <td>Tr</td> <td>—</td> </tr> </table>		2, 80	4, 6		D	M	Sand	3	2	Silt	12	8	Clay	85	90	Feldspar	Tr	—	Clay	5	5	Volcanic glass	Tr	1	Dolomite	—	Tr	Black MnO ₂ ?	—	48	Nannofossils	83	40	Radiolarians	8	4	Sponge spicules	4	2	Silicoflagellates	Tr	—
	2, 80	4, 6																																																					
	D	M																																																					
Sand	3	2																																																					
Silt	12	8																																																					
Clay	85	90																																																					
Feldspar	Tr	—																																																					
Clay	5	5																																																					
Volcanic glass	Tr	1																																																					
Dolomite	—	Tr																																																					
Black MnO ₂ ?	—	48																																																					
Nannofossils	83	40																																																					
Radiolarians	8	4																																																					
Sponge spicules	4	2																																																					
Silicoflagellates	Tr	—																																																					
AG	CP 15 (NP 18 - NP 20)						1																																																
CG	<i>Thyrocystis bromia</i>						2																																																
	Barren						3																																																
							4																																																

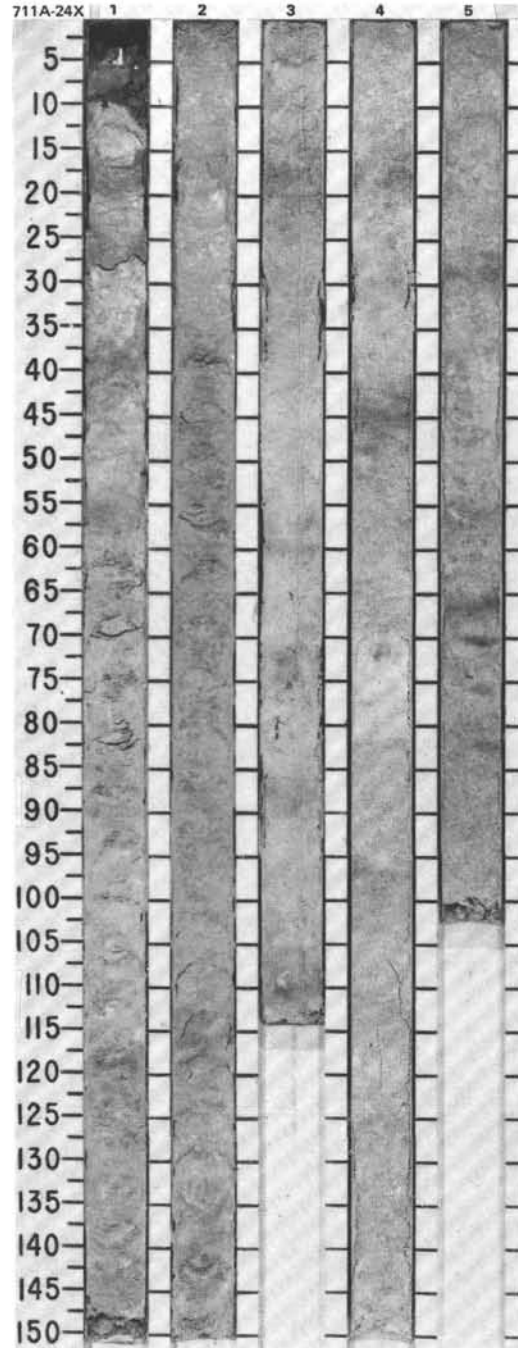


TIME-ROCK UNIT	BIOSTRAT. ZONE/ FOSSIL CHARACTER				PALEOMAGNETICS	PHYS. PROPERTIES	CHEMISTRY	SECTION	METERS	GRAPHIC LITHOLOGY	DRILLING DISTURB.	SED. STRUCTURES	SAMPLES	LITHOLOGIC DESCRIPTION																						
	FORAMINIFERS	NANNOFOSSILS	RADIOLARIANS	DIATOMS																																
MIDDLE EOCENE	P 11													<p>CLAY-BEARING NANNOFOSSIL CHALK and RADIOLARIAN-BEARING NANNOFOSSIL CHALK</p> <p>Major lithologies: Clay-bearing nannofossil chalk, very pale brown (10YR 7/3, 7/4, 8/3), bioturbated. Radiolarian-bearing nannofossil chalk, creamy white (10YR 9/3), in Section 1, 60-95 cm, Section 2, 60-70 cm, and Section 4, 75-80 and 85-94 cm.</p> <p>Minor lithologies: Clay-bearing radiolarian ooze, brownish yellow/orange (10YR 6/6) and brown (10YR 5/3), four thin layers 2-6 cm thick in Section 3, 36-38 and 117-121 cm, and Section 4, 80-85 and 94-101 cm. Turbidite layer, light gray (10YR 7/2), 20 cm thick with sharp base and gradational upper contact as well as graded, in Section 5, 14-34 cm.</p> <p>SMEAR SLIDE SUMMARY (%):</p> <table border="0"> <tr><td>1, 85</td></tr> <tr><td>D</td></tr> </table> <p>TEXTURE:</p> <table border="0"> <tr><td>Sand</td><td>5</td></tr> <tr><td>Silt</td><td>10</td></tr> <tr><td>Clay</td><td>85</td></tr> </table> <p>COMPOSITION:</p> <table border="0"> <tr><td>Feldspar</td><td>Tr</td></tr> <tr><td>Clay</td><td>5</td></tr> <tr><td>Dolomite</td><td>Tr</td></tr> <tr><td>Foraminifers</td><td>Tr</td></tr> <tr><td>Nannofossils</td><td>75</td></tr> <tr><td>Radiolarians</td><td>15</td></tr> <tr><td>Sponge spicules</td><td>5</td></tr> </table>	1, 85	D	Sand	5	Silt	10	Clay	85	Feldspar	Tr	Clay	5	Dolomite	Tr	Foraminifers	Tr	Nannofossils	75	Radiolarians	15	Sponge spicules	5
1, 85																																				
D																																				
Sand	5																																			
Silt	10																																			
Clay	85																																			
Feldspar	Tr																																			
Clay	5																																			
Dolomite	Tr																																			
Foraminifers	Tr																																			
Nannofossils	75																																			
Radiolarians	15																																			
Sponge spicules	5																																			
RP								0.5																												
AG	13c	CP 14 (NP 16 - NP 17)						1.0																												
CG		<i>Podocystis mitra</i>																																		
		Barren																																		
								2																												
								3																												
								4																												
								5																												
								CC																												



SITE 711 HOLE A CORE 24X CORED INTERVAL 4648.8-4658.4 mbsl; 220.7-230.3 mbsf

TIME-ROCK UNIT	BIOSTRAT. ZONE/ FOSSIL CHARACTER				PALEOMAGNETICS	PHYS. PROPERTIES	CHEMISTRY	SECTION	METERS	GRAPHIC LITHOLOGY	DRILLING DISTURB.	SED. STRUCTURES	SAMPLES	LITHOLOGIC DESCRIPTION	
	FORAMINIFERS	NANNOFOSSILS	RADIOLARIANS	DIFATOMS											
MIDDLE EOCENE	P 9	CP 13b (NP 15)	<i>Podocyrhis ampla</i>	Barren				0.5						<p>CLAY-BEARING RADIOLARIAN-BEARING NANNOFOSSIL CHALK</p> <p>Major lithology: Clay-bearing radiolarian-bearing nannofossil chalk, very pale brown (10YR 8/3) and light yellowish brown (10YR 6/4). General mottling and bioturbation throughout the core.</p> <p>SMEAR SLIDE SUMMARY (%):</p> <p>1, 80 D</p> <p>TEXTURE:</p> <p>Sand 30 Clay 70</p> <p>COMPOSITION:</p> <p>Volcanic glass 1 Foraminifers 2 Nannofossils 70 Radiolarians 20 Sponge spicules 5 Calcspheres(?) 2</p>	
FP							1	1.0							
AM							2								
CG							3								
							4								
							5								

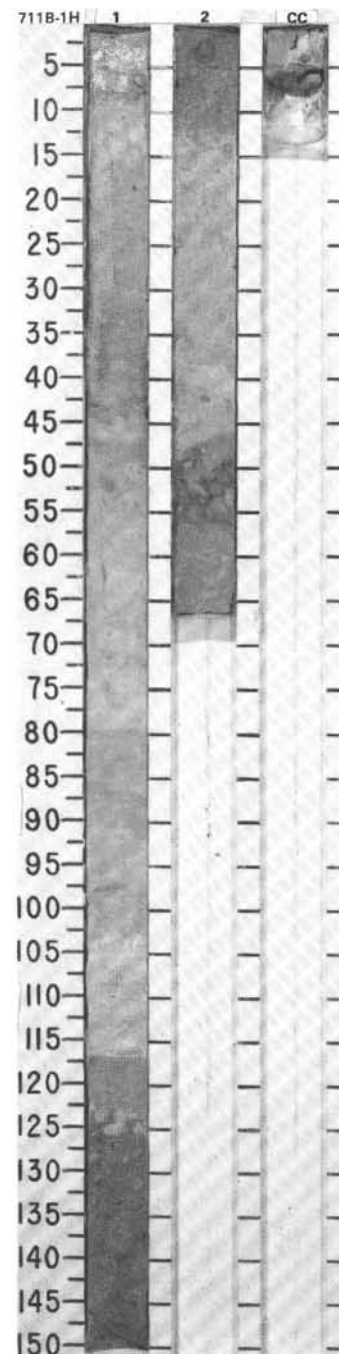
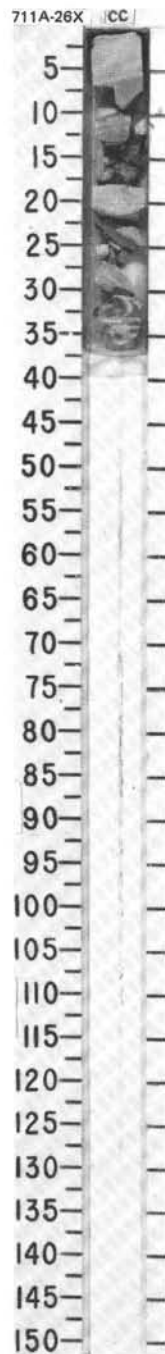


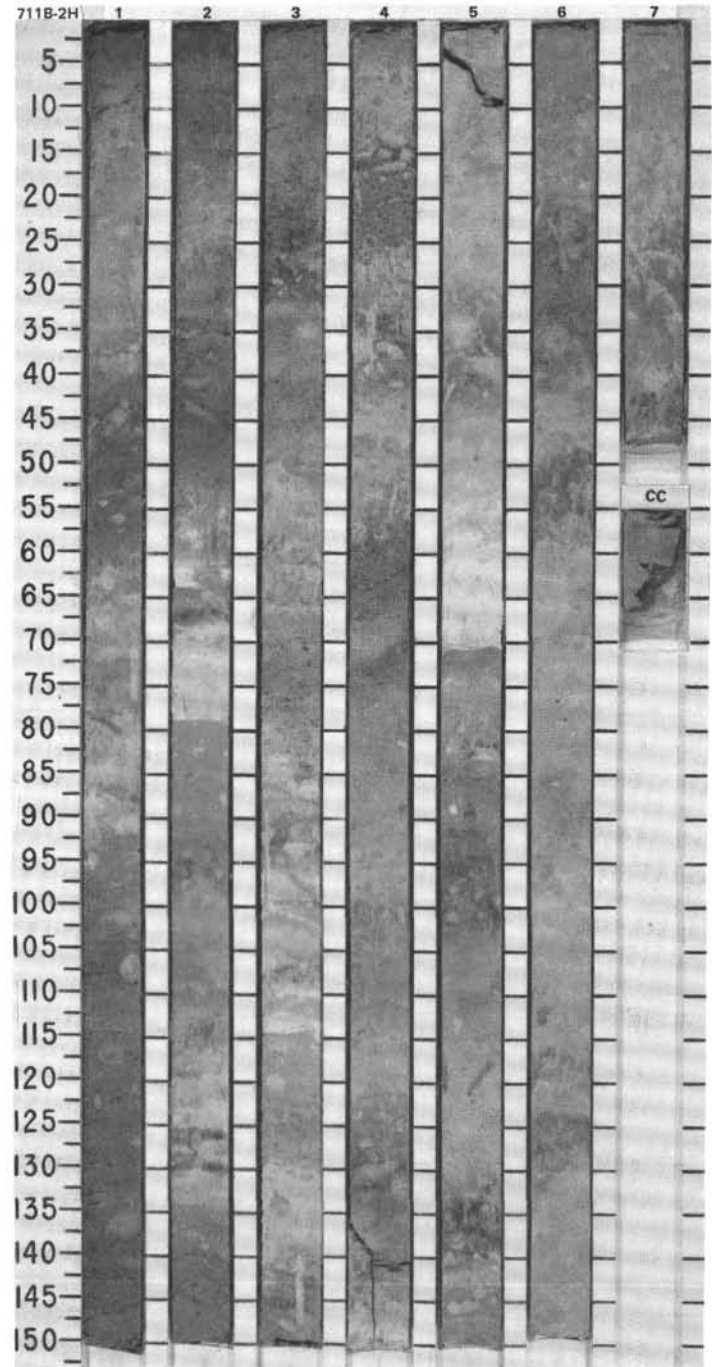
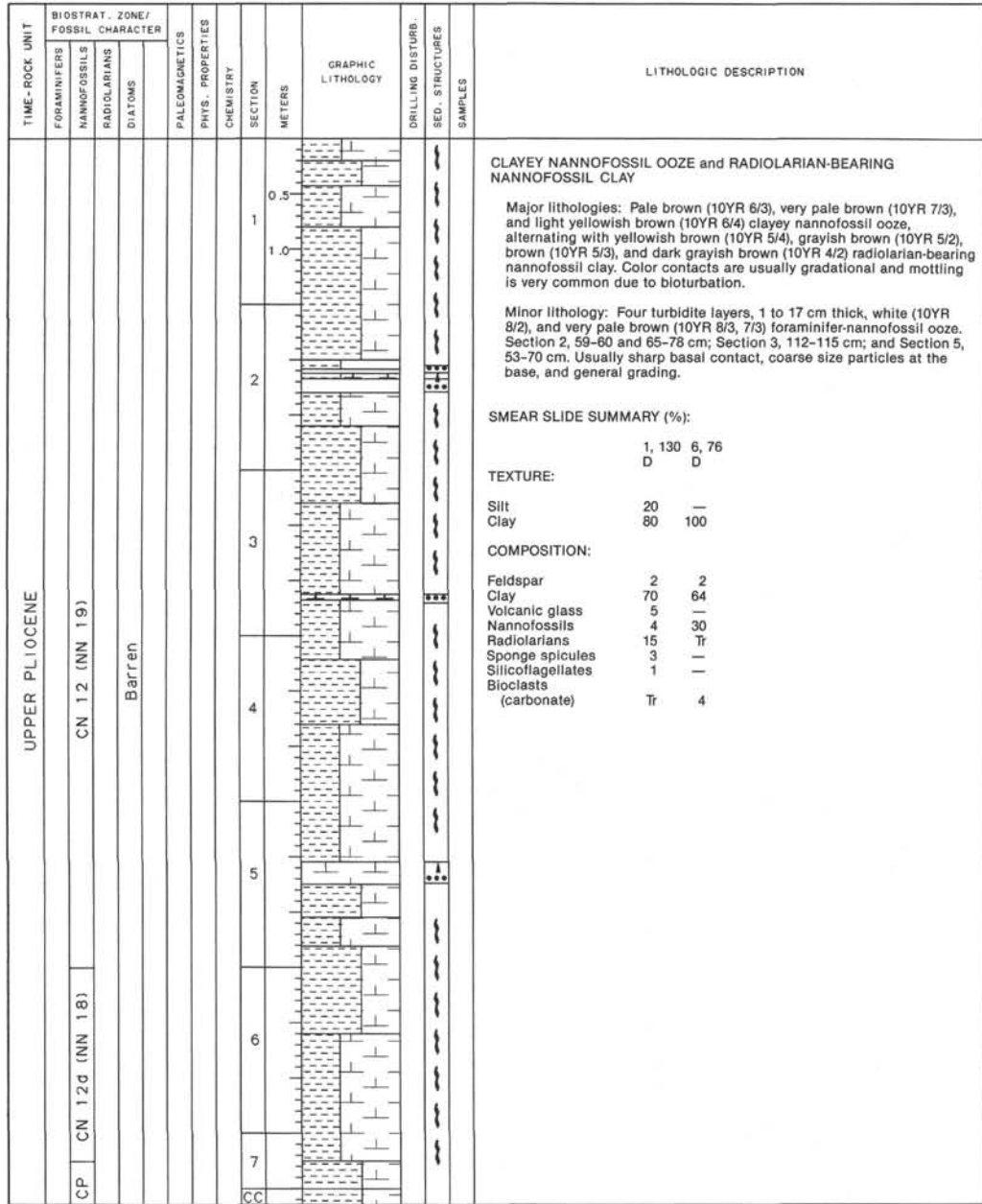
SITE 711 HOLE A CORE 26X CORED INTERVAL 4668.1-4677.8 mbsl; 240.0-249.7 mbsf

TIME-ROCK UNIT	BIOSTRAT. ZONE/ FOSSIL CHARACTER			PALEOMAGNETICS	PHYS. PROPERTIES	CHEMISTRY	SECTION	METERS	GRAPHIC LITHOLOGY	DRILLING DISTURB. BED. STRUCTURES	SAMPLES	LITHOLOGIC DESCRIPTION
	FORAMINIFERS	NANNOFOSSILS	RADIOLARIANS DIATOMS									
LOWER EOCENE	CP 12 (NP 14) AM		Barren						▲▲▲▲▲▲▲▲			CHERT Major lithology: Numerous pieces of banded chert, very pale brown (10YR 8/4) to yellowish brown (10YR 5/4).

SITE 711 HOLE B CORE 1H CORED INTERVAL 4429.7-4431.8 mbsl; 0.0-2.1 mbsf

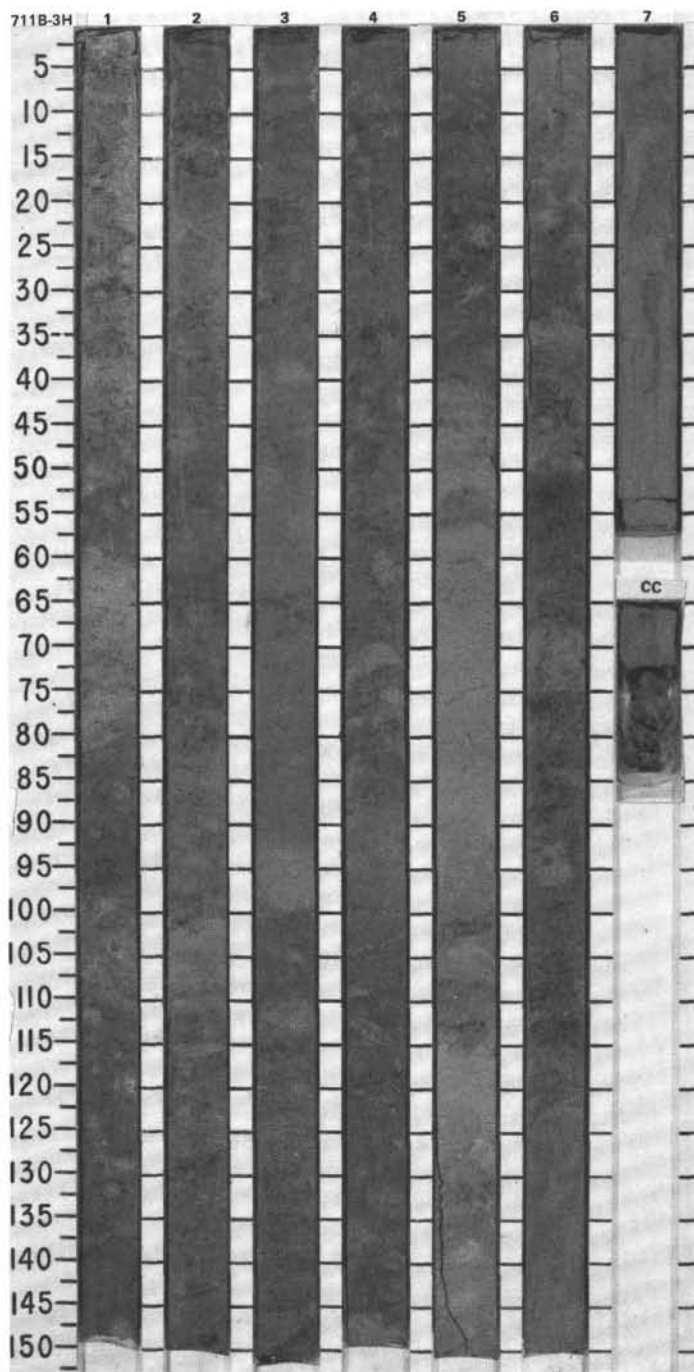
TIME-ROCK UNIT	BIOSTRAT. ZONE/ FOSSIL CHARACTER			PALEOMAGNETICS	PHYS. PROPERTIES	CHEMISTRY	SECTION	METERS	GRAPHIC LITHOLOGY	DRILLING DISTURB. BED. STRUCTURES	SAMPLES	LITHOLOGIC DESCRIPTION
	FORAMINIFERS	NANNOFOSSILS	RADIOLARIANS DIATOMS									
PLEISTOCENE	CN 14-CN 15	AP	RP <i>N. reinholdii</i>					0.5 1.0 2				CLAYEY NANNOFOSSIL OOZE Major lithology: Clayey nannofossil ooze, light yellowish brown (10YR 6/4), pale brown (10YR 6/3) and very pale brown (10YR 8/3), interbedded with yellowish brown (10YR 5/4). All color contacts are gradational and mottled due to extensive bioturbation. Minor lithology: One turbidite layer, graded, 16 cm thick, nannofossil foraminifer ooze, very pale brown (10YR 7/3) and light brownish gray (10YR 6/2). Section 1, 101-117. SMEAR SLIDE SUMMARY (%): TEXTURE: 1, 40 D Silt 15 Clay 85 COMPOSITION: Clay 20 Dolomite Tr Accessory minerals: Zeolite(?) Tr Foraminifers 5 Nannofossils 65 Diatoms 3 Radiolarians 6 Sponge spicules 1 Silicoflagellates Tr





SITE 711 HOLE B CORE 3H CORED INTERVAL 4441.4-4451.1 mbsl; 11.7-21.4 mbsf

TIME-ROCK UNIT	BIOSTRAT. ZONE/ FOSSIL CHARACTER			PALEOMAGNETICS	PHYS. PROPERTIES	CHEMISTRY	SECTION	METERS	GRAPHIC LITHOLOGY	DRILLING DISTURB. SEC. STRUCTURES	SAMPLES	LITHOLOGIC DESCRIPTION																																	
	FORAMINIFERS	NANNOFOSSILS	RADIOLARIANS DIATOMS																																										
LOWER PLEISTOCENE		CP 12c7 (NN 17?)						0.5				<p>NANNOFOSSIL-BEARING and CLAY</p> <p>Major lithologies: Dark grayish brown (10YR 4/2), grayish brown (10YR 5/2), brown (10YR 5/3), and light brownish gray (10YR 6/2) nannofossil-bearing and clay, alternating with light yellowish brown (10YR 6/4) nannofossil-bearing clay; often a mixture of both lithologies due to intense mottling related to heavy bioturbation. The lower part of the core is totally disturbed by drilling (flow in) from Section 6, 125 cm.</p> <p>SMEAR SLIDE SUMMARY (%):</p> <table> <tr> <td></td> <td>2, 53</td> <td>5, 80</td> </tr> <tr> <td>D</td> <td></td> <td>D</td> </tr> </table> <p>* TEXTURE:</p> <table> <tr> <td>Silt</td> <td>—</td> <td>10</td> </tr> <tr> <td>Clay</td> <td>100</td> <td>90</td> </tr> </table> <p>COMPOSITION:</p> <table> <tr> <td>Feldspar</td> <td>Tr</td> <td>—</td> </tr> <tr> <td>Clay</td> <td>100</td> <td>90</td> </tr> </table> <p>Accessory minerals:</p> <table> <tr> <td>Opales</td> <td>Tr</td> <td>Tr</td> </tr> <tr> <td>Foraminifers (fragments)</td> <td>—</td> <td>Tr</td> </tr> <tr> <td>Nannofossils</td> <td>—</td> <td>10</td> </tr> <tr> <td>Radiolarians</td> <td>Tr</td> <td>Tr</td> </tr> <tr> <td>Sponge spicules</td> <td>—</td> <td>Tr</td> </tr> </table>		2, 53	5, 80	D		D	Silt	—	10	Clay	100	90	Feldspar	Tr	—	Clay	100	90	Opales	Tr	Tr	Foraminifers (fragments)	—	Tr	Nannofossils	—	10	Radiolarians	Tr	Tr	Sponge spicules	—	Tr
		2, 53	5, 80																																										
	D		D																																										
	Silt	—	10																																										
	Clay	100	90																																										
	Feldspar	Tr	—																																										
	Clay	100	90																																										
Opales	Tr	Tr																																											
Foraminifers (fragments)	—	Tr																																											
Nannofossils	—	10																																											
Radiolarians	Tr	Tr																																											
Sponge spicules	—	Tr																																											
	Barren						1.0																																						
	Barren						2			*																																			
	CN 10b						3																																						
	Barren						4																																						
							5			*																																			
	Barren						6																																						
							7		FLOW IN																																				
							CC		FLOW IN																																				



SITE 711 HOLE B CORE 5H CORED INTERVAL 4460.7-4470.4 mbsf; 31.0-40.7 mbsf

TIME-ROCK UNIT	BIOSTRAT. ZONE/FOSSIL CHARACTER			PALEOMAGNETICS	PHYS. PROPERTIES	CHEMISTRY	SECTION	METERS	GRAPHIC LITHOLOGY	DRILLING DISTURB.	SED. STRUCTURES	SAMPLES	LITHOLOGIC DESCRIPTION
	FORAMINIFERS	NANNOFOSSILS	RADIOLARIANS										
UPPER MIOCENE													
		CP 9a (NN 11)					1	0.5					
							2	1.0					
							3						
		CP 8? (NN 10?)					4						
							5						
		Barren					6						
FP	Barren					7							
						CC							

NANNOFOSSIL CLAY and VOLCANIC GLASS-BEARING CLAY

Major lithologies: Very pale brown (10YR 7/4, 7/3), light yellowish brown (10YR 6/4), and pale brown (10YR 6/3) moderately bioturbated nannofossil clay, passing downcore (from Section 5) to a very homogeneous, featureless, pale brown (10YR 6/3) and grayish brown (10YR 5/2) volcanic glass-bearing clay.

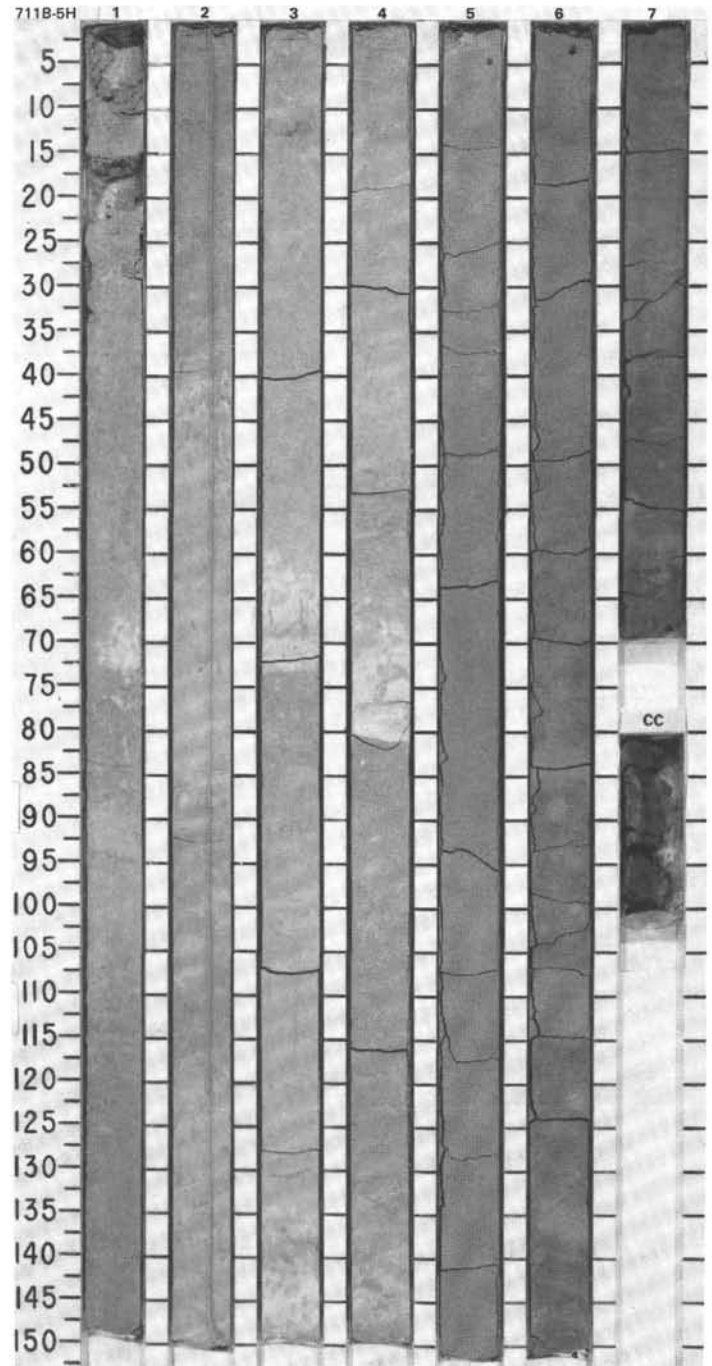
Minor lithology: Three, possibly five, turbidite layers, white (10YR 8/2, N9) and very pale brown (10YR 8/3) nannofossil ooze, 3-10 cm thick. Section 1, 70-73 cm; Section 3, 59-69 and 142-149 cm; and Section 4, 70-80 and 142-157 cm.

SMEAR SLIDE SUMMARY (%):

	2, 74 D	3, 70 D	5, 74 D	5, 120 D
TEXTURE:				
Sand	—	1	—	—
Silt	10	30	—	5
Clay	90	69	100	95

COMPOSITION:

	35	15	98	97
Clay				
Volcanic glass	—	—	1	Tr
Accessory minerals:				
Opauques	—	—	1	—
Foraminifers	—	—	—	—
Fragments	Tr	2	—	—
Nannofossils	65	83	—	3
Radiolarians	—	—	Tr	—



TIME-ROCK UNIT	BIOSTRAT. ZONE/ FOSSIL CHARACTER				PHYS. PROPERTIES	CHEMISTRY	SECTION	METERS	GRAPHIC LITHOLOGY	DRILLING DISTURB.	SED. STRUCTURES	SAMPLES	LITHOLOGIC DESCRIPTION
	FORAMINIFERS	NANNOFOSSILS	RADIOLARIANS	DIATOMS									
LOWER-MIDDLE MIOCENE													
	CP	CN 4 - CN 3 (NN 4 - NN 5)	Barren	Barren			0.5 1.0						
							2			*			
							3			*			
							4						
							5			?	*		
						6							
						CC							

VOLCANIC GLASS-BEARING CLAY and NANNOFOSSIL CLAY

Major lithologies: Dark grayish brown (10YR 4/2) and light yellowish brown (10YR 6/4) volcanic glass-bearing clay, usually occurring as large patches, in the top four sections; alternating in Sections 5 and 6 with a grayish brown (10YR 5/2), light yellowish brown (10YR 6/4), and very pale brown (10YR 7/4) mottled and bioturbated nannofossil clay.

Minor lithology: White (N9) and very pale brown (10YR 8/3) nannofossil ooze in three, possibly four, turbidite layers, 2-13 cm thick. Section 5, 98-92, 103-116, and 144-146 cm, and CC, 0-10 cm. [Usually the few cm just below the turbidite layer have a characteristic light yellowish brown color (10YR 6/4), similar to the color of the blebs scattered within the clay; both might be diagenetic in origin. See 115-711B-8H.]

SMEAR SLIDE SUMMARY (%):

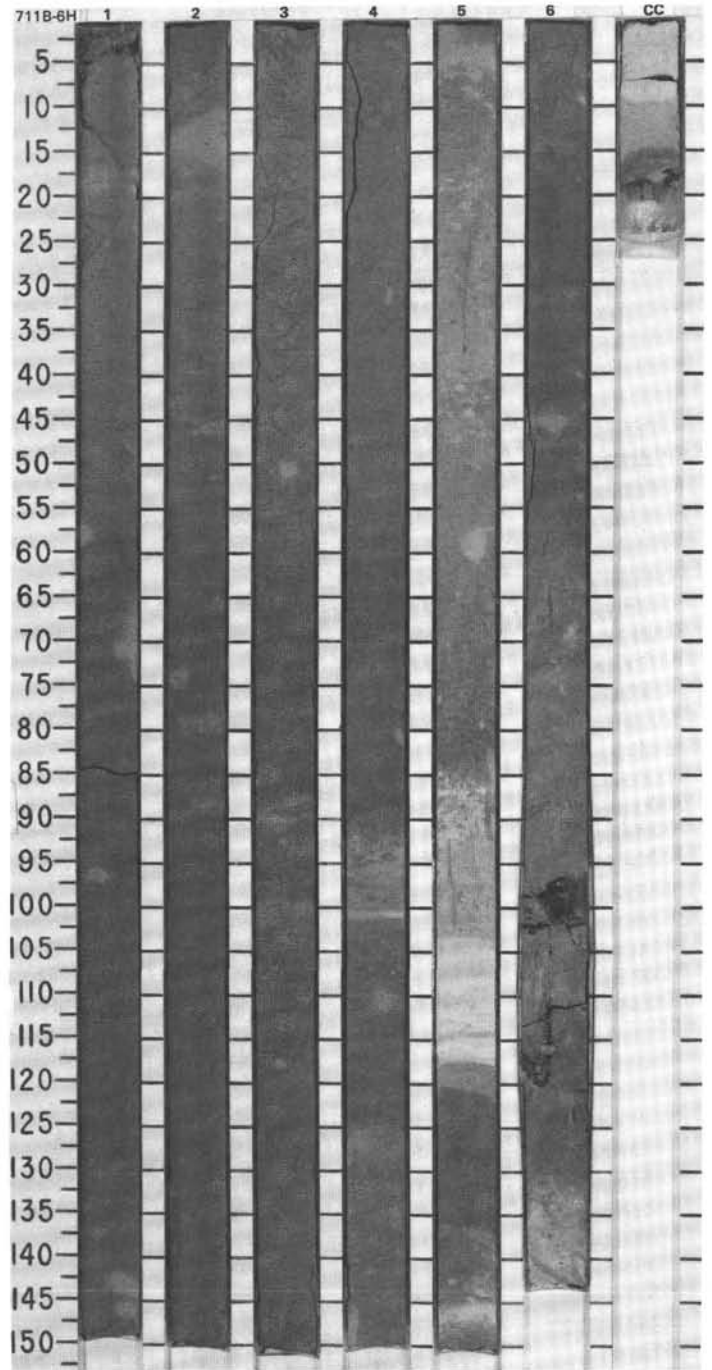
	2, 14	2, 71	5, 100
	D	D	D

TEXTURE:

Silt	3	—	30
Clay	97	100	70

COMPOSITION:

Quartz	—	Tr	—
Clay	96	99	5
Volcanic glass	3	1	—
Accessory minerals:			
Opauques	1	Tr	—
Nannofossils	Tr	—	95



SITE 711 HOLE B CORE 11H CORED INTERVAL 4518.3-4528.0 mbsl; 88.9-98.6 mbsf

TIME-ROCK UNIT	BIOSTRAT. ZONE/ FOSSIL CHARACTER				PALEOMAGNETICS	PHYS. PROPERTIES	CHEMISTRY	SECTION	METERS	GRAPHIC LITHOLOGY	DRILLING DISTURB.	SED. STRUCTURES	SAMPLES	LITHOLOGIC DESCRIPTION
	FORAMINIFERS	NANNOFOSSILS	RADIOLARIANS	DIATOMS										
UPPER OLILOCENE									0.5 1.0					<p>CLAY-BEARING NANNOFOSSIL OOZE</p> <p>Major lithology: White (10YR 8/2), light gray (2.5Y 7/2), and pale yellow (2.5Y 7/4) clay-bearing nannofossil ooze, homogeneous and featureless, slight bioturbation.</p> <p>Minor lithology: One probable turbidite layer, 17 cm thick, white (N9), little evidence of coarsening of material, but similar to previous layer, with grading.</p> <p>SMEAR SLIDE SUMMARY (%):</p> <p>Texture: 5, 80 D</p> <p>Silt 6 Clay 94</p> <p>COMPOSITION:</p> <p>Clay 15 Volcanic glass 1 Foraminifers Tr Nannofossils 79 Radiolarians 2 Sponge spicules 3</p>
AM								2						
	CP 19a (NP 24)													
	Barrén													
	Barrén													
								3						
								4						
								5					*	
								6						
								7						
								CC						

